GEMS & GEMOLOGY

TABLE OF CONTENTS

pg. 97

pg. 109

pg. 115

pg. 145

SUPPORT YOUR LOCAL RESEARCHER

Last February, many leading gemologists attended the very successful First World Emerald Congress in Bogotá, Colombia. Of particular concern to the participants was the topic of emerald treatments—that is, the use of different fillers to improve the apparent clarity of the stone. All were aware of the negative publicity that emerald filling has received in recent months, and of the fact that some fillers are less effective or less durable than others. At the Congress, representatives from many of the major gemological laboratories sat together on a single panel to discuss this problem. A constant refrain from the audience, which included dealers as well as retailers, was: When were the GIA Gem Trade Laboratory, the Gübelin Gemmological Laboratory, SSEF, AGTA, and even *Gems & Gemology*, among others, going to resolve the treatment issue?

We, however, cannot address such problems without help from you in the trade. A meaningful gemological study—whether done in the U.S., Europe, Asia, or South America—often requires large numbers of samples, hundreds of hours of testing, and the participation of several experts to analyze the results. For example, the trace-element-chemistry project reported by Sam Muhlmeister and colleagues in this issue used 283 natural and synthetic rubies, from 14 localities and 12 synthetics manufacturers. As Dr. Mary Johnson reported at the Emerald Congress, the emerald treatment study that GIA is currently spearheading required almost 300 emerald samples, all natural, from a number of known localities. Several fillers are being tested by various means to determine both their effectiveness and their durability under normal conditions of wear and care.

Often the greatest delay in conducting such a study is in acquiring the samples. Unlike universities or government research institutions, the research conducted by most gemological laboratories is not supported by outside funding. You are the experts on buying and selling gems, so most of you know what it costs to purchase 300 one-half to one carat emeralds or rubies. In addition, even though for many projects the samples do not have to be large or expensive, it is critical that they be representative of the particular locality, manufacturing process, or treatment under investigation—information that often can be provided only by members of the trade. As a result, researchers may have to work for years to obtain the stones for a single research project. For the ruby study, some samples were donated, many were loaned, and others were purchased. Our hats are off to all of the people who participated (more than 30 individuals and companies for that study alone). Still, some dealers leave request letters unanswered or make promises they cannot keep, consuming precious time. Then, when the pressure is on from consumers and the media, these same dealers want to know what's taking so long.

As the gem and jewelry industry is faced with ever-more-pressing issues regarding the disclosure of treatments and synthetics, comprehensive research will become even more important. Knowledge gained from the scientific study of gem materials and their treatments is necessary to maintain confidence in the industry by our colleagues and consumers alike. The use of broad, representative sets of samples, accompanied by reliable information about the sources (or treatments) of the stones, is critical to many of these research projects.

So, please, think about it. And the next time you're asked, send some stones, provide information, share your experience and . . . support your local researcher.
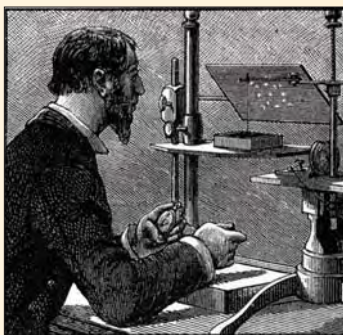
Alice S. Keller
EDITOR

SEPARATING NATURAL AND SYNTHETIC RUBIES ON THE BASIS OF TRACE-ELEMENT CHEMISTRY

By Sam Muhlmeister, Emmanuel Fritsch, James E. Shigley, Bertrand Devouard, and Brendan M. Laurs

Natural and synthetic gem rubies can be separated on the basis of their trace-element chemistry as determined by energy-dispersive X-ray fluorescence (EDXRF) spectrometry. This method is especially important for rubies that do not have diagnostic inclusions or growth features, since such stones are difficult to identify using traditional gem testing methods. The results of this study indicate that the presence of nickel, molybdenum, lanthanum, tungsten, platinum, lead, or bismuth proves synthetic origin, but these elements were not detectable in most of the synthetic rubies tested. Alternatively, the concentrations of titanium, vanadium, iron, and gallium—considered together, as a trace-element "signature"—provide a means for separating nearly all synthetic from natural rubies. EDXRF can also help identify the geologic environment in which a ruby formed, and thus imply a geographic origin.

ABOUT THE AUTHORS

Mr. Muhlmeister (smeister@gia.edu) is research associate, and Dr. Shigley is director, at GIA Research in Carlsbad, California. Dr. Fritsch (fritsch@cnrs-imn.fr) is professor of physics at the University of Nantes, France. Dr. Devouard is assistant professor at Clermont-Ferrand University, France. Mr. Laurs, a geologist and gemologist, is senior editor of Gems & Gemology, Gemological Institute of America, Carlsbad.

Please see acknowledgments at end of article.

Correct gem identification is crucial to the gem and jewelry trade. However, accurate information on a gem's origin rarely accompanies a stone from the mine, or follows a synthetic through the trade after it leaves its place of manufacture. Today, natural and synthetic rubies from a variety of sources are seen routinely (figure 1). Usually, careful visual observation and measurement of gemological properties are sufficient to make important distinctions (Schmetzer, 1986a; Hughes, 1997). In some cases, however, traditional gemological methods are not adequate; this is particularly true of rubies that are free of internal characteristics or that contain inclusions and growth features that are ambiguous as to their origin (Hänni, 1993; Smith and Bosshart, 1993; Smith, 1996). The consequences of a misidentification can be in the tens of thousands, and even hundreds of thousands, of dollars.

Ruby is a gem variety of corundum (Al_2O_3) that is colored red by trivalent chromium (Cr^{3+}). Besides Cr, most rubies contain other elements in trace amounts that were incorporated during their growth, whether in nature or in the laboratory. For the purpose of this article, we consider trace elements to be those elements other than aluminum, oxygen, and chromium. These trace elements (such as vanadium [V] and iron [Fe]) substitute for Al^{3+} in the corundum crystal structure, or they may be present as various mineral inclusions (such as zirconium [Zr] in zircon) or as constituents in fractures. The particular assemblage of trace elements (i.e., which ones are present and their concentrations) provides a distinctive chemical signature for many gem materials. Since the trade places little emphasis on establishing the manufacturer of synthetic products, this article will focus on how trace-element chemistry, as determined by EDXRF, can be used for the basic identification of natural versus synthetic rubies. It will also explore how EDXRF can

Figure 1. These six natural and synthetic rubies are typical of material that might be submitted to a gemological laboratory for identification. From top to bottom and left to right: 1.29 ct Kashan flux-grown synthetic ruby, 1.10 ct natural ruby, 0.93 ct Czochralski-pulled synthetic ruby, 0.95 ct Ramaura synthetic ruby, 1.05 ct natural ruby from Tanzania, and 0.57 ct Swarovski flame-fusion synthetic ruby with flux-induced fingerprints. The 1.10 ct natural ruby was reported to have come from Mogok, but trace-element chemistry indicated that the stone was from a basalt-hosted deposit (such as Thailand); microscopy also indicated a basaltic origin. Photo © GIA and Tino Hammid.
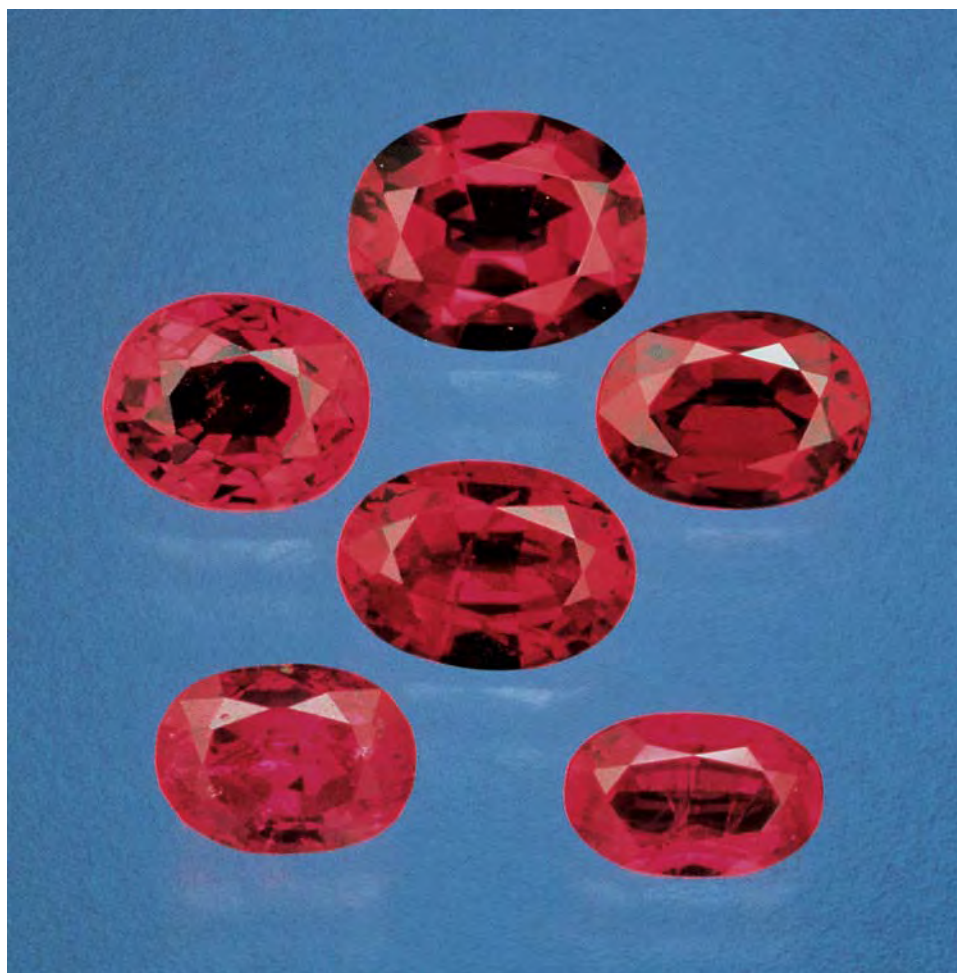
help determine the geologic origin of a natural ruby, which is useful for identifying the country of origin.

BACKGROUND

Previous research has indicated the potential of trace-element chemistry for separating natural from synthetic rubies (Hänni and Stern, 1982; Stern and Hänni, 1982; Kuhlmann, 1983; Schrader and Henn, 1986; Tang et al., 1989; Muhlmeister and Devouard, 1991; Yu and Mok, 1993; Acharya et al., 1997), and also for differentiating rubies from different localities (Harder, 1969; Kuhlmann, 1983; Tang et al., 1988, 1989; Delé-Dubois et al., 1993; Osipowicz et al., 1995; Sanchez et al., 1997). The two most common analytical techniques for determining ruby chemistry are electron microprobe and EDXRF. Other methods include wavelength dispersive X-ray fluorescence spectrometry, neutron activation analysis, proton-induced X-ray emission (PIXE) analysis, and optical emission spectroscopy. Most of these methods involve instrumentation that is not readily

available to gemological laboratories, or use techniques that may damage the sample. EDXRF, however, is nondestructive and has become standard equipment in many gemological laboratories.

Qualitative EDXRF analyses have shown that synthetic rubies contain relatively few trace elements, and that the presence of molybdenum (Mo) indicates a flux origin; natural rubies, on the other hand, show a greater number of trace elements, and Myanmar rubies show relatively low Fe and high V (Muhlmeister and Devouard, 1991; Yu and Mok, 1993). Analyses by electron microprobe (Delé-Dubois et al., 1993) and PIXE (Tang et al., 1988, 1989; Sun, 1992; Osipowicz et al., 1995) have revealed the same trends for Myanmar rubies, and have indicated that Thai stones show high Fe and low V; these studies have also shown significant variations in trace elements in rubies from the same deposit. PIXE analyses of rubies from several deposits have detected numerous trace elements, including silicon (Si), sulfur (S), chlorine, potassium

Figure 2. The discovery of new gem localities presents constant challenges for the gemologist. These two rubies (2.59 ct total weight) are from Mong Hsu, Myanmar, which first became known only in the early 1990s. Photo © Tino Hammid.

(K), calcium (Ca), titanium (Ti), V, Cr, manganese (Mn), Fe, and gallium (Ga); in contrast, with the exception of Cr, synthetic stones from Chatham, Inamori, and Seiko showed no significant trace elements, Kashan synthetic rubies showed some Ti, and Knischka and Ramaura synthetics contained Fe (Tang et al., 1989). Using optical emission spectroscopy, Kuhlmann (1983) reported the following trace elements (besides Cr) at levels >0.001 wt.% in these synthetics: Chatham and Verneuil—Fe, Si, Mo, beryllium (Be); Knischka—Fe, Si, Be, copper (Cu); Kashan—Si, Ti, Fe, Cu, Mn, Be. In natural rubies, the following (besides Cr) were detected at levels >0.001 wt.%: Mogok, Myanmar—V, Fe, Ti, Si, tin (Sn), Mn, Be; Jegdalek, Afghanistan—Si, Fe, Be; Umba Valley, Tanzania—Fe, Si, Ti, Cr, V, Mn; Morogoro, Tanzania—Ti, Si, Cr, Fe, V; Tsavo Park, Kenya—Cr, Fe, Si, Ti, V; Rajasthan, India—Fe, Si, Ti, Sn, Cu, V, Mn, Be.

In recent years, a number of new synthetic ruby products have entered the market, including those grown by the flux method (Smith and Bosshart, 1993; Henn and Bank, 1993; Henn, 1994; Hänni et al., 1994); by the hydrothermal method (Peretti and Smith, 1993); and by the Czochralski technique with natural ruby as the feed material, marketed as "recrystallized" (Kammerling et al., 1995b,c; Nassau, 1995). Other synthetic materials that have caused identification problems for the contemporary gemologist include flame-fusion synthetic rubies with flux-induced "fingerprints" (Koivula,

1983; Schmetzer and Schupp, 1994; Kammerling et al., 1995a) and Czochralski-pulled synthetic rubies that are inclusion-free (Kammerling and Koivula, 1994).

Natural rubies can also present identification problems. Heat treatment can significantly alter the appearance of the inclusions in natural ruby (Gübelin and Koivula, 1986; Themelis, 1992; Hughes, 1997). Fluid inclusions commonly rupture when heated, creating fractures that can be subsequently filled by the fluid or partially repaired on cooling (Gübelin and Koivula, 1986). These secondary fingerprints—common in heat-treated rubies from Mong Hsu, Myanmar, for example—are similar to the white, high-relief fingerprint-like inclusions commonly seen in flux synthetics (Laughter, 1993; Smith and Surdez, 1994; Peretti et al., 1995).

In addition, the locality of a natural ruby can have a significant impact on its market value (figure 2). Although the importance of "country of origin" in helping establish a natural ruby's value is a topic of ongoing debate (Liddicoat, 1990; Hughes, 1990a), it is nonetheless a significant consideration in some trading circles, especially for larger stones.

GEOLOGIC ORIGINS OF GEM-QUALITY RUBIES

Rubies are mined from both primary deposits (the host rock where the ruby formed) and secondary deposits (i.e., alluvial—stream transported, or eluvial—weathered in place) [Simonet, 1997]. Because of its durability and relatively high specific gravity, ruby is readily concentrated into secondary deposits; the processes of weathering and alluvial transport tend to destroy all but the best material, so these deposits can be quite valuable. In general, primary deposits are economically important only if the ruby is concentrated in distinct mineable areas, such as layers within marble.

The conditions under which ruby forms are important to gemologists, because the chemical composition, inclusions, and growth features visible in fashioned stones are influenced by the composition, pressure, and temperature of the ruby-forming environment (see, e.g., Peretti et al., 1996). The trace elements in a ruby are incorporated into the crystal structure, or are present as mineral inclusions (table 1) or as constituents in fractures. Therefore, the geologic environment influences the assemblage of trace elements present. Corundum (Al_2O_3) crystallizes only in silica-deficient environments because, in the presence of Si, the Al is used to form more common minerals such as kyanite,

TABLE 1. Geology and mineralogy of gem-quality ruby deposits.

Deposit type	Geology	Typical associated minerals	Typical mineral inclusions	Localities[a]
Basalt-hosted	Xenocrysts in alkali basalt (alluvial and eluvial deposits)	Sapphire, clinopyroxene, zircon, Fe-rich spinel, garnet; sometimes sapphirine	Pyrrhotite (commonly altered to goethite), apatite; sometimes spinel, almandine garnet	Australia—Barrington (Sutherland, 1996a,b; Sutherland and Coenraads, 1996; Webb, 1997; Sutherland et al., 1998) Cambodia—Pailin (Jobbins and Berrangé, 1981; Sutherland et al., 1998) Thailand—Chanthaburi, at Bo Rai–Bo Waen (Charaljavanaphet, 1951; Gübelin, 1971; Keller, 1982; Vichit, 1987; Coenraads et al., 1995) Vietnam—southern, at Dak Nong (Kane et al., 1991; Poirot, 1997)
Marble-hosted	Calcite or dolomite marble, commonly interlayered with schists and gneisses; may or may not be cut by granite intrusions (primary and alluvial deposits)	Calcite, dolomite, spinel, pargasite, phlogopite, rutile, Cr-muscovite, chlorite, tremolite, tourmaline, apatite, sphene, anorthite, margarite, pyrrhotite, pyrite, ilmenite, graphite, fluorite	Calcite, dolomite, rutile, apatite, pyrite, phlogopite, boehmite; sometimes spinel, zircon, margarite, graphite, pyrrhotite	Afghanistan—Jegdalek (Hughes, 1994; Bowersox and Chamberlin, 1995) China—Aliao Mountains, Yunnan Province (Keller and Fuquan, 1986; ICA Gembureau, 1991) India—southern (Viswanatha, 1982) Myanmar—Mogok (Iyer, 1953; Keller, 1983; Gübelin and Koivula, 1986; Kammerling et al., 1994) Myanmar—Mong Hsu (Peretti and Mouawad, 1994; Smith and Surdez, 1994; Peretti et al., 1995) Nepal—Taplejung district (Harding and Scarratt, 1986; Smith et al., 1997) Pakistan—Hunza (Bank and Okrusch, 1976; Okrusch et al., 1976; Gübelin, 1982; Hunstiger, 1990b) Pakistan—Kashmir ("Kashmir Yields Ruby, Tourmaline," 1992; Kane, 1997) Russia—Ural Mountains (Kissin, 1994) Tanzania—Morogoro (Hänni and Schmetzer, 1991) Tajikistan—eastern Pamir Mtns. (Henn et al., 1990b; Smith, 1998) Vietnam—northern, at Luc Yen (Henn and Bank, 1990; Henn, 1991; Kane et al., 1991; Delé-Dubois et al., 1993; Poirot, 1997)
Metasomatic	Desilicated pegmatite cutting ultramafic rock or marble (primary, eluvial, and alluvial deposits)	Plagioclase, vermiculite, phlogopite, muscovite, tourmaline (highly variable)	Rutile, boehmite; sometimes apatite, zircon, spinel, vermiculite, muscovite, pyrrhotite, graphite (highly variable)	India—southern (Viswanatha, 1982; Menon et al., 1994) Kenya—Mangari (Pohl et al., 1977; Pohl and Horkel, 1980; Bridges, 1982; Hunstiger, 1990b; Levitski and Sims, 1997) Tanzania—Umba (Solesbury, 1967; Zwaan, 1974; Hänni, 1987) Vietnam—central, at Quy Chau (Kane et al., 1991; Poirot, 1997)
Metasomatic	Desilicated aluminous schist/gneiss adjacent to ultramafic rock (primary, eluvial, and alluvial deposits)	Plagioclase, amphibole, epidote, tourmaline, micas, sillimanite, kyanite (highly variable)	Rutile, plagioclase, apatite, zircon, graphite, sillimanite, amphibole, ilmenite (highly variable)	India—southern (Viswanatha, 1982; Hunstiger, 1990a) Kenya—Mangari (Pohl et al., 1977; Pohl and Horkel, 1980; Hunstiger, 1990b; Key and Ochieng, 1991; Levitski and Sims, 1997) Malawi—Chimwadzulu Hill (Rutland, 1969; Henn et al., 1990a) Sri Lanka—Ratnapura, Elahera (Dahanayake and Ranasinghe, 1981, 1985; Munasinghe and Dissanayake, 1981; Dahanayake, 1985; Rupashinge and Dissanayake, 1985; Gunawardene and Rupasinghe, 1986)

[a]Although there are known deposit types in the countries listed, there may also be deposits (e.g., alluvial) that have not yet been characterized. Consequently, we do not know the specific geologic environment for all of the rubies obtained for this study.

feldspars, and micas. The scarcity of gem corundum—especially ruby—results from this requirement for Si-depleted conditions in the presence of the appropriate chromophore(s) (i.e., Cr for ruby and Fe and Ti for blue sapphire), under the appropriate temperature and pressure conditions. The mechanisms by which gem corundum forms are still debated by geologists (see, e.g., Levinson and Cook,

Figure 3. This specimen (4.6 cm high) from Jegdalek, Afghanistan, shows a ruby embedded in calcite marble, along with traces of associated minerals. Courtesy of H. Obodda; photo © Jeffrey Scovil.

1994). With the exception of a few occurrences, gem-quality ruby has been found in three types of primary deposits (again, see table 1): basalt-hosted, marble-hosted, and metasomatic. (The latter two form by different metamorphic processes, as explained below.)

Basalt-Hosted Deposits. Some of the world's largest ruby deposits, past and present, are secondary deposits associated with alkali basalts (e.g., Cambodia and Thailand). However, the formation conditions of this type of corundum are the least understood. The occurrence of corundum in basalt is similar to that of diamond in kimberlite: The ruby and sapphire crystals (xenocrysts) are transported in molten rock from lower levels of the earth's crust (or upper mantle) to the surface. During transport from depths of 15–40 km (Levinson and Cook, 1994), the corundum is partially resorbed, as shown by the rounded edges and surface etch patterns typically seen on basalt-hosted corundum (Coenraads, 1992).

From evidence revealed by trace elements, mineral inclusions, fluid inclusions, and associated mineral assemblages observed in rare corundum-bearing assemblages (as xenoliths), geologists have suggested that both metamorphic- and igneous-formed rubies may be present in a given basalt-hosted deposit (see, e.g., Sutherland and Coenraads, 1996; Sutherland et al., 1998). The metamorphic rubies in such deposits may be derived from regional metamorphism of aluminous rocks (such as shales, laterites, and bauxites) that were subducted to great depths (Levinson and Cook, 1994). Two models have been proposed for the igneous origin of gem corundum: (1) from magma mixing at mid-crustal levels (Guo et al., 1996a,b), or (2) from the pegmatite-like crystallization of silica-poor magma in the deep crust or upper mantle (Coenraads et al., 1995). Regardless of the specific origin, the mineral inclusions and associated minerals suggest that the corundum formed in an environment containing Fe, S, and geochemically incompatible elements (Coenraads, 1992). This geochemical (or trace-element) "signature" is consistent with the relatively enriched Fe content that is characteristically shown by basalt-hosted rubies (see Results section, below).

Marble-Hosted Deposits. Some of the world's finest rubies form in marble-hosted deposits, such as those in Myanmar. These deposits are commonly thought to have formed as a result of the regional metamorphism of limestone by heat and pressure (see, e.g., Okrusch et al., 1976). At some localities, the close association of granitic intrusions with the ruby-bearing marble has led some researchers to consider them "metasomatic" (e.g., Mogok; Iyer, 1953); that is, chemical interaction between the marble and fluids associated with the intrusions caused ruby mineralization. Therefore, marble-hosted ruby deposits may form from regional metamorphism or contact metasomatism, or from a combination of the two (Konovalenko, 1990).

Depending on the composition of the original limestone, ruby-bearing marbles may be composed of calcite ($CaCO_3$) and/or dolomite [$CaMg(CO_3)_2$]. Ruby and associated minerals, such as spinel and micas (again, see table 1), form in layers that are irregularly distributed within the marble (figure 3). These ruby-bearing assemblages are thought to represent impure horizons within the original limestone, where Al-rich clays or sediments (such as bauxite) were deposited (see, e.g., Platen, 1988; Okrusch et al., 1976). The composition of the asso-

ciated minerals (table 1) indicates that these impure layers contain traces of Si, S, K, Ti, V, Cr, and, in general, are low in Fe. Rubies from certain marble-type deposits (such as Mogok) are prized for their "pure" red color (i.e., absence of brown modifying hues), which is supposedly due to their lack of iron; this is consistent with the low iron content of their marble host rocks.

Metasomatic Deposits. Metasomatism is a metamorphic process whereby chemical components are exchanged in the presence of fluids. One important mechanism is "desilication," in which Si is mobilized (i.e., removed from the rock), leaving Al behind to form corundum. Metasomatic deposits of gem ruby can be divided into two groups: (1) desilicated pegmatites intruding silica-poor rocks such as serpentinite (as, e.g., at Umba, Tanzania: Solesbury, 1967) or marble (as at Quy Chau, Vietnam; Poirot, 1997); and (2) desilicated schists and gneisses that have been altered by metasomatic fluids in the presence of ultramafic (low Si; high Mg, Fe) rock (e.g., Malawi: Rutland, 1969; again, see table 1). As stated above, the ruby deposits at Mogok may also be metasomatic; if so, they would constitute a third type of metasomatic deposit—marble that has been altered by pegmatite-derived fluids.

The trace-element chemistry of rubies formed in metasomatic deposits is variable because of the different rock types and the particular local geochemical conditions under which these rubies formed (see, e.g., Kuhlmann, 1983). For example, rubies from different metasomatic deposits at Mangari, Kenya, show different characteristics: At the John Saul mine, "pure" red ruby coloration is common; at the Penny Lane deposit, the ruby is "darker" (Bridges, 1982; Levitski and Sims, 1997). These color variations most likely result from the variable composition of the host rocks; that is, at John Saul, the host rocks contain lower concentrations of Fe than at Penny Lane. Other metasomatic-type ruby localities with variable host rocks are in India (see, e.g., Viswanatha, 1982) and Sri Lanka (see, e.g., Dahanayake and Ranasinghe, 1985; Rupasinghe and Dissanayake, 1985).

MANUFACTURE OF SYNTHETIC RUBY

Synthetic rubies were introduced to the gem market in 1885. Originally sold as natural rubies from a fictitious mine near Geneva, and hence named "Geneva ruby," they were later proved to be synthetic (Nassau and Crowningshield, 1969; Nassau,

Figure 4. Synthetic rubies were first manufactured more than 100 years ago. Today, several types are available in the gem marketplace. Here, a Chatham flux-grown synthetic ruby is set in 14k gold. Ring courtesy of Chatham Created Gems, photo © Tino Hammid.

1980, 1995). The producer of these early synthetic rubies was never disclosed. The first scientific paper describing ruby synthesis using the flame-fusion process was published by Auguste Verneuil in 1904, two years after his first success. The flame-fusion process used today to grow rubies is largely unchanged from the one Verneuil introduced at the turn of the century (Nassau and Crowningshield, 1969; Nassau, 1980; Hughes, 1990b). Although flame-fusion material is still the most common synthetic corundum used in jewelry, other techniques are commercially available (figure 4; table 2).

Ruby manufacturing methods can be divided into two general categories: melt and solution. Melt-grown synthetic rubies—including flame-fusion, Czochralski, and floating zone—are produced by melting and crystallizing aluminum oxide powder to which traces of Cr and (possibly) various trace elements have been added. With the Czochralski and floating-zone methods, crystallization typically takes place in an iridium crucible; with flame-fusion, crystallization occurs on a rotating boule, without a container. The chemistry of melt-grown synthetic rubies is usually relatively "pure"—that is, they contain detectable amounts of relatively few elements—in comparison to other synthetic rubies, because the melt generally contains few additives.

Solution-grown synthetic rubies are crystallized from a solution in which aluminum and trace elements are dissolved. There are two types of growth solutions: flux and hydrothermal. A variety of chemical fluxes are used (again, see table 2), and the solutions are contained within a metal crucible, usually platinum. Hydrothermal synthetic rubies are grown from a water-rich solution enclosed in a pressurized autoclave. These synthetic rubies may contain trace elements originating from the flux or the hydrothermal solution, and possibly from the crucible or autoclave.

MATERIALS AND METHODS

Materials. For this study, we examined 121 natural and 162 synthetic rubies, most of which were faceted. These samples were chosen to represent the known commercially available sources of gem-quality material. The stones ranged from 0.14 to 52.06 ct, with most samples between 0.50 and 3.00 ct. The majority were transparent, but some were translucent; many had eye-visible inclusions. The samples were provided by individuals who had reliable information on the country of origin, although in some cases the specific deposit was not known. Note that some corundums with Lechleitner synthetic ruby overgrowth were included in this study, although they are not true synthetic rubies (Schmetzer, 1986b; Schmetzer and Bank, 1987). Red diffusion-treated corundum and "recrystallized" synthetic ruby were also analyzed.

At least seven representative samples were obtained for most localities and manufacturers, although the actual number varied from one to 31 for each type. Due to the limited number of samples from some deposits or manufacturers, and the possible future compositional variations of these rubies, the results of this study should only be considered an indication of the chemistry from these sources. Also, the trace-element data in this study are valid only for rubies, and do not necessarily apply to corundum of other colors (including pink). The fol-

TABLE 2. Manufacturing methods and possible sources of trace elements in synthetic rubies.

Manufacturing method/manufacturer[a]	Growth material	References
Melt	**Feed**	
Czochralski-pulled	Alumina and Cr_2O_3	Rubin and Van Uitert, 1966; Nassau, 1980
Flame-fusion	Alumina and Cr_2O_3	Verneuil, 1904; Nassau, 1980; Yaverbaum, 1980
Floating zone	Alumina and Cr_2O_3	Nassau, 1980; Sloan and McGhie, 1988
Induced fingerprint	(Flame-fusion synthetic rubies with induced "fingerprints" by any of various fluxes)	Koivula, 1983; Schmetzer and Schupp, 1994; Kammerling et al., 1995a
Solution—Flux	**Fluxes**	
Chatham	Li_2O-MoO_3-PbF_2 and/or PbO	Schmetzer, 1986b
Douros	PbF_2 or PbO_4	Smith and Bosshart, 1993; Hänni et al., 1994
Kashan	Na_3AlF_6	Henn and Schrader, 1985; Schmetzer, 1986b; Weldon, 1994
Knischka	Li_2O-WO_3-PbF_2, PbO, $Na_2W_2O_7$, and Ta_2O_5	Knischka and Gübelin, 1980; Schmetzer, 1986b, 1987; Galia, 1987; Brown and Kelly, 1989
Lechleitner	Flux overgrowth (using Li_2O-MoO_3-PbF_2 and/or PbO flux) on natural corundum	Schmetzer, 1986b; Schmetzer and Bank, 1987
Ramaura	Bi_2O_3-PbF_2, also rare-earth dopant[b] added to flux as well as La_2O_3[c]	Kane, 1983; Schmetzer, 1986b
Solution—Hydrothermal	**Solution**	
Tairus (Russia)	Alumina or aluminum hydrates partially dissolved in an aqueous medium with Cr compounds such as $Na_2Cr_2O_7$	Nassau, 1980; Yaverbaum, 1980; Peretti and Smith, 1993; Peretti et al., 1997; Qi and Lin, 1998

[a]The following containers are typically used during manufacture: Melt—iridium crucible (except no container is used for flame-fusion), Flux—platinum crucible, Hydrothermal—metal autoclave containing Fe, Ni, and Cu, possibly lined with silver, gold, or platinum.
[b]Produces a yellow fluorescence, which is usually absent in faceted material (Kane, 1983).
[c]Promotes the growth of facetable crystals.

lowing were not included in the study samples: material from localities not known to provide crystals suitable for faceting, synthetic rubies grown for experimental purposes only, and phenomenal rubies (e.g., star rubies). Although it is possible to obtain analyses of larger mounted stones with EDXRF, we did not include mounted samples.

Methods. We used a TN Spectrace 5000 EDXRF spectrometer for the chemical analyses. This instrument can detect the elements sodium (atomic number 11) through uranium (atomic number 92), using an X-ray tube voltage of up to 50 kV and a current of 0.01 mA to 0.35 mA. Two sets of analytical conditions were used to maximize sensitivity: for sodium (atomic number 11) through sulfur (atomic number 16)—a voltage of 15 kV, current of 0.15 mA, no filter, and a count time of 200 seconds; for chlorine (atomic number 17) through bromine (atomic number 35)—a voltage of 25 kV, current of 0.25 mA, 0.127 mm aluminum filter, and a count time of 200 seconds. Each sample was run once under the two separate instrument conditions, in order to generate one analysis.

We used the spectra derived from these procedures to obtain "semi-quantitative" data for the elements Al, Ca, Ti, V, Cr, Mn, Fe, and Ga using the Fundamental Parameters (FP) method of Criss and Birks (1968; see also Jenkins, 1980). (Oxygen was assumed present in stoichiometric proportions, and Fe is reported as FeO [i.e., +2 oxidation state]). In addition, the presence of heavier elements (e.g., Zr, Ni, Cu, Mo, lanthanum [La], tungsten [W], and lead [Pb]) was noted from the spectra, but these elements were not analyzed quantitatively. The samples were analyzed for Si; however, because of peak overlap with Al, results for Si were unreliable and are not reported in this study.

The following standards were used for calibration and to check the instrument's performance: colorless Czochralski-pulled synthetic corundum for Al; tsavorite garnet for Al and Ca; and almandine garnet for Al, Mn, and Fe. The compositions of the standards were quantitatively determined at the California Institute of Technology by Paul Carpenter using an electron microprobe.

We used a 3 mm diameter X-ray beam collimator to limit the beam size to about 20 mm^2. (However, the actual area analyzed varied depending on the size of the sample; on most, it was less than 20 mm^2.) This area was analyzed to a depth of approximately 0.1 mm. Whenever possible, we ori-

ented each sample to avoid prominent color zoning or conspicuous mineral inclusions. We usually analyzed the table facet; for some samples, we analyzed the pavilion. We did not include analyses if we suspected that the presence of diffraction peaks caused erroneous quantitative results.

Both the accuracy and the sensitivity of the analyses are affected by the size of the area analyzed, because this determines the number of counts obtained for a given element. Table 3 illustrates the differences in detection limits for rubies of three different sizes. In general, the detection limits decreased with increasing sample size. Above approximately 1 ct, there were only minor improvements in the detection limits.

The concentrations of each element in the sample are calculated from the counting statistics and the FP algorithm, and they are expressed as weight percent oxides. The number of counts determined for each element had to be normalized to 100% to compensate for the different sample sizes. Because the concentrations reported are not directly calculated from the peak counts, our analyses are considered semi-quantitative. For comparison purposes, we had five natural rubies from our study analyzed by Dr. W. B. Stern of the University of Basel using his EDXRF. Dr. Stern's results for these samples were very similar to our own. Based on multiple analyses of three of the samples used in this study, we found the repeatability of the trace-element data to be generally within 10%–20%.

RESULTS

Qualitative Results. *Synthetic Rubies.* The following elements were detected in all of the synthetic

---

TABLE 3. Variation in EDXRF detection limits according to sample size.[a]

Oxide (wt.%)	0.20 ct	0.65 ct	1.27 ct
Al_2O_3	0.15	0.13	0.06
Cr_2O_3	0.007	0.003	0.002
CaO	0.044	0.013	0.017
TiO_2	0.012	0.006	0.005
V_2O_3	0.009	0.004	0.003
MnO	0.011	0.005	0.003
FeO	0.005	0.002	0.001
Ga_2O_3	0.006	0.002	0.001

[a]*Calculated after Jenkins, 1980.*

---

ruby growth types (but not all samples) we examined: Ca, Ti, Cr, Mn, and Fe. Ga and V were also detected in the products of all specific manufacturers except the one Inamori sample we examined. The greatest variety of trace elements was detected in the flux-grown synthetics. In addition to the elements noted above, the Chatham flux synthetic rubies had Mo (six out of 21 samples), the Douros contained Pb (seven out of 15), and the Knischka samples showed W (five out of 14). La was seen only in Ramaura flux-grown synthetic rubies (12 out of 31), as previously reported by Schmetzer (1986b); Pt was also detected in one Ramaura synthetic ruby, Pb in four, and Bi (bismuth) in three. All of the flame-fusion synthetic rubies with flux-induced fingerprints revealed traces of Mo or Zr; otherwise, the melt-grown synthetics contained no trace elements other than those mentioned above. Traces of Ni were detected in 15 samples, and Cu in six samples, of the Tairus hydrothermal synthetic rubies (as previously reported by Peretti and Smith, 1993; Peretti et al., 1997; and Qi and Lin, 1998). One Tairus sample also contained cobalt, which we did not detect in any of the other synthetic or natural samples.

Natural Rubies. Traces of Ca, Ti, V, Cr, Mn, Fe, and Ga were noted in rubies from all of the localities we analyzed. Zr was detected in seven of the eight rubies analyzed from India, all of which contained numerous zircon inclusions. Cu was detected in one sample from Mong Hsu, Myanmar.

Semi-Quantitative Results. In addition to Al, the following elements were analyzed semi-quantitatively: Ca, Ti, V, Cr, Mn, Fe, and Ga. The natural rubies we examined typically contained a greater variety and higher quantity of these elements than the synthetics (tables 4 and 5; figures 5–8), which is consistent with the results reported by Kuhlmann (1983) and Tang et al. (1989).

Synthetic Rubies. Compared to many natural rubies, most of the synthetic samples contained little V and Ga (table 5; figures 5 and 6). In general, the melt-grown synthetic rubies contained the lowest concentrations of the elements listed above, especially Fe (figure 7; see also Box A). Two of the 10 flame-fusion samples had relatively high Ti (nearly 0.05 wt.% TiO_2; figure 8); one of these also contained relatively high V (nearly 0.02 wt.% V_2O_3), and the other contained the highest Cr level measured on the synthetics in this study (2.41 wt.% Cr_2O_3), with the exception of the red diffusion-treated corundum (see Box B). All the other synthetic rubies had Cr contents that ranged from about 0.07 to 1.70 wt.% Cr_2O_3, without any discernable trends. The floating-zone synthetic rubies were the only

	Basalt-hosted		Marble-hosted					Metasomatic	
Oxide (wt.%)	Cambodia (1)[b]	Thailand (15)	Afghanistan (15)	Mogok, Myanmar (19)	Mong Hsu, Myanmar (11)	Nepal (3)	Southern Yunnan (2)	Kenya (8)	Umba Valley, Tanzania (4)
Al_2O_3	99.09	98.91–99.25 (99.06)	96.39–99.66 (98.31)	98.73–99.67 (99.27)	96.83–99.25 (98.69)	99.51–99.60 (99.57)	98.48–99.28 (98.88)	95.13–99.63 (98.22)	97.94–98.23 (98.11)
Cr_2O_3	0.417	0.237–0.732 (0.419)	0.205–0.575 (0.350)	0.255–1.02 (0.562)	0.576–1.19 (0.887)	0.190–0.347 (0.260)	0.608–1.29 (0.950)	0.222–1.70 (0.675)	0.246–0.571 (0.372)
CaO	0.018	bdl–0.036 (0.023)	bdl–3.11 (0.784)	bdl–0.065 (0.029)	bdl–0.063 (0.030)	bdl–0.044 (0.025)	0.064–0.072 (0.068)	0.028–0.193 (0.068)	bdl–0.033 (0.023)
TiO_2	0.021	0.008–0.033 (0.020)	0.009–0.091 (0.045)	0.015–0.047 (0.026)	0.019–0.207 (0.078)	0.059–0.096 (0.080)	0.007–0.024 (0.016)	0.020–0.042 (0.033)	bdl–0.017 (0.009)
V_2O_3	0.004	bdl–0.007 (0.004)	bdl–0.016 (0.009)	0.028–0.171 (0.066)	0.024–0.104 (0.048)	0.014–0.024 (0.017)	0.017–0.022 (0.020)	0.003–0.048 (0.018)	0.002–0.006 (0.004)
MnO	0.003	0.003–0.008 (0.005)	bdl–0.005 (bdl)	bdl–0.013 (0.004)	bdl–0.012 (0.006)	bdl	0.005–0.014 (0.010)	bdl–0.009 (0.005)	0.003–0.007 (0.006)
FeO	0.439	0.299–0.722 (0.468)	0.009–0.133 (0.070)	0.006–0.080 (0.028)	bdl–0.022 (0.010)	0.012–0.038 (0.029)	0.012–0.072 (0.042)	0.005–0.040 (0.020)	1.21–1.67 (1.46)
Ga_2O_3	0.006	0.004–0.009 (0.005)	bdl–0.011 (0.006)	bdl–0.026 (0.012)	bdl–0.014 (0.009)	0.009–0.025 (0.018)	0.008–0.008 (0.008)	0.012–0.048 (0.033)	0.008–0.023 (0.014)

TABLE 4. Summary of natural ruby chemistry.[a]

[a]*Values shown are normalized wt.%. Minimum and maximum values are given, along with the average (in parentheses below each range). bdl = below detection limits (varies according to size of sample; see table 3).* [b]*Number of samples in parentheses.*
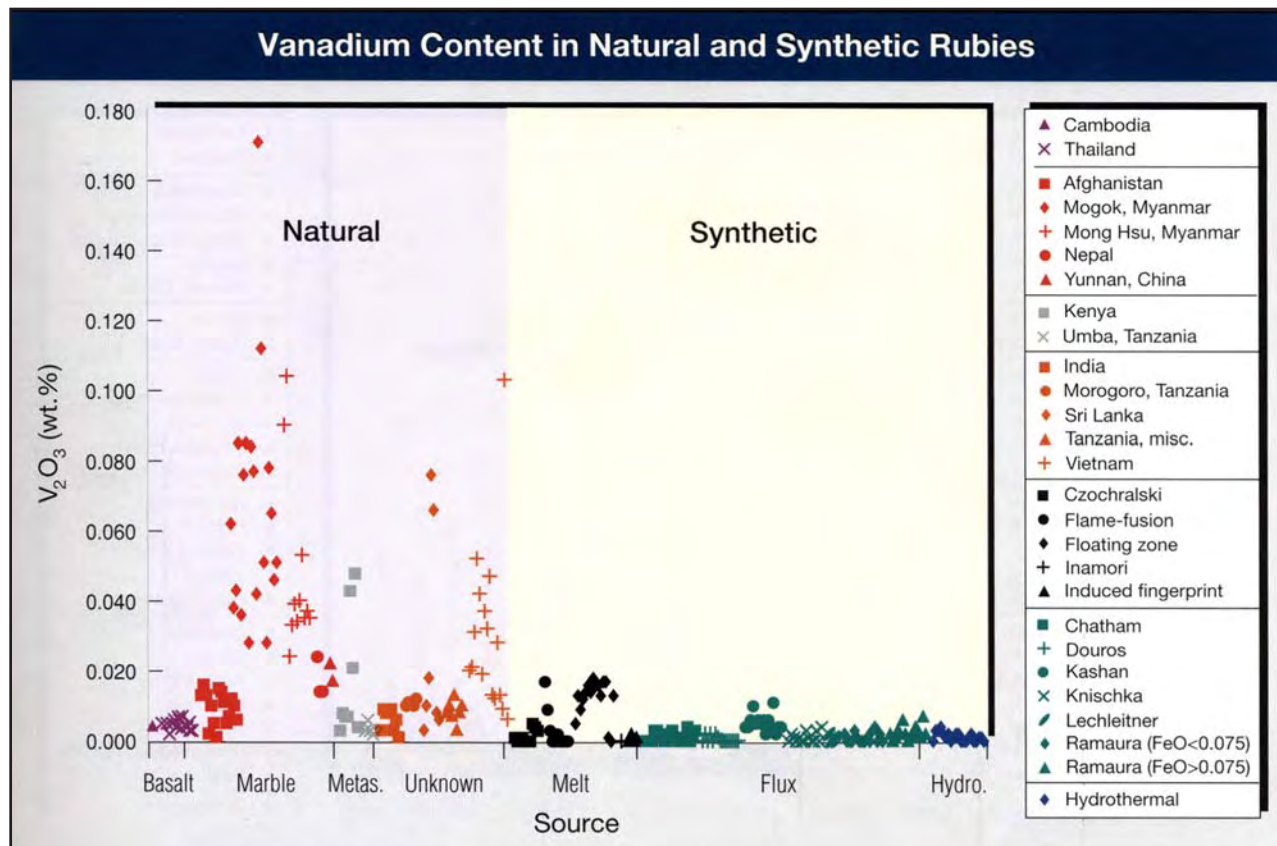
Figure 5. Most synthetic rubies contain little vanadium compared to natural rubies. In general, rubies from marble-hosted deposits contained the highest V content, although those from Afghanistan showed atypically low V. (Note that the Czochralski samples in these graphs are all produced by Union Carbide, as distinct from the Inamori Czochralski-pulled sample that was also analyzed.)

	Unknown deposit type				
India (8)	Morogoro, Tanzania (5)	Sri Lanka (7)	Tanzania, misc. (7)	Vietnam (16)
98.80–99.36 (99.10)	98.35–98.69 (98.52)	97.95–99.63 (99.14)	98.69–99.44 (99.08)	97.31–99.49 (98.70)
0.192–0.518 (0.358)	1.10–1.51 (1.30)	0.182–1.00 (0.327)	0.448–1.16 (0.713)	0.344–2.38 (1.01)
bdl–0.025 (bdl)	0.027–0.046 (0.035)	bdl–0.072 (0.024)	0.017–0.100 (0.052)	0.007–0.153 (0.062)
0.013–0.024 (0.017)	0.023–0.038 (0.032)	0.017–0.170 (0.083)	0.021–0.046 (0.031)	0.011–0.268 (0.071)
bdl–0.009 (0.006)	0.010–0.012 (0.011)	0.003–0.076 (0.027)	0.003–0.013 (0.008)	0.006–0.103 (0.030)
bdl–0.004 (0.002)	0.007–0.014 (0.010)	bdl–0.010 (0.003)	bdl–0.009 (0.004)	0.002–0.027 (0.011)
0.184–0.947 (0.502)	0.043–0.137 (0.093)	0.032–0.494 (0.178)	0.003–0.175 (0.098)	0.015–0.482 (0.103)
0.004–0.008 (0.007)	0.004–0.010 (0.007)	0.004–0.024 (0.011)	0.008–0.020 (0.013)	0.005–0.034 (0.014)

synthetic samples with a relatively high average V content (0.012 wt.% V_2O_3).

Variable trace-element contents were measured in the flux-grown synthetic rubies. The Chatham samples contained insignificant amounts of most trace elements, except for 0.024 wt.% Ga_2O_3 in one sample. The Douros synthetics contained elevated Fe (0.055–0.241 wt.% FeO), and the highest concentration of Ga of all the natural and synthetic rubies tested for this study (0.051–0.079 wt.% Ga_2O_3). The Kashan synthetic rubies showed very low Fe, and they had the most Ti of all the synthetics analyzed (0.042–0.174 wt.% TiO_2). One Knischka sample also contained elevated Ti (0.159 wt.% TiO_2), and another showed high Ga (0.071 wt.% Ga_2O_3). The Knischka synthetic rubies contained about the same amount of Fe as the Douros samples, with the exception of one Knischka sample that contained 1.15 wt.% FeO; this anomalous sample contained the greatest amount of Fe of all the synthetics analyzed. Ramaura synthetic rubies typically contained some Ga (up to 0.017 wt.% Ga_2O_3) and Fe
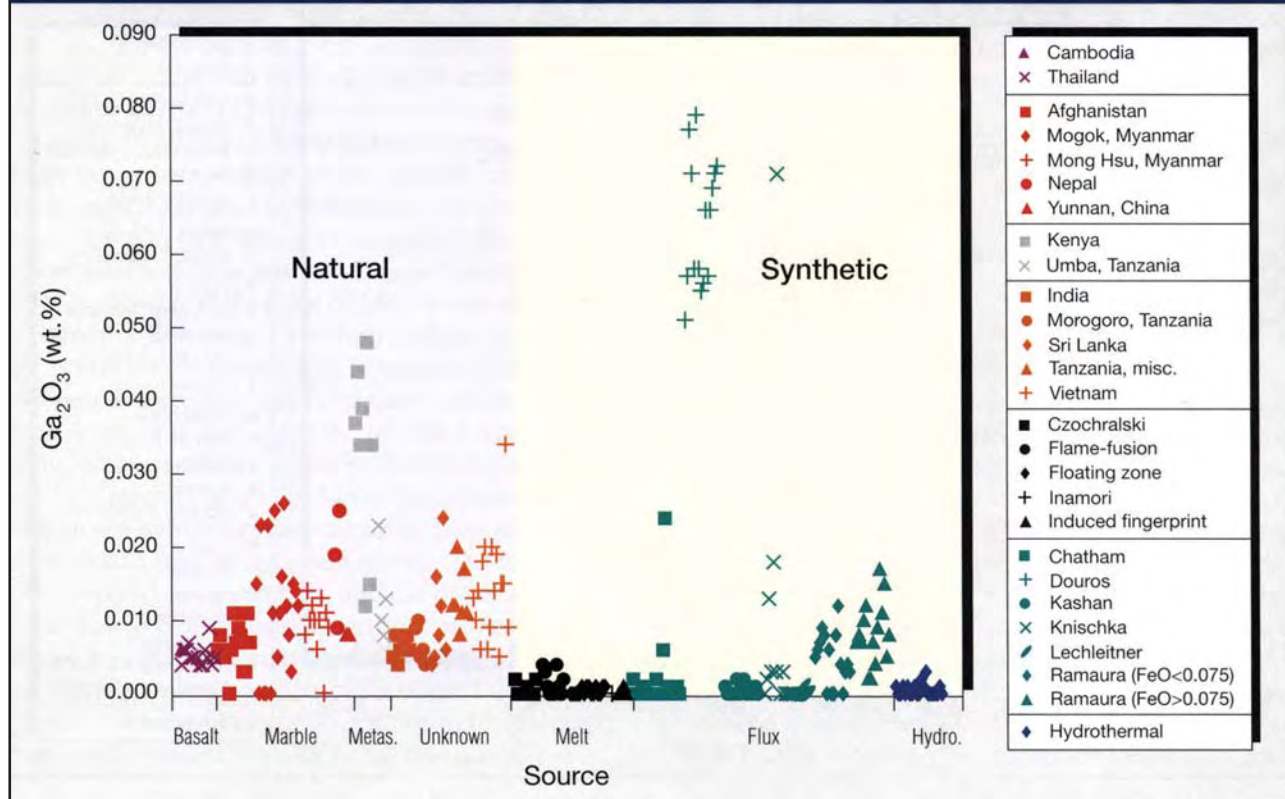
Figure 6. Gallium is another key trace element for separating natural from synthetic rubies. While fewer than one-seventh of the natural stones contained less than 0.005 wt.% Ga_2O_3, more than three-quarters of the synthetic samples did. However, Douros synthetic rubies (and one Knischka sample) were exceptions to this, with more than 0.050 wt.% Ga_2O_3.

TABLE 5. Summary of synthetic ruby chemistry.[a]

Oxide (wt.%)	Melt					Flux		
	Czochralski: Union Carbide (10)[e]	Flame-fusion (10)	Floating zone (16)	Czochralski: Inamori (1)[b]	Induced finger-print flame-fusion (4)	Chatham (21)	Douros (15)	Kashan (15)
Al_2O_3	98.67–99.34 (98.86)	97.47–99.80 (99.15)	99.08–99.59 (99.40)	99.37	98.25–99.40 (98.84)	98.22–99.53 (98.98)	98.06–99.79 (99.32)	99.32–99.77 (99.57)
Cr_2O_3	0.634–1.28 (1.08)	0.184–2.41 (0.788)	0.366–0.869 (0.521)	0.595	0.583–1.71 (1.12)	0.444–1.66 (0.956)	0.067–1.50 (0.484)	0.121–0.506 (0.291)
CaO	bdl–0.020 (bdl)	bdl–0.056 (0.034)	bdl–0.035 (0.024)	0.022	bdl–0.028 (0.018)	bdl–0.089 (0.040)	bdl–0.022 bdl	bdl–0.067 (0.023)
TiO_2	bdl–0.007 (0.002)	bdl–0.044 (0.013)	bdl–0.011 (bdl)	bdl	bdl–0.017 (0.009)	bdl–0.027 (0.009)	0.005–0.034 (0.013)	0.042–0.174 (0.096)
V_2O_3	bdl–0.005 bdl	bdl–0.017 (0.003)	bdl–0.018 (0.012)	bdl	bdl	bdl–0.004 (0.001)	bdl	bdl–0.011 (0.005)
MnO	0.004–0.010 (0.007)	bdl–0.014 (0.005)	bdl–0.005 (0.003)	0.007	0.003–0.014 (0.007)	bdl–0.010 (0.006)	bdl–0.009 (0.004)	bdl–0.015 (0.003)
FeO	0.001–0.005 (0.003)	0.002–0.019 (0.007)	bdl–0.038 (0.006)	0.005	0.002–0.008 (0.005)	0.004–0.018 (0.010)	0.055–0.241 (0.085)	0.001–0.016 (0.007)
Ga_2O_3	bdl–0.002 (0.001)	bdl–0.004 (0.002)	bdl–0.001 bdl	bdl	bdl–0.001 bdl	bdl–0.024 (0.002)	0.051–0.079 (0.064)	bdl–0.002 (0.001)

[a]Values are normalized wt.%. Minimum and maximum values are given, along with the average (in parentheses below each range). bdl= below detection limits (varies according to size of sample; see table 3).   [b]Number of samples in parentheses.
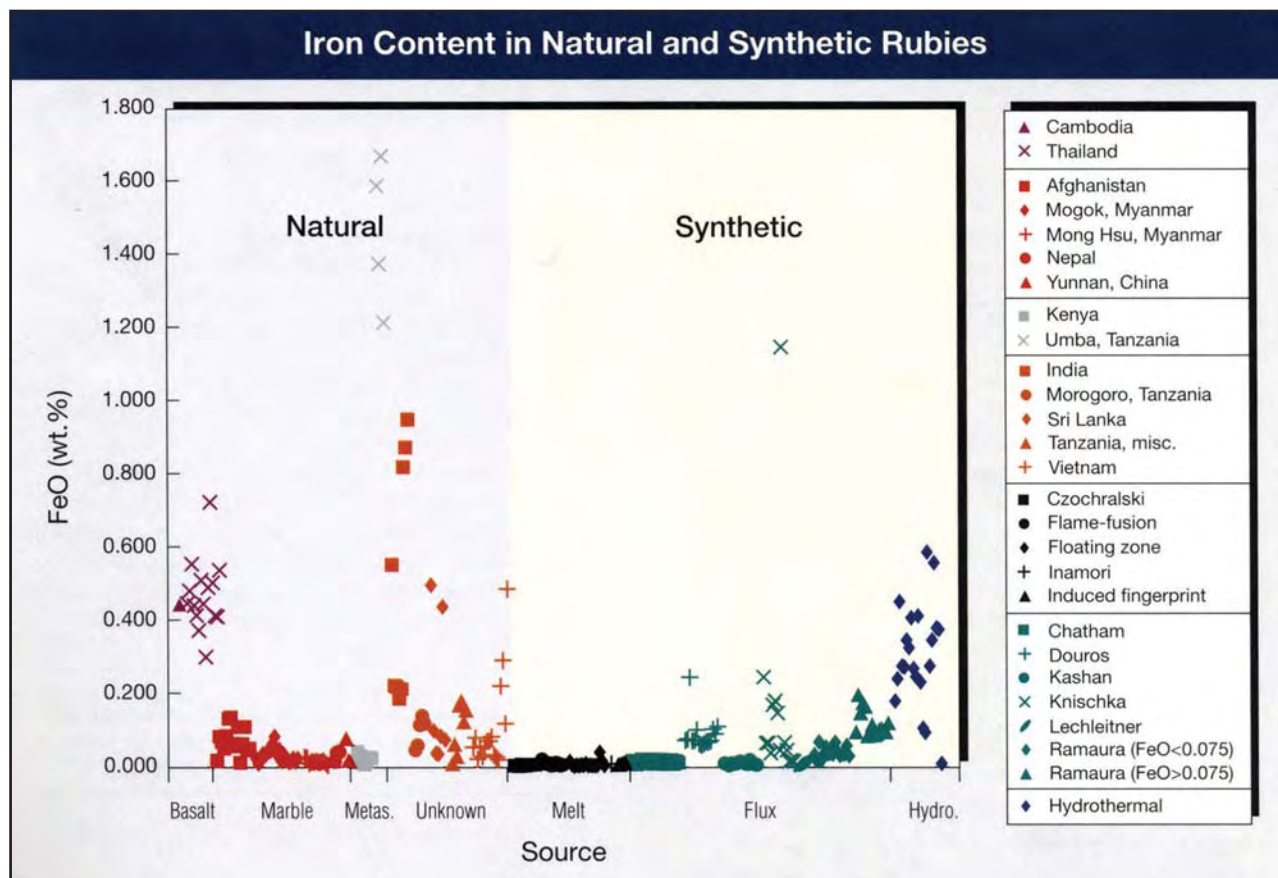
Figure 7. Iron is also useful for separating natural from synthetic rubies, especially when used in conjunction with vanadium. Only one of the melt-grown synthetic rubies and approximately half of the flux-grown synthetic rubies displayed an FeO content greater than 0.02 wt.%, while three-quarters of the natural stones did. Hydrothermal synthetic rubies had the highest overall Fe contents of the synthetics we analyzed.

	Flux (cont'd)			Hydrothermal
Knischka (14)	Lechleitner (4)	Ramaura[c] (FeO < 0.075) (15)	Ramaura[d] (FeO > 0.075) (15)	Tairus (21)
97.81–99.51 (98.97)	98.34–99.55 (99.00)	98.45–99.77 (99.23)	98.17–99.66 (99.01)	97.95–99.89 (98.51)
0.266–1.15 (0.690)	0.413–1.57 (0.933)	0.171–1.45 (0.688)	0.128–1.65 (0.822)	0.084–1.74 (1.12)
bdl–0.104 (0.034)	bdl–0.046 (0.031)	bdl–0.061 (0.033)	bdl–0.065 (0.039)	bdl–0.054 (0.030)
bdl–0.159 (0.023)	0.011–0.044 (0.026)	bdl–0.012 bdl	bdl–0.010 bdl	0.007–0.034 (0.023)
bdl–0.004 bdl	bdl	bdl–0.004 bdl	bdl–0.007 bdl	bdl–0.004 bdl
bdl–0.013 (0.006)	0.003–0.015 (0.008)	0.002–0.014 (0.006)	bdl–0.011 (0.005)	BDL–0.015 (0.008)
0.012–1.15 (0.159)	0.004–0.008 (0.006)	0.014–0.065 (0.037)	0.079–0.192 (0.112)	0.006–0.584 (0.302)
bdl–0.071 (0.008)	bdl–0.001 bdl	bdl–0.012 (0.005)	0.002–0.017 (0.008)	bdl–0.003 (0.001)

[c] Includes all "Burma tone" samples.
[d] Includes all "Thai tone" samples.

(0.014–0.192 wt.% FeO), with those Ramaura synthetic rubies marketed as "Thai tone" richer in Fe than those marketed as "Burma tone."

The Tairus hydrothermal synthetic rubies contained relatively high Fe (up to 0.584 wt.% FeO) and traces of Ti (up to 0.034 wt.% TiO_2).

Natural Rubies. In general, there was greater variability in the trace-element chemistry of the natural rubies than of the synthetics, but there were also some distinct trends according to geologic occurrence. Basalt-hosted rubies were the most consistent: Samples from Thailand and Cambodia showed relatively high Fe (0.299–0.722 wt.% FeO) and low V (up to 0.007 wt.% V_2O_3). Marble-hosted rubies showed the opposite trend: low Fe (up to 0.133 wt.% FeO) and high V (typically 0.02–0.09 wt.% V_2O_3), with the exception of Afghan rubies, which showed low V contents (less than 0.02 wt.% V_2O_3). The Afghan rubies contained the highest levels of Ca measured in this study (up to 3.11 wt.% CaO). Rubies from Myanmar contained the most V measured in this study (up to 0.171 wt.% V_2O_3). Some
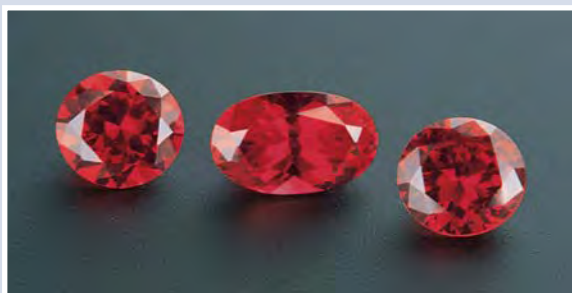
Mong Hsu samples contained up to 0.207 wt.% TiO_2 (high Ti was also reported by Smith and Surdez [1994] and Peretti et al. [1995]).

The rubies from metasomatic deposits showed wide variations in composition. Samples from Umba in Tanzania had the greatest Fe measured in this study (1.21–1.67 wt.% FeO), combined with low V and Ti. Rubies from Kenya, however, showed low Fe and the most Ga (0.12–0.48 wt.% Ga_2O_3) measured in the natural samples.

DISCUSSION

Chemical Variations in Synthetic and Natural Rubies. *Synthetic Rubies.* Verneuil's original flame-fusion process required that the feed powder used be free of Fe, since Fe caused the boule to turn brown (Verneuil, 1904; Nassau, 1980). Today's melt-grown products are still essentially Fe-free, and they typically contain none or very small amounts of other elements besides Cr. Flux-grown synthetic rubies revealed the most trace elements, which is consistent with the variety of fluxes used to manufacture these synthetics (again, see table 2). Li, F, Na, Al, Mo, Ta (tantalum), W, Pb, or Bi may be present in the flux in which these rubies were grown or treated (for synthetic rubies with "induced fingerprints") [Schmetzer, 1986a,b, 1987; Schmetzer and Schupp, 1994; Kammerling et al., 1995a]. Lanthanum has been used experimentally to help grow crystals with rhombohedral rather than flat, tabular habits
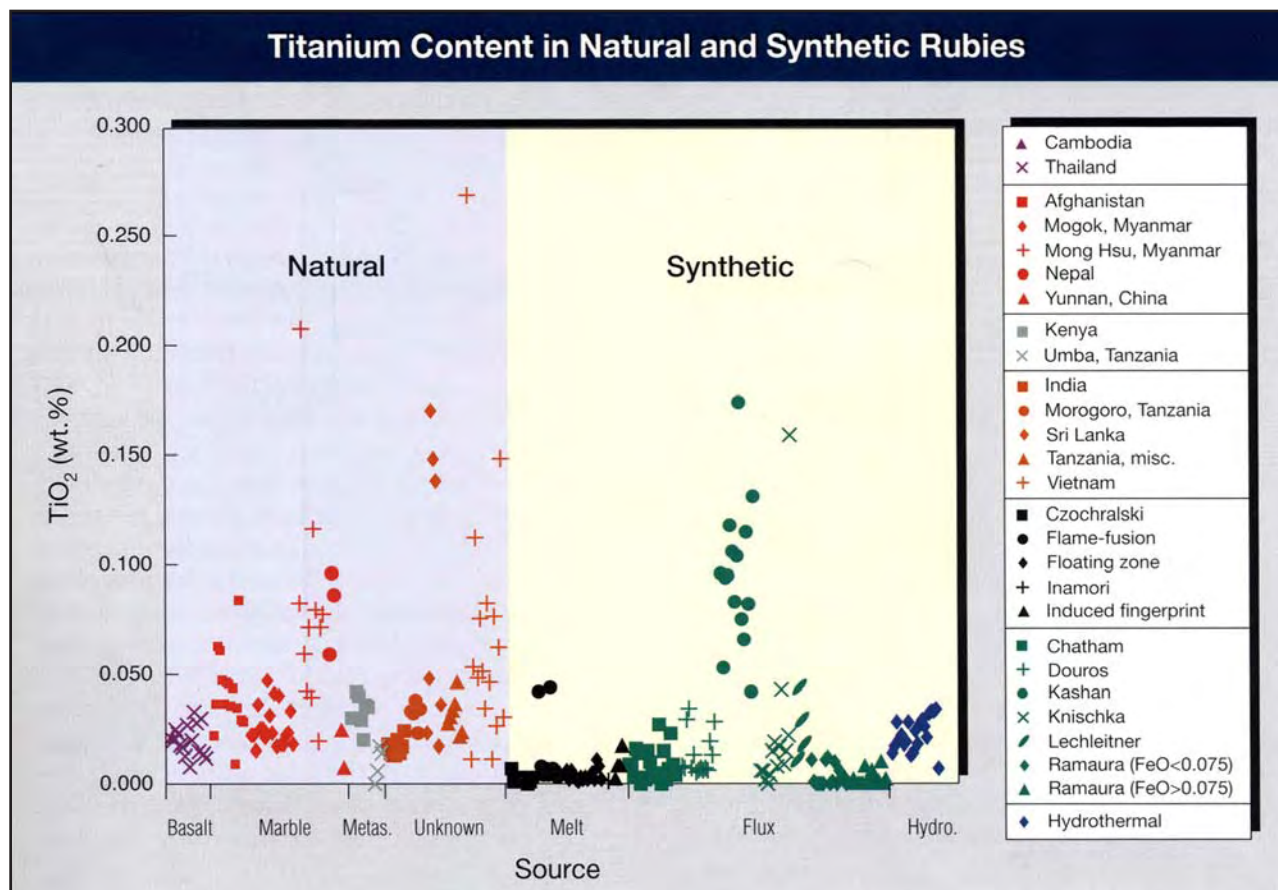
Figure 8. Natural rubies contain, on average, more titanium than synthetic rubies, but there was significant overlap in this study. Therefore, Ti alone is not useful for separating most natural from synthetic rubies. Among the synthetic rubies we analyzed, the Kashan samples had the highest Ti contents, while melt-grown and some flux-grown synthetics had the lowest.

(Chase, 1966), which significantly increases cutting yield from the rough. Because their charges and atomic radii are different from Al^{3+}, some of the elements detected (e.g., Mo, La, W, Pt, Pb, and Bi) do not readily enter the corundum structure. It is interesting to note, therefore, that the samples in which these elements were detected had no flux inclusions visible with 63$\leftrightarrow$ magnification. In the Tairus hydrothermal samples, the Fe, Ni, and Cu that we detected were probably derived from the autoclave in which they were grown (see, e.g., Peretti and Smith, 1993).

Natural Rubies. Some of the elements detected in the natural rubies (i.e., Ca and Zr) do not readily substitute for Al^{3+} in the corundum crystal structure, and were probably present in mineral inclusions. The Afghan rubies, in particular, contained abundant inclusions, and these samples showed elevated amounts of Ca. Zr was detected in those Indian samples that contained abundant zircon

inclusions. The other trace elements measured in the natural samples (Fe, V, Ti, and Ga) can substitute for Al^{3+}, and their abundance reflects the geologic environment of formation (see below).

Distinguishing Natural from Synthetic Ruby. According to this study, the presence of Mo, La, W, Pt, Pb or Bi proves that a ruby is synthetic. Ni and Cu suggest synthetic origin; however, both of these elements could be present in sulfide inclusions within natural rubies, and Cu has been detected in natural rubies (Kuhlmann, 1983; Osipowicz et al., 1995; Sanchez et al., 1997).
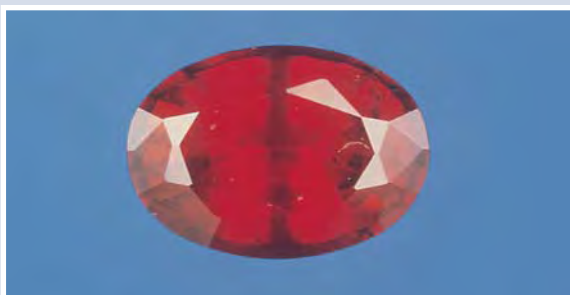
Although no single trace element proves natural origin, trace-element assemblages can provide the distinction for nearly all samples. Many of the synthetic rubies contained low amounts of Fe (<0.02 wt.% FeO), whereas most of the natural stones had more than 0.02 wt.% FeO (again, see figure 7 and table 4). Tairus hydrothermal synthetic rubies contained elevated Fe, but the common presence of Ni

BOX B: TRACE-ELEMENT CHEMISTRY OF
RED DIFFUSION-TREATED CORUNDUM

In the diffusion-treatment process, faceted pale-colored to colorless corundum is embedded in a powder that consists of aluminum oxide and color-causing trace elements, within an alumina crucible. Prolonged heating of the crucible to high temperatures (usually 1600°–1850°C) causes the chemicals to diffuse into a thin outer layer of treated color over the entire surface of the stone. Blue diffusion-treated corundum first appeared in the late 1970s, although it did not become widely available until 1989 (Kane et al., 1990). Red diffusion-treated corundum was introduced in the early 1990s (McClure et al., 1993; figure B-1).

Although diffusion treatment initially caused a great deal of concern in the jewelry trade, it is relatively easy to identify with standard gemological techniques. When observed in immersion with diffused transmitted light, diffusion-treated corundum displays uneven or patchy coloration, color concentration along facet junctions, and a high relief when compared to natural or synthetic stones. Other identifying features include spherical voids in the diffusion layer, dense concentrations of very small white inclusions just under the surface, and anomalous refractive index readings—including different readings from different facets and some R.I. values over the limit of the refractometer (McClure et al., 1993).

In the event, however, that a deeper diffusion layer is achieved, perhaps making some of these identifying features less obvious, we decided to include red diffusion-treated corundum in this study to determine the effectiveness of EDXRF analysis in making this separation. Because the color of a diffusion-treated stone is present only in a thin surface layer, this layer has to be significantly darker than a similarly colored natural or synthetic ruby to achieve an equivalent depth of color. Thus, the layer of diffused color must have a high Cr concentration. To document this characteristic, we analyzed 23 samples from a number of sources using EDXRF (table B-1). The analyses revealed high to extremely high Cr contents (2.72–13.16 wt.% Cr_2O_3). In fact, the diffusion-treated sample with the least amount of Cr contained even more of this element than any of the other samples analyzed for this study; the next-highest Cr content (2.41 wt.% Cr_2O_3) was measured in a flame-fusion synthetic ruby. The enriched Cr concentrations measured in diffusion-treated corundum probably cause the anomalously high R.I. readings that are commonly measured on this material (see, e.g., McClure et al., 1993).

Figure B-1. EDXRF analyses of red diffusion-treated corundums such as this 2.55 ct stone showed that this material had a higher Cr content than any of the other samples examined for this study.

TABLE B-1. Trace-element chemistry of red diffusion treated corundum.

Oxide (wt.%)	Min.	Max.	Average[a]	Std. Dev.[b]
Al_2O_3	85.85	96.92	92.30	3.06
Cr_2O_3	2.72	13.16	7.13	2.81
CaO	0.011	0.283	0.087	0.087
TiO_2	0.004	0.478	0.215	0.149
V_2O_3	bdl	0.010	0.002	0.003
MnO	bdl	0.035	0.006	0.011
FeO	0.077	0.501	0.188	0.153
Ga_2O_3	bdl	0.023	0.011	0.005

[a]Average of 23 samples.
[b]By definition, about two-thirds of the analyses will fall within one standard deviation of the average.

Iron vs. Vanadium Content in Natural and Synthetic Rubies

Figure 9. This graph of FeO content vs. V_2O_3 content illustrates the usefulness of these elements in making the separation between natural and synthetic rubies, even though there is some overlap between these populations. Most of the synthetic samples cluster near the origin of the diagram (due to their lower Fe and V contents), while the natural samples plot further from the origin and also display greater variations in their contents of Fe or V.
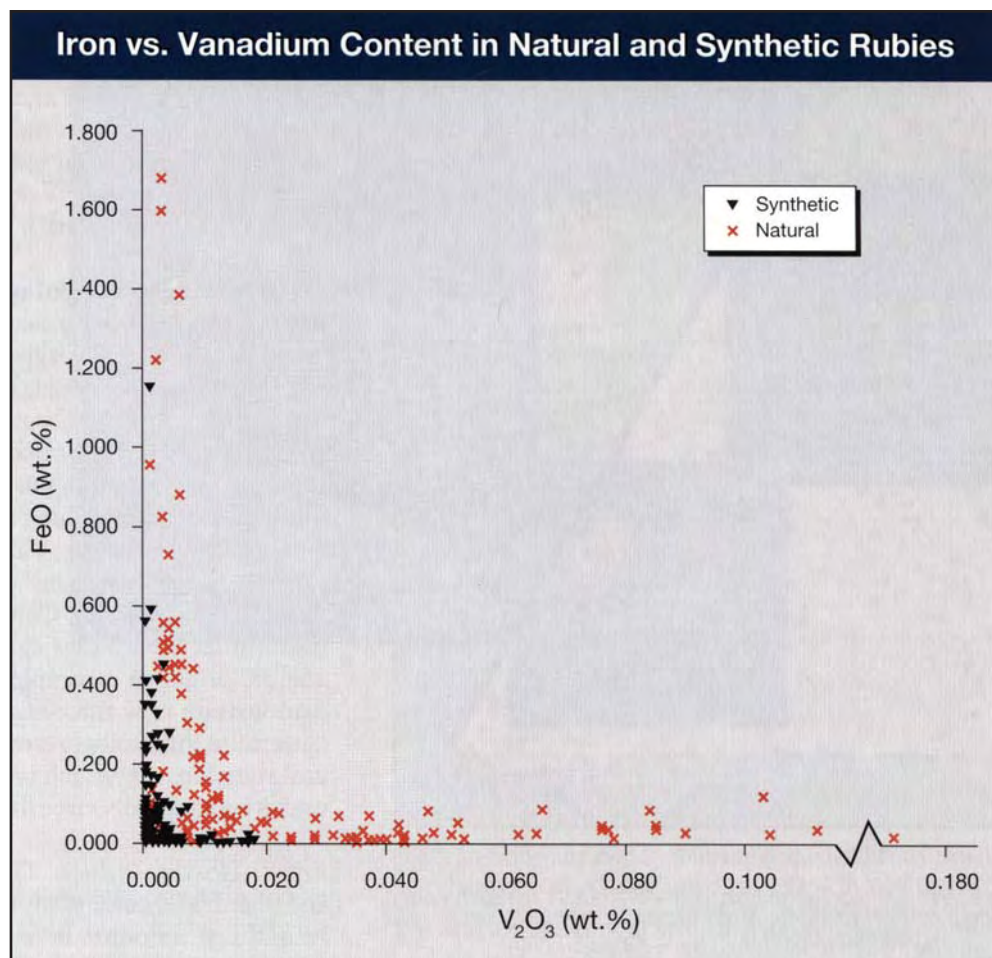
and Cu, combined with a lack of V and Ga, identifies them as synthetic.

Relatively high concentrations of V were measured in the natural rubies. Few of the synthetic rubies we examined contained detectable amounts of V, which is consistent with the findings of Kuhlmann (1983) and Tang et al. (1989). However, a low V content is not proof of synthetic origin, since several of the natural rubies we analyzed contained relatively low V (again, see figure 5). Nevertheless, many synthetics, especially melt products, can be identified by their relative lack of both Fe and V (figure 9). In contrast to the synthetics, natural rubies contained a broad range of Fe and V contents. Therefore, with the exception of one anomalous (Knischka) sample, the data for synthetics are clustered below 0.60 wt.% FeO, and 0.02 wt.% V_2O_3, toward the corner of the graph in figure 9.

Although most synthetics contained very little Ga—and in many cases, none—a few samples (i.e., Ramaura, Knischka, and Chatham) showed Ga contents similar to those recorded in natural samples

(again, see figure 6). Douros synthetic rubies have a consistently high Ga content, which is unique among both synthetic and natural rubies. In our analyses, a concentration above 0.050 wt.% Ga_2O_3 with some Fe, little or no Ti, and no V strongly indicates Douros as the source. When Ga is plotted together with V and Fe in a triangular diagram (figure 10), further distinctions can be made. The triangular V-Fe-Ga diagram shows a ratio of these three elements, rather than their actual concentrations. Many of the synthetics plot near the edges of the triangle. These samples are distributed fairly evenly between the V and Fe apexes (i.e., little or no Ga, variable Fe/V ratio), or extend halfway from Fe to the Ga apex (i.e., little or no V, variable Fe/Ga ratio with Fe>Ga). The natural samples, by contrast, are distributed throughout much of the triangle. Within the triangle, the considerable overlap in the region between the Fe and V apexes is due mostly to the Ga-enriched composition of the Douros synthetic rubies.

Synthetic rubies generally contain less Ti than
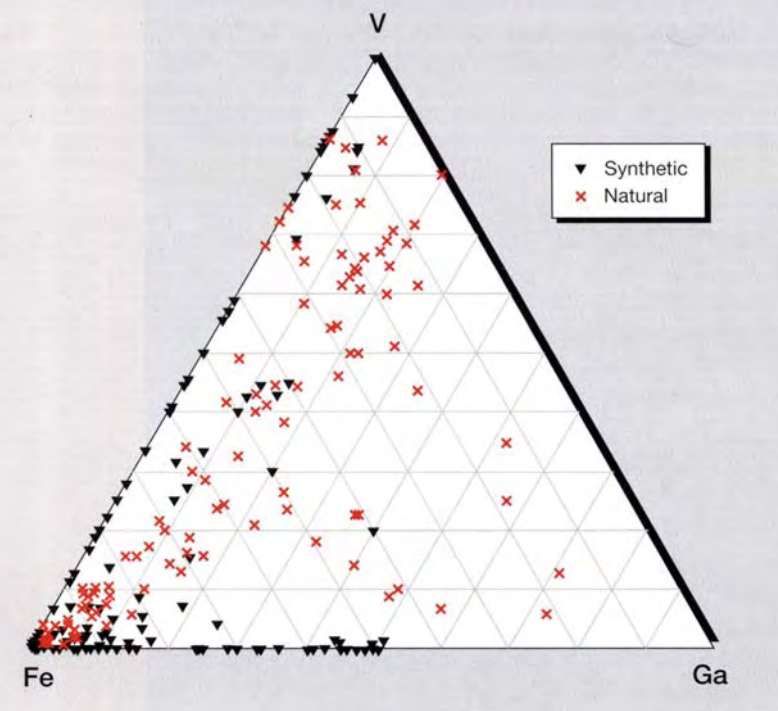
V-Fe-Ga Diagram: Natural vs. Synthetic

Figure 10. This triangular plot shows the ratio of the contents of V_2O_3, FeO, and Ga_2O_3 in natural and synthetic rubies. Most of the synthetics plot near the Fe apex or along the V-Fe and Fe-Ga edges, reflecting the low V and Ga contents. Natural stones plot throughout the area of the triangle, which is consistent with their more complex trace-element chemistry.

do natural rubies (again, see figure 8), although there is a large overlap between the natural stones and the flux and hydrothermal synthetics. Therefore, we did not find Ti alone useful for separating natural from synthetic rubies. Kashan synthetic rubies have a high Ti content (>0.042 wt.% TiO_2; table 4), but low V, Fe, and Ga concentrations. This distinctive chemistry makes it easy to identify most Kashan rubies by EDXRF.

We did not find Cr to be useful for separating natural from synthetic rubies. However, red diffusion-treated corundum consistently shows high to extremely high concentrations of Cr, which is diagnostic (see Box B).

Even if abundant chemical evidence is available, it is important to combine chemical data with standard gemological observations when making a ruby identification. For example, one flame-fusion synthetic contained 0.017 wt.% V_2O_3, as well as a sig-

nificant amount of Ti and some Fe. Attempting to determine this ruby's origin based on trace-element chemistry alone would lead one to erroneously conclude that the sample was natural, yet curved striae were clearly visible with a microscope.

Determining the Geologic Origin of a Natural Ruby. Using EDXRF trace-element data, we could often determine the type of geologic deposit in which a stone originated, but not its specific locality (table 4). However, optical microscopy, growth structure analysis, and laser Raman microspectroscopy studies have provided useful data on the internal features that are present in rubies from various localities (see, e.g., Gübelin, 1974; Gübelin and Koivula, 1986; Delé-Dubois et al., 1993; Peretti et al., 1995; Smith, 1996). Combining EDXRF data with these other techniques can help establish the geographic origin of a sample. Our purpose here is to demonstrate how trace-element chemistry can help determine the geologic environment in which a natural ruby formed, which is one step toward identifying its geographic source (figure 11).

Basalt-Hosted Rubies. The rubies from Thailand and Cambodia contained relatively high contents of Fe and low amounts of V. Although the formation conditions of basalt-hosted rubies are not well known, the compositions of associated minerals and mineral inclusions are consistent with the Fe-rich compositional trends measured in this study. In a triangular plot of V-Fe-Ga, the basalt-hosted rubies form a tight cluster at the Fe apex (i.e., high Fe, little or no Ga or V; figure 12).

Marble-Hosted Rubies. A low Fe content characterized the rubies from Afghanistan, Myanmar, Nepal, and China (southern Yunnan), and is consistent with the Fe-deficient geochemistry of the host marbles. With the exception of Afghanistan, the marble-hosted rubies contained high amounts of V (table 4, figure 5). Elevated V contents are consistent with the fact that this element, like Cr, is concentrated into clays during weathering and the formation of residual bauxites (Wedepohl, 1978), which are thought to account for the aluminous layers in ruby-bearing marbles (see, e.g., Okrusch et al., 1976). Most of the marble-hosted rubies plot in a diagnostic area within figure 12, toward the V apex (i.e., V>Fe and V>Ga). Afghan rubies are an exception, however; because they contain relatively low V compared to Fe, some samples plot near the Fe apex.

Figure 11. In some gem markets, the geographic origin is an important consideration toward its value. EDXRF analysis can help establish the geologic origin in many cases. Shown here (clockwise from the left) are: a crystal from Mogok, Myanmar (Hixon ruby, 196.1 ct; specimen courtesy of the Los Angeles County Museum of Natural History, photo © Harold a & Erica Van Pelt), a 2.98 ct step cut from Thailand (photo © Tino Hammid), a round brilliant from Myanmar (stone courtesy of Amba Gem Corp., New York; photo © Tino Hammid), and an 8.33 ct oval brilliant from Sri Lanka (photo courtesy of ICA/Bart Curren).

Metasomatic Rubies. As one would expect from the variable composition of their host rocks, metasomatic rubies have widely varying trace-element chemistries. This was apparent in our samples. Rubies from Kenya plotted over a wide area of the V-Fe-Ga diagram (figure 12). Two of the analyses overlapped with the field of marble-hosted rubies, while the remainder of the samples plotted in a distinctive area closer to the Ga apex (i.e., Ga>Fe and Ga>V). Because of their enriched Fe content, the Umba rubies plotted within the field for basalt-hosted rubies. Overall, the variable composition of rubies from metasomatic deposits makes separation by trace elements alone ambiguous. However, if such data are combined with gemological observations (e.g., the presence of carbonate inclusions in marble-hosted rubies), then a more meaningful distinction between deposit types could be made.

CONCLUSION

Trace-element chemistry as provided by EDXRF spectrometry is effective for separating natural and synthetic rubies. It can also help determine the deposit type of a natural ruby. Because of the chemistry of the laboratory growth environment, certain trace elements are diagnostic of a synthetic product. Ni, Cu, Mo, La, W, Pt, Pb, and Bi were found only in synthetic rubies. When present, Mo, La, W, Pt, Pb, and Bi are diagnostic of flux synthetic rubies, and Ni and Cu are indicative of (Tairus) hydrothermal synthetic rubies. In those cases where these elements are not detected, the concentrations of Ti, V, Fe, and Ga provide a means for separating nearly all natural stones from synthetic rubies. Generally, the natural stones in our study contained higher concentrations of these four elements than the synthetics.

However, it is important that a sample's entire trace-element signature be considered when attempting this separation. For example, the presence of significant amounts of V should not be considered proof of natural origin, since some melt-grown synthetic rubies contained V in amounts similar to those typically seen in natural stones. Furthermore, trace-element chemistry should be used in conjunction with traditional gemological methods, because a few synthetic rubies had trace-element assemblages that suggested a natural origin.

Trace-element chemistry can also help determine the geologic origin of a sample, although for these distinctions, too, EDXRF should be used in conjunction with traditional methods such as microscopy. Rubies from basalt-hosted deposits typically contained little V and moderate to high Fe. The opposite trends were seen in rubies from mar-

V-Fe-Ga Diagram: Deposit Type

Basalt-hosted
▲ Cambodia
✕ Thailand

Metasomatic
■ Kenya
✕ Umba, Tanzania

Marble-hosted
■ Afghanistan
◆ Mogok
+ Mong Hsu
● Nepal
▲ Yunnan, China
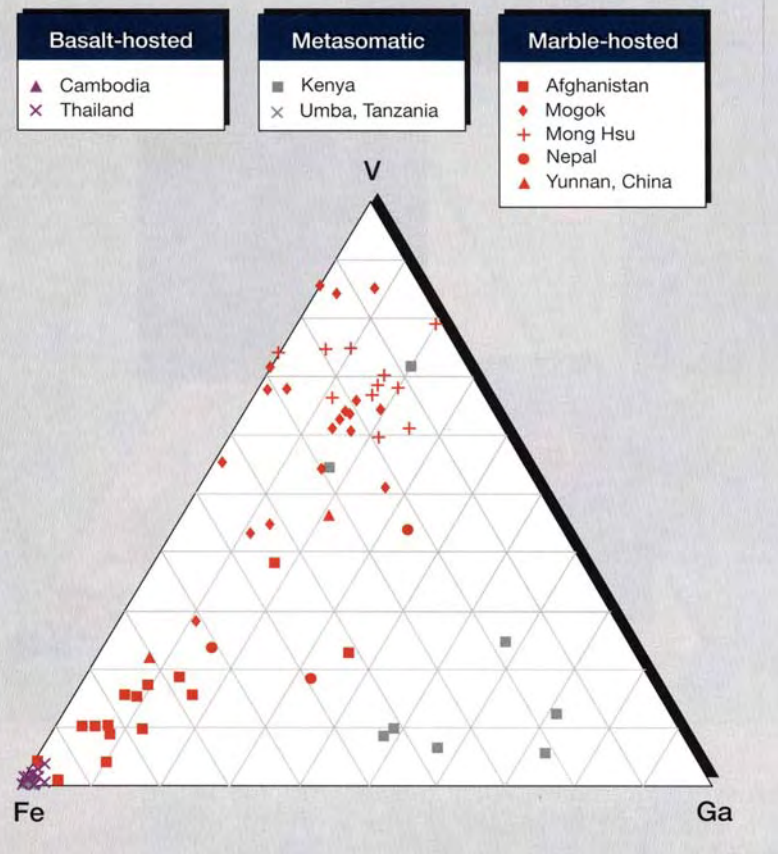
Figure 12. Natural rubies from different deposit types are plotted on this V-Fe-Ga diagram. All of the rubies from basalt-hosted deposits plot near the Fe apex, due to their high-Fe, low-V contents. Most of the marble-hosted rubies plot closer to the center of the diagram, toward the V apex; however, due to their low V contents, the marble-hosted Afghan rubies plot closer to the Fe apex. Metasomatic rubies are less systematic due to their variable growth environment: Some plotted near the Fe apex (Umba), whereas others showed a wide distribution (Kenya).

ble-hosted deposits. Rubies from metasomatic deposits, however, displayed a wide variety of trace-element chemistries, so it may be difficult to establish origin for some of these stones. Combining trace-element chemistry with traditional gemological methods, such as microscopy, will strengthen the means for determining the geographic origin of rubies.

Difficulties with separating natural from synthetic rubies using traditional gemological techniques will, in all likelihood, persist in the future, as

producers continue to improve the quality of their product or possibly change the trace-element contents. As rubies from new localities, new manufacturers, or new processes are introduced to the market, they will have to be characterized to keep this database current. It should be recognized that although trace-element chemistry can correctly separate nearly all natural and synthetic rubies, it does not substitute for careful gemological measurements and observations. Rather, chemical analysis provides a useful supplement to standard gemological techniques for ruby identification.

REFERENCES

Acharya R.N., Burte P.P., Manohar S.B. (1997) Multielement analysis of natural ruby samples by neutron activation using the single comparator method. *Journal of Radioanalytical and Nuclear Chemistry*, Vol. 220, No. 2, pp. 223–227.

Bank H., Okrusch M. (1976) Über Rubinvorkommen in Marmoren von Hunza (Pakistan). *Zeitschrift der Deutschen Gemmologischen Gesellschaft*, Vol. 25, No. 2, pp. 67–85.

Bowersox G.W., Chamberlin B.E. (1995) Ruby (Yakut) and sapphire (Yakut Habut) deposits of Jegdalek and Gandamak. In *Gemstones of Afghanistan*, Geoscience Press, Tucson, AZ, pp. 95–119.

Bridges C.R. (1982) *Gemstones of East Africa*. In D. M. Eash, Ed., *Proceedings of the International Gemological Symposium*, Gemological Institute of America, Santa Monica, CA, pp. 263–275.

Brown G. (1996) ? Reconstructed rubies of South African origin. *South African Gemmologist*, Vol. 10, Nos. 2 and 3, pp. 33–35.

Brown G., Kelly S.M.B. (1989) Knischka-created rubies. *Australian Gemmologist*, Vol. 17, No. 5, pp. 199–204.

Charaljavanaphet J. (1951) Gem deposits at Bo Na-Wong, Tok-Phrom, Bo-Rai in Chanthaburi and Trat Provinces and Bo Phloi in Kanchanaburi Province. *Geologic Reconnaissance of the Mineral Deposits of Thailand*, U.S. Geological Survey Bulletin 984, pp. 148–150.

Chase A.B. (1966) Habit modification of corundum crystals grown from molten PbF_2-Bi_2O_3. *Journal of the American Ceramics Society*, Vol. 49, No. 5, pp. 233–236.

Coenraads R.R. (1992) Surface features on natural rubies and sapphires derived from volcanic provinces. *Journal of Gemmology*, Vol. 23, No. 3, pp. 151–160.

Coenraads R.R., Vichit P., Sutherland F.L. (1995) An unusual sapphire-zircon-magnetite xenolith from the Chanthaburi gem province, Thailand. *Mineralogical Magazine*, Vol. 59, pp. 465–479.

Criss J.W., Birks L.S. (1968) Calculation methods for fluorescent X-ray spectrometry. *Analytical Chemistry*, Vol. 40, No. 7, pp. 1080–1086.

Dahanayake K. (1985) Modes of occurrence and provenance of gemstones of Sri Lanka. *Mineralium Deposita*, Vol. 15, pp. 81–86.

Dahanayake K., Ranasinghe A.P. (1981) Source rocks of gem materials: A case study from Sri Lanka. *Mineralium Deposita*, Vol.. 16, pp. 103–111.

Dahanayake K., Ranasinghe A.P. (1985) Geology and mineralogy of gemming terrains of Sri Lanka. *Bulletin of the Geological Society of Finland*, No. 57, Part 1–2, pp. 139–149.

Delé-Dubois M.-L., Fournier J., Peretti A. (1993) Rubis du Vietnam. *Revue de Gemmologie a.f.g.*, No. 114, pp. 7–10.

Galia W. (1987) Eine neue Generation synthetischer Rubine von P.O. Knischka unter Verwendung natürlicher Nährsubstanz. *Zeitschrift der Deutschen Gemmologischen Gesellschaft,* Vol. 36, No. 1/2, pp. 19–31.

Gübelin E. (1971) New analytical results of the inclusions in Siam rubies. *Journal of Australian Gemmology*, Vol. 12, No. 7, pp. 242–252.

Gübelin E. (1974) *Internal World of Gemstones*, ABC Edition, Zurich, Switzerland.

Gübelin E. (1982) Die Edelsteinvorkommen Pakistans—1. Teil: Die Rubine aus dem Hunzatal. *Lapis,* Vol. 7, No. 5, pp. 19–26.

Gübelin E.J., Koivula J.I. (1986) *Photoatlas of Inclusions in Gemstones*, ABC Edition, Zurich, Switzerland.

Gunawardene M., Rupasinghe M.S. (1986) The Elahera gem field in central Sri Lanka. *Gems & Gemology*, Vol. 22, No. 2, pp. 80–95.

Guo J., O'Reilly S.Y., Griffin W.L. (1996a) Corundum from basaltic terrains: A mineral inclusion approach to the enigma. *Contributions to Mineralogy and Petrology*, Vol. 122, pp. 368–386.

Guo J., O'Reilly S.Y., Griffin W.L. (1996b) Zircon inclusions in corundum megacrysts: I. Trace element geochemistry and clues to the origin of corundum megacrysts in alkali basalts. *Geochimica et Cosmochimica Acta*, Vol. 60, No. 13, pp. 2347–2363.

Hänni H.A. (1987) On corundums from Umba Valley, Tanzania. *Journal of Gemmology*, Vol. 20, No. 5, pp. 278–284.

Hänni H.A. (1993) A new synthetic ruby from Greece poses challenges for gemologists. *Rapaport Diamond Report*, Vol. 16, No. 30, pp. 27–28.

Hänni H.A., Schmetzer K. (1991) New rubies from the Morogoro area, Tanzania. *Gems & Gemology*, Vol. 27, No. 3, pp. 156–167.

Hänni H.A., Schmetzer K., Bernhardt H.J. (1994) Synthetic rubies by Douros: A new challenge for gemologists. *Gems & Gemology*, Vol. 30, No. 2, pp. 72–86.

Hänni H.A., Stern W.B. (1982) Über die gemmologische Bedeutung des Gallium-Nachweises in Korunden. *Zeitschrift der Deutschen Gemmologischen Gesellschaft*, Vol. 31, No. 4, pp. 255–261.

Harder H. (1969) Farbgebende Spurenelemente in den natürlichen Korunden. *Neues Jahrbuch für Mineralogie Abhandlungen*, Vol. 110, No. 2, pp. 128–141.

Harding R.R., Scarratt K. (1986) A description of ruby from Nepal. *Journal of Gemmology*, Vol. 20, No. 1, pp. 3–10.

Henn U. (1991) Burma-type rubies from Vietnam. *Australian Gemmologist*, Vol. 17, No. 12, pp. 505–509.

Henn U. (1994) A new type of synthetic ruby from Russia. *Australian Gemmologist*, Vol. 18, No. 11, pp. 362–364.

Henn U., Bank H. (1990) A gemological examination of ruby from Vietnam. *ICA Gazette*, November, pp. 9–10.

Henn U., Bank H. (1993) Flux-grown synthetic rubies from Russia. *Journal of Gemmology*, Vol. 23, No. 7, pp. 393–396.

Henn U., Bank H., Bank F.H. (1990a) Red and orange corundum (ruby and padparadscha) from Malawi. *Journal of Gemmology*, Vol. 22, No. 2, pp. 83–89.

Henn U., Bank H., Bank-Scherner M. (1990b) Rubine aus dem Pamir-Gebirge, UdSSR. *Zeitschrift der Deutschen Gemmologischen Gesellschaft*, Vol. 39, No. 4, pp. 201–205.

Henn U., Schrader H. (1985) Some aspects of identification of Kashan synthetic rubies. *Journal of Gemmology*, Vol. 19, No. 6, pp. 469–478.

Hughes R.W. (1990a) A question of origin. *Gemological Digest*, Vol. 3, No. 1, pp. 16–32.

Hughes R.W. (1990b) *Corundum,* Butterworth-Heinemann, London.

Hughes R.W. (1994) The rubies and spinels of Afghanistan—a brief history. *Journal of Gemmology*, Vol. 24, No. 4, pp. 256–267.

Hughes R.W. (1997) *Ruby & Sapphire*, RWH Publishing, Boulder, Colorado.

Hunstiger C. (1990a) Darstellung und Vergleich primärer Rubinvorkommen in metamorphen Muttergesteinen: Petrographie und Phasenpetrologie; Teil II. *Zeitschrift der Deutschen Gemmologischen Gesellschaft*, Vol. 39, No. 1, pp. 49–63.

Hunstiger C. (1990b) Darstellung und Vergleich primärer Rubinvorkommen in metamorphen Muttergesteinen: Petrographie und Phasenpetrologie; Teil III. *Zeitschrift der Deutschen Gemmologischen Gesellschaft*, Vol. 39, No. 2/3, pp. 121–145.

ICA Gembureau (1991) Ruby discovered in China is similar to Vietnamese. *ICA Gazette*, August, p. 11.

Iyer L.A.N. (1953) The geology and gem-stones of the Mogok Stone Tract, Burma. *Memoirs of the Geological Survey of India*, Vol. 82, pp. 7–100.

Jenkins R. (1980) *An Introduction to X-Ray Spectrometry*, Heyden, Philadelphia.

Jobbins E.A., Berrangé J.P. (1981) The Pailin ruby and sapphire gemfield, Cambodia. *Journal of Gemmology*, Vol. 17, No. 8, pp. 555–567.

Kammerling R.C., Koivula J.I. (1994) Microscopic features of synthetic rubies, Part 1: Melt Products. *Canadian Gemmologist*, Vol. 15, No. 3, pp. 82–85.

Kammerling R.C., Fritsch E., Koivula J.I. (1995a) Swarogem's new synthetic ruby with induced fingerprints. *Jewellery News Asia*, No. 127, pp. 70–76.

Kammerling R.C., Koivula J.I., Fritsch E. (1995b) Gem news: "Recrystallized" synthetics. *Gems & Gemology*, Vol. 31, No. 1, p. 71.

Kammerling R.C., Koivula J.I., Fritsch E. (1995c) Gem news: Update on "recrystallized" corundum. *Gems & Gemology*, Vol. 31, No. 2, p. 136.

Kammerling R.C., Scarratt K., Bosshart G., Jobbins E.A., Kane R.E., Gübelin E.J., Levinson A.A. (1994) Myanmar and its gems—an update. *Journal of Gemmology*, Vol. 24, No. 1, pp. 3–40.

Kane R.E. (1983) The Ramaura synthetic ruby. *Gems & Gemology*, Vol. 19, No. 3, pp. 130–148.

Kane R.E. (1997) Kashmir ruby—a preliminary report on the deposit at Nangimali, Azad Kashmir, Pakistan. *Proceedings of the 26th International Gemological Congress*, September 27–October 3, Idar-Oberstein, Germany, pp. 28–30.

Kane R.E., Kammerling R.C., Koivula J.I., Shigley J.E., Fritsch E. (1990) The identification of blue diffusion-treated sapphires. *Gems & Gemology*, Vol. 26, No. 2, pp. 115–133.

Kane R.E., McClure S.F., Kammerling R.C., Khoa N.D, Mora C., Repetto S., Khai N.D., Koivula J.I. (1991) Rubies and fancy sapphires from Vietnam. *Gems & Gemology*, Vol. 27, No. 3, pp. 136–155.

Kashmir yields ruby, tourmaline (1992) *National Jeweler*, Vol. 36, No. 7, p. 17.

Keller P.C. (1982) The Chanthaburi-Trat gem field, Thailand. *Gems & Gemology*, Vol. 18, No. 4, pp. 186–196.

Keller P.C. (1983) The rubies of Burma: A review of the Mogok stone tract. *Gems & Gemology*, Vol. 19, No. 4, pp. 209–219.

Keller P.C., Fuquan W. (1986) A survey of the gemstone resources of China. *Gems & Gemology*, Vol. 22, No. 1, pp. 3–13.

Key R.M., Ochieng J.O. (1991) The growth of rubies in southeast Kenya. *Journal of Gemmology*, Vol. 22, No. 8, pp. 484–496.

Kissin A.J. (1994) Ruby and sapphire from the southern Ural Mountains, Russia. *Gems & Gemology*, Vol. 30, No. 4, pp. 243–252.

Knischka P.O., Gübelin E. (1980) Synthetische Rubine mit Edelsteinqualität, isometrischem Habitus und hoher Zahl unbeschädigter Kristallflächen. *Zeitschrift der Deutschen Gemmologischen Gesellschaft*, Vol. 29, No. 3/4, pp. 155–185.

Koivula J.I. (1983) Induced fingerprints. *Gems & Gemology*, Vol. 19, No. 4, pp. 220–227.

Konovalenko S.I. (1990) Mineral associations of corundum bearing marbles and the problem of ruby genesis. *Proceedings of the 15th General Meeting of the International Mineralogical Association*, Beijing, China, pp. 679–680.

Kuhlmann H. (1983) Emissionsspektralanalyse von natürlichen und synthetischen Rubinen, Sapphiren, Smaragden und Alexandriten. *Zeitschrift der Deutschen Gemmologischen Gesellschaft*, Vol. 32, No. 4, pp. 179–195.

Laughter T. (1993) How do you do? I'm from Mong Hsu. *JewelSiam*, Vol. 4, No. 5, pp. 38–41.

Levinson A.A., Cook F.A. (1994) Gem corundum in alkali basalt: Origin and occurrence. *Gems & Gemology*, Vol. 30, No. 4, pp. 253–262.

Levitski A.G., Sims D.H.R. (1997) Surface geochemical techniques in gemstone exploration at the Rockland ruby mine, Mangare area, SE Kenya. *Journal of Geochemical Exploration*, Vol. 59, No. 2, pp. 87–98.

Liddicoat R.T. Jr. (1990) The country of origin question. *Gems & Gemology*, Vol. 26, No. 4, p. 247.

McClure S.F., Kammerling R.C., Fritsch E. (1993) Update on diffusion-treated corundum: Red and other colors. *Gems & Gemology*, Vol. 29, No. 1, pp. 16–28.

Menon R.D., Santosh M., Yoshida M. (1994) Gemstone mineralization in southern Kerala, India. *Journal of the Geological Society of India*, Vol. 44, pp. 241–252.

Muhlmeister S., Devouard B. (1991) Trace element chemistry of natural and synthetic rubies. *Proceedings of the International Gemological Symposium 1991*, A. S. Keller, Ed., Gemological Institute of America, Santa Monica, CA, pp. 139–140.

Munasinghe T., Dissanayake C.B. (1981) The origin of gemstones of Sri Lanka. *Economic Geology*, Vol. 76, No. 5, pp. 1216–1225.

Nassau K. (1980) *Gems Made by Man*, Chilton Book Co., Radnor, PA.

Nassau K. (1995) Reconstituted, reconstructed, recrystallized, regrown-again! *Jewelers' Circular-Keystone*, Vol. 166, No. 9, pp. 94–97.

Nassau K., Crowningshield R. (1969) The nineteenth century, Verneuil, and the mystery of "reconstructed" ruby.... *Lapidary Journal*, Vol. 23, No. 1, pp. 114–119; No. 2, pp. 313–314, 334–338.

Okrusch M., Bunch T.E., Bank H. (1976) Paragenesis and petrogenesis of a corundum-bearing marble at Hunza (Kashmir). *Mineralium Deposita*, Vol. 11, pp. 278–297.

Osipowicz T., Tay T.S., Orlic I., Tang S.M., Watt F. (1995) Nuclear microscopy of rubies: Trace elements and inclusions. *Nuclear Instruments and Methods in Physics Research B*, No. 104, pp. 590–594.

Peretti A., Mouawad F. (1994) Fluorite inclusions in Mong Hsu ruby. *JewelSiam*, Vol. 5, No. 4, pp. 136–137.

Peretti A., Mullis J., Mouawad F. (1996) The role of fluorine in the formation of colour zoning in rubies from Mong Hsu, Myanmar. *Journal of Gemmology*, Vol. 25, No. 1, pp. 3–19.

Peretti A., Mullis J., Mouawad F., Guggenheim R. (1997) Inclusions in synthetic rubies and synthetic sapphires produced by hydrothermal methods (Tairus, Novosibirsk, Russia). *Journal of Gemmology*, Vol. 25, No. 8, pp. 540–561. [See abstract on pp. 155–156 of this issue of *Gems & Gemology*.]

Peretti A., Schmetzer K., Bernhardt H.J., Mouawad F. (1995) Rubies from Mong Hsu. *Gems & Gemology*, Vol. 31, No. 1, pp. 2–26.

Peretti H.A. [*sic*], Smith C.P. (1993) A new type of synthetic ruby on the market: Offered as hydrothermal rubies from Novosibirsk. *Australian Gemmologist*, Vol. 18, No. 5, pp. 149–156.

Platen H.v. (1988) Zur Genese von Korund in metamorphen Bauxiten und Tonen. *Zeitschrift der Deutschen Gemmologischen Gesellschaft*, Vol. 37, No. 3/4, pp. 129–137.

Pohl W., Horkel A. (1980) Notes on the geology and mineral resources of the Mtito-Andei-Taita area (southern Kenya). *Mitteilungen der Oesterreichischen Geologie Gesellschaft*, Vol. 73, pp. 135–152.

Pohl W., Niedermayr G., Horkel A. (1977) Geology of the Mangari ruby mines, Kenya. *Austria Mineral Exploration Project*, Report No. 9, 70 pp.

Poirot J.-P. (1997) Rubis et saphirs du Viêt-Nam. *Revue de Gemmologie a.f.g.*, No. 131, June, pp. 3–5.

Qi L., Lin S. (1998) Tairus hydrothermal synthetic ruby. *China Gems*, Vol. 7, No. 1, pp. 122–124 [in Chinese].[See abstract on p. 156 of this issue of *Gems & Gemology*.]

Rubin J.J., Van Uitert L.G. (1966) Growth of sapphire and ruby by the Czochralski technique. *Materials Research Bulletin*, Vol. 1, pp. 211–214.

Rupasinghe M.S., Dissanayake C.B. (1985) Charnockites and the genesis of gem minerals. *Chemical Geology*, Vol. 53, pp. 1–16.

Rutland E.H. (1969) Corundum from Malawi. *Journal of Gemmology*, Vol. 11, No. 8, pp. 320–323.

Sanchez J.L., Osipowicz T., Tang S.M., Tay T.S., Win T.T. (1997) Micro-PIXE analysis of trace element concentrations of natural rubies from different locations in Myanmar. *Nuclear Instruments and Methods in Physics Research B*, No. 130, pp. 682–686.

Schmetzer K. (1986a) *Rubine*. E. Schweizerbart'sche Verlagsbuchhandlung (Nägele u. Obermiller), Stuttgart, Germany.

Schmetzer K. (1986b) Production techniques of commercially available gem rubies. *Australian Gemmologist*, Vol. 16, No. 3, pp. 95–100.

Schmetzer K. (1987) Production techniques of commercially available Knischka synthetic rubies—an additional note. *Australian Gemmologist*, Vol. 16, No. 5, pp. 192–194.

Schmetzer K., Bank J. (1987) Synthetische Lechleitner-Rubine mit natürlichen Kernen und synthetischen Überzügen. *Zeitschrift der Deutschen Gemmologischen Gesellschaft.* Vol. 36, No. 1/2, pp. 1–10.

Schmetzer K., Schupp F.-J. (1994) Flux-induced fingerprint patterns in synthetic ruby: An update. *Gems & Gemology*, Vol. 30, No. 1, pp. 33–38.

Schrader H.W., Henn U. (1986) On the problems of using the gallium content as a means of distinction between natural and synthetic gemstones. *Journal of Gemmology*, Vol. 20, No. 2, pp. 108–113.

Simonet C. (1997) La géologie des gisements de saphirs. *Revue de Gemmologie*, No. 132, pp. 21–23. [See abstract on p. 151 of this issue of *Gems & Gemology*.]

Sloan G.J., McGhie A.R. (1988) *Techniques of Melt Crystallization. Techniques of Chemistry*, Vol. 19, John Wiley & Sons, New York.

Smith C.P. (1996) Introduction to analyzing internal growth structures: Identification of the negative *d* plane in natural ruby. *Gems & Gemology*, Vol. 32, No. 3, pp. 170–184.

Smith C.P. (1998) Rubies and pink sapphires from the Pamir mountain range in Tajikistan, former USSR. *Journal of Gemmology*, Vol. 26, No. 2, pp. 103–109.

Smith C.P., Bosshart G. (1993) New flux-grown synthetic rubies from Greece. *JewelSiam*, Vol. 4, No. 4, pp. 106–114.

Smith C.P., Gübelin E.J., Bassett A.M., Manandhar M.N. (1997) Rubies and fancy-color sapphires from Nepal. *Gems & Gemology*, Vol. 33, No. 1, pp. 24–41.

Smith C.P., Surdez N. (1994) The Mong Hsu ruby: A new type of Burmese ruby. *JewelSiam*, Vol. 4, No. 6, pp. 82–98.

Solesbury F.W. (1967) Gem corundum pegmatites in NE Tanganyika. *Economic Geology*, Vol. 62, pp. 983–991.

Stern W.B., Hänni H.A. (1982) Energy dispersive X-ray spectrometry: A non-destructive tool in gemmology. *Journal of Gemmology*, Vol. 18, No. 4, pp. 285–296.

Sun T.T. (1992) Analysis of Burmese and Thai rubies by Pixe [*sic*]. *Zeitschrift der Deutschen Gemmologischen Gesellschaft*, Vol. 41, No. 4, pp. 191–192.

Sutherland F.L. (1996a) Alkaline rocks and gemstones, Australia: A review and synthesis. *Australian Journal of Earth Sciences*, Vol. 43, pp. 323–343.

Sutherland F.L. (1996b) Volcanic minerals and rocks around Australia. *The Volcanic Earth*, UNSW Press, Sydney, Australia, Chap. 10, pp. 146–165.

Sutherland F.L., Coenraads R.R. (1996) An unusual ruby-sapphire-sapphirine-spinel assemblage from the Tertiary Barrington volcanic province, New South Wales, Australia. *Mineralogical Magazine*, Vol. 60, pp. 623–638.

Sutherland F.L., Schwarz D., Jobbins E.A., Coenraads R.R., Webb G. (1998) Distinctive gem corundum suites from discrete basalt fields: Barrington, Australia, and West Pailin, Cambodia, gemfields. *Journal of Gemmology*, Vol. 26, No. 2, pp. 65–85.

Tang S.M., Tang S.H., Mok K.F., Retty A.T., Tay T.S. (1989) A study of natural and synthetic rubies by PIXE. *Applied Spectroscopy*, Vol. 43, No. 2, pp. 219–222.

Tang S.M., Tang S.H., Tay T.S., Retty A.T. (1988) Analysis of Burmese and Thai rubies by PIXE. *Applied Spectroscopy*, Vol. 42, No. 1, pp. 44–48.

Themelis T. (1992) The effect of heat on inclusions in corundum. *The Heat Treatment of Ruby and Sapphire*. Gemlab Inc., Chap. 3, pp. 63–79.

Verneuil A. (1904) Mémoire sur la reproduction du rubis par fusion. *Annales de Chimie et de Physique*, Vol. 8, No. 3, pp. 20–48.

Vichit P. (1987) Gemstones in Thailand. *Journal of the Geological Society of Thailand*, Vol. 9, No. 1–2, pp. 108–133.

Viswanatha M.N. (1982) Economic potentiality of gem tracts of southern India and other aspects of gem exploration and marketing. *Records of the Geological Survey of India*, Vol. 114, Pt. 5, pp. 71–89.

Webb G. (1997) Gemmological features of rubies and sapphires from the Barrington Volcano, Eastern Australia. *Australian Gemmologist*, Vol. 19, No. 11, pp. 471–475.

Wedepohl K.H., Ed. (1978) *Handbook of Geochemistry*, Springer-Verlag, Berlin.

Weldon R. (1994) Yes, that is a Kashan! *Jewelers' Circular Keystone*, Vol. 165, No. 10, pp. 38–42.

Yaverbaum L.H. (1980) Corundum. *Synthetic Gems Production Techniques*, Noyes Data Corp., Park Ridge, New Jersey, p. 4–34.

Yu P., Mok D. (1993) Separation of natural and synthetic rubies using X-ray fluorescence analysis. *Journal of the Gemmological Association of Hong Kong*, Vol. 16, pp. 57–59.

Zwaan P.C. (1974) Garnet, corundum, and other gem minerals from Umba, Tanzania. *Scripta Geologica*, Vol. 20, pp. 19–30.

RAMAN INVESTIGATIONS ON TWO HISTORICAL OBJECTS FROM BASEL CATHEDRAL: THE RELIQUARY CROSS AND DOROTHY MONSTRANCE

By Henry A. Hänni, Benno Schubiger, Lore Kiefert, and Sabine Häberli

Two ecclesiastical objects of the late Gothic period (1350–1520) were investigated to identify the gemstones that adorn them. Both are from the treasury of Basel Cathedral (Basler Münster, Basel, Switzerland). To avoid potential damage, the identifications were conducted using only optical microscopy and Raman spectroscopy. Most of the mounted materials were found to be varieties of quartz, either as polished single pieces or as doublets with evidence of what may once have been dyed cement. Glass of various colors was also identified, as were peridot, sapphire, garnet, spinel, and turquoise.

In 1996, the SSEF Swiss Gemmological Institute investigated the adornments on two ecclesiastical objects from the treasury of Basel Cathedral: the Reliquary cross and the Dorothy monstrance (fig-

ABOUT THE AUTHORS

Dr. Hänni (haennih@ubaclu.unibas.ch), FGA, is director of the SSEF Swiss Gemmological Institute, Basel, and professor of gemology at Basel University, Switzerland. Dr. Kiefert, FGA, is research scientist at the SSEF Swiss Gemmological Institute, Basel, Switzerland. Dr. Schubiger is curator of the Art History Department of the Historical Museum of Basel. Ms. Häberli, FGA, is an art historian working as assistant curator at the Art History Department of the Historical Museum of Basel.

ures 1 and 2). These objects have been described previously with regard to their historical and cultural importance (Burckhardt, 1933; Barth, 1990), but not with regard to the materials themselves.

Only rarely does a gemologist get the opportunity to examine the stones adorning historical religious items. The investigations of Meixner (1952), CISGEM (1986), Köseoglu (1987), Querré et al. (1996), Bouquillon et al. (1995), Querré et al. (1995), and Scarratt (1998) are notable exceptions. The prudence and concern of museum curators is undoubtedly a major reason why so many important historical and religious pieces of jewelry and other artwork lack precise descriptions of their materials. Another explanation is that the fancy names and historical terminology for gemstones in old inventories are often simply accepted, without taking into account

Figure 1. The Reliquary cross from the treasury of Basel Cathedral, Basel, Switzerland, is believed to have been manufactured around 1440. Fashioned from silver with rock crystal quartz, it is adorned with a variety of "stones"—including glass and quartz doublets, as well as natural gem materials. The 37 cm high piece is currently in the collection of the Historical Museum of Basel. Photo by P. Portner, Basel.

Figure 2. The Dorothy (also known as Offenburg, in honor of the donor) monstrance, another piece from the treasury of Basel Cathedral, is believed to have been manufactured around 1440 as well. The "stones" in this religious artifact, which is constructed from silver with partial gilt, also include glass and doublets, as well as various natural gem materials. It is 55 cm high and currently resides in the Historical Museum of Basel. Photo by P. Portner, Basel.

BOX A: RAMAN ANALYSIS

Laser Raman microspectrometry has a unique combination of properties that make it useful in tackling gemological problems. These properties include a high spatial resolution that permits the study of inclusions as small as one micrometer. With a high-power objective and spatial light filtering, the system can be focused to a point *inside* a sample. This allows the analysis of layered compounds or inclusions inside gemstones with minimal contribution from the main bulk species. In addition, the analysis is rapid, requires no sample preparation, and, most importantly, is (with a few known exceptions) damage-free.

The Raman effect is a light-scattering technique that uses a monochromatic light source (usually a visible laser). While most of the light focused on a sample is scattered and contains no useful information (so-called "Rayleigh," or elastic, scattering), a small amount, typically one photon in 10^6-10^8, is re-emitted after having lost some energy. This shifted, or "Stokes," radiation appears as lines in a spectrum that is characteristic for the substance under study. Most materials that the gemologist or mineralogist will encounter have a distinctive Raman spectrum, which is dependent on the material's crystal structure and atomic bonding. Even subtle changes within a single material, such as alterations in crystallinity and composition, often can be detected. However, the operator must be aware that Raman spectra can change depending on the orientation of the sample (just as color can change with pleochroism). Also, inclusions within fluorescent minerals (such as ruby) must be at or very near the surface, because of interference caused by fluorescence. The only major subset of materials that cannot be studied are metals and alloys.

Using the "extended scanning" facility, the operator can measure a complete spectrum from 100 up to 9000 cm^{-1} with a resolution of 2 cm^{-1}. This allows not only Raman measurements, but also simultaneous Raman and luminescence studies, to be performed between 520 and 1000 nm. The spectrum obtained can be identified by comparison with known spectra, which means that a large set of reference spectra is an important condition for the successful use of the method.

A number of references are available for basic descriptions of the technique (McMillan and Hofmeister, 1988; McMillan, 1989) and its mineralogical (Griffin, 1987; Smith, 1987; Malézieux, 1990; Ostertag, 1996) and gemological applications (Dhamelincourt and Schubnel, 1977; Delé-Dubois et al., 1980; Pinet et al., 1992; Schubnel, 1992; Lasnier, 1995; Hänni et al., 1997). Geologic and gemological applications of the Raman method were also discussed at the Georaman 96 Congress (as summarized by E. Fritsch in Johnson and Koivula, 1996) and the 2nd Australian Conference on Vibrational Spectroscopy (Kiefert et al., 1996).

---

contemporary nomenclature rules and the fact that gemstone names today agree (more or less) with modern mineralogical identifications. However, the scarcity of both analytical techniques and research organizations specialized in nondestructive methods may be the primary reason for so many vague descriptions of the materials used in such objects. The Louvre Museum in Paris is one of relatively few repositories that have a well-equipped analytical laboratory; at the Louvre, various microprobes are used to investigate a wide variety of very delicate, rare, historical objects (Querré et al., 1995).

The present article reports on the examination of two historical religious objects with two nondestructive means—microscopy and Raman spectroscopy—available at the SSEF. Specifically, this article describes the identification of cut "stones" used in Christian ceremonial objects of the 15th century, during the late Gothic period. The two religious artifacts—a reliquary cross (i.e., one that contains some aspect, or relic, of a holy person) and a monstrance (a transparent vessel, surrounded by metalwork)—were brought to SSEF for gem identification in 1996. Such unique objects should, of course, be tested only by techniques that ensure no risk of damage. Among the available techniques, visible-range spectroscopy does not provide characteristic data for many (especially colorless) materials. Fourier-transform infrared (FTIR) spectroscopy might be appropriate, but Raman microspectrometry better accommodates large objects (figure 3) and provides a more rapid analysis (see Box A). We com-

bined Raman analysis with observation through a microscope to arrive at the results presented below. We hope that this article will give the gemologist dealing with antique objects information about a relatively new nondestructive method of identification. We also hope that more historians will take Raman spectroscopy into account when they are considering how to describe or catalogue pieces in their inventory with respect to the gem materials they contain.

HISTORICAL BACKGROUND

Places of worship in many cultures are characterized by magnificent construction and rich decoration as an expression of religious devotion. Such sacred places frequently are reservoirs for gifts and votive offerings from believers, some of whom may be quite wealthy. Such gifts can result in the accumulation of a significant treasury of gold, silver, and gems.

Both of the objects described here are part of the treasury of Basel Cathedral, in Basel, Switzerland. The Cathedral treasury is fascinating not only for the artistic quality and richness of its pieces, but especially for its long history (as described in Burckhardt, 1933; Barth, 1990). Through donations and, in the odd case, purchases during the 500 years from the early 11th century until the advent of the Reformation in the early 16th century, hundreds of examples of the handiwork of goldsmiths and other artisans were collected in the cathedral of the Bishopric of Basel. These incense burners, chalices, crosses, monstrances, and various other religious artifacts were the centerpieces during mass or other church ceremonies. The key piece in this collection, and also the oldest object (made in 1020), is the Golden altarpiece, which is now at the Cluny Museum in Paris. It previously belonged to Emperor Heinrich II of the Holy Roman Empire (973–1024).

Before the Reformation, Basel Cathedral had the richest church treasury in the region that is today southern Germany and Switzerland. The treasury was spared destruction during the Reformation when the members of the cathedral chapter hid the items in a cupboard in the vestry of the cathedral in 1528, right before they fled the city. The treasures remained hidden in the vestry, removed only occasionally for inventory, until 1827.

Subsequent local politics in Basel, however, finally led to the breakup of this collection. In 1833, Basel Canton divided into the half cantons of Basel-Stadt (city) and Basel-Land, and the ancient
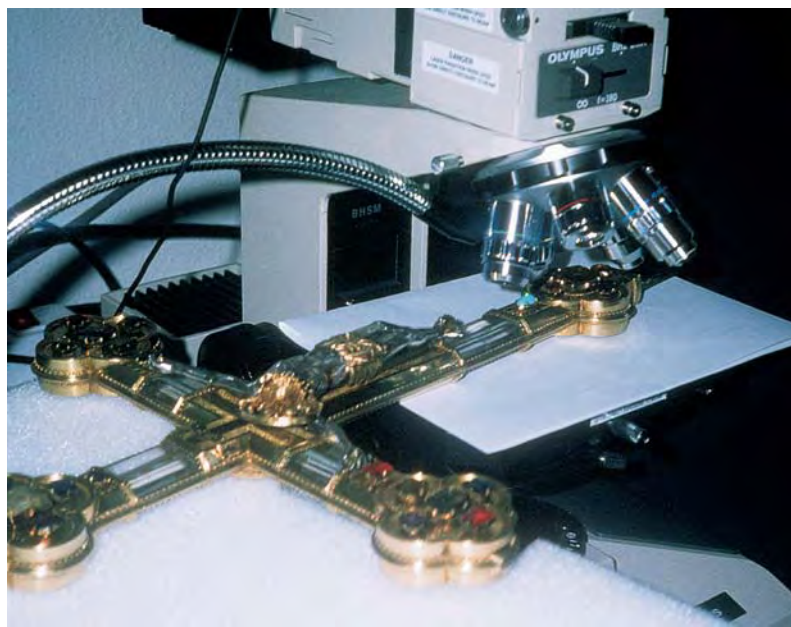
Figure 3. The Reliquary cross is shown here under the Raman microscope. To record the spectra of the different stones, the investigators had to carefully adjust the rather bulky object and direct the laser beam to the surface of the specific stone.

Cathedral treasury was likewise divided. The canton of Basel-Land received two-thirds of the treasury, which it sold at auction in its capital city Liestal in 1836. Whereas the city of Basel retained its share of the treasury items, the Basel-Land pieces were dispersed in many directions. Today, those pieces that have not been destroyed or lost can be found in museums in Berlin, Paris, London, New York, St. Petersburg, Vienna, and Zürich, as well as in Basel in the church of St. Clara. A large number are now in the Historical Museum of Basel, which over the last hundred years has purchased approximately two-thirds of the existing objects from the treasury, including the portion that remained with Basel-Stadt and 11 pieces that had been sold by Basel-Land. The Reliquary cross and the Dorothy (or Offenburg) monstrance (again, see figures 1 and 2), on which we conducted our gemological investigations, came from this collection. The Reliquary cross purportedly contains relics of St. Catherine and St. Jacob, whereas the monstrance is believed to contain a relic of St. Dorothy.

A precise dating of the two objects is not possible, because little information is available on the origin or history of the pieces. The first record of them is in the Cathedral treasury inventory of 1477. However, on the basis of stylistic features and what

TABLE 1. Physical properties of the gem materials set in the Reliquary Cross.

No.	Shape/cut	Color	Measurements (mm)	Internal features	Identification
A. Quatrefoil at left					
1	Octagonal, faceted	Violet	9.5 × 8.4	Color zoning	Amethyst
2	Octagonal, faceted	Yellow	11.8 × 9.6	Bubbles	Paste/glass
3	Rectangular, cut corners	Blue	9.6 × 8.0	Bubbles	Paste/glass
4	Rectangular, cut corners, domed table	Red	10.7 × 8.6	Tiny red particles in cement layer	Doublet with quartz top and dyed red cement
5	Octagonal, engraved man's head	Brown	18.2 × 11.8	Two-phase inclusions	Smoky quartz
6	Rectangular, cut corners	Red	9.6 × 8.0	Tiny particles in cement layer	Doublet with quartz top and dyed red cement
7	Colorless piece, drilled, with metal core	Colorless	25.5 × 22.8	Drilled, with metal core	Quartz
B. Quatrefoil on top					
1	Rectangular, domed table	Blue	9.2 × 7.7	Bubbles	Paste/glass
2	Octagonal, domed table	Violet	9.6 × 8.6	Color banding	Amethyst
3	Rectangular, domed table	Blue	9.1 × 7.7	Elongated bubbles	Paste/glass
4	Octagonal, cut corners	Violet	9.8 × 8.6	Two-phase inclusions	Amethyst
5	Rectangular, domed table	Yellow	17.1 × 13.9	Bubbles	Doublet with glass top
6	Octagonal, cut corners	Violet	8.8 × 7.0	Two-phase inclusions	Amethyst-quartz
7	Colorless piece, drilled, with metal core	Colorless	30.1 × 24.6	Drilled, with metal core	Quartz
C. Quatrefoil on right					
1	Rectangular, cut corners	Violet	8.7 × 6.5	Two-phase inclusions	Amethyst
2	Rectangular	Red	9.6 × 9.1	Bubbles and red	Doublet with quartz top particles in cement layer
3	Rectangular, domed table	Blue	9.6 × 8.6	Bubbles	Paste/glass
4	Rectangular, cut corners	Yellow	9.6 × 9.1	Bubbles	Paste/glass
5	Octagonal, cut corners, engraved woman's head	Brown	15.0 × 12.3	Two-phase inclusions	Smoky quartz
6	Octagonal, cut corners	Violet	10.2 × 7.0	Two-phase inclusions	Amethyst
7	Colorless piece, drilled, with metal core	Colorless	25.4 × 23.4	Drilled with metal core	Quartz
D. Quatrefoil on bottom					
1	Rectangular, cut corners, domed table	Red	9.7 × 7.5	Bubbles and red particles in cement layer	Doublet with quartz top and dyed red cement
2	Octagonal, cut corners	Violet	10.7 × 8.8	Two-phase inclusions	Amethyst
3	Octagonal, domed table	Yellow	12.8 × 10.2	Elongated bubbles	Paste/glass
4	Octagonal, cut corners	Violet	11.2 × 8.8	Color banding; inclusions	Amethyst
5	Octagonal, cut corners	Brownish yellow	23.5 × 21.4	Two-phase inclusions	Citrine
6	Oval, cabochon	Light greenish blue	11.8 × 7.5	Black veins	Turquoise
7	Colorless piece, drilled, with metal core	Colorless	42.9 × 24.4	Drilled, with metal core	Quartz
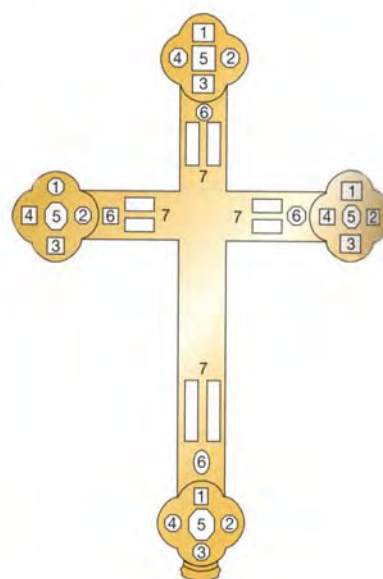
little is known of their history, both objects are believed to date from approximately 1440 (Burckhardt, 1933; Barth, 1990). Specifically, the style of the mold-made crucifix figure and the engraved foliage scrolls on the back of the cross are typical of this period. It is likely, too, that the donor of the Dorothy monstrance, Henmann Offenburg (1397–1459), had it made to hold a relic of Saint Dorothy that he brought from Rome after being knighted there in 1433.

TABLE 2. Physical properties of the gem materials set in the Dorothy monstrance.

No.	Shape/cut	Color	Measurements (mm)	Internal features	Identification
1	Polished pebble	"Olive" green	10.7 × 9.3	Slight turbidity	Peridot
2	Polished pebble	Colorless	6.3 diameter	Elongated bubbles	Paste/glass
3	Octagonal lozenge, sl. domed table	Blue	13.2 × 10.7	Spheric bubbles	Paste/glass
4	Octagonal, slightly domed table	Colorless	11.8 × 9.1	Cement layer, decomposed	Doublet with quartz top
5	Octagonal, slightly domed table	Blue	12.3 × 9.7	Spheric bubbles	Paste/glass
6	Round disc engraved goat	Orange	12.0 × 11.0	None observed	Chalcedony, var. carnelian
7	Octagonal, slightly domed table	Colorless	11.0 × 8.6	Cement layer, decomposed	Doublet with quartz top
8	Octagonal, slightly domed table	Blue	6.6 × 5.8	Elongated bubbles	Paste/glass
9	Oval, engraved woman's head	Cream and grey layers	13.5 × 21.5	Weak banding	Agate, layered onyx
10	Round cabochon	Green	6.0 × 5.5	Spherical bubbles	Paste/glass
11	Oval, unpolished	Black	14.0 × 10.0	None observed	Black chalcedony
12	Oval, cabochon	Light blue	9.5 × 8.3	Bubbles	Paste/glass doublet
13	Octagonal, slightly domed table	Blue	13.3 × 11.3	Bubbles	Paste/glass
14	Octagonal, slightly domed table	Colorless	11.1 × 8.6	Cement layer, decomposed	Doublet with quartz top
15	Octagonal, slightly domed table	Blue	14.2 × 11.1	Bubbles	Paste/glass
16	Rectangular, blocky	Violet	6.2 × 5.2	None observed	Amethyst
17	Oval, cabochon	Blue	5.0 × 4.0	Turbid growth layers	Sapphire
18	Octagonal, cabochon	Red	5.9 × 4.8	Rutile needles and mineral inclusions	Garnet
19	Round, cabochon	Pink	4.7 diameter	Mineral inclusions	Spinel
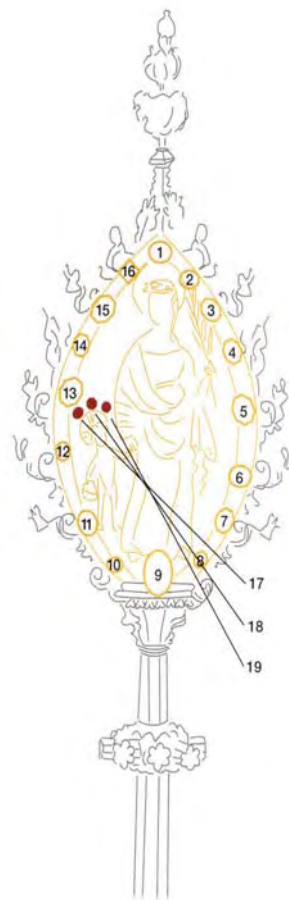
MATERIALS AND METHODS

The Reliquary cross and Dorothy monstrance both contain a variety of stones mounted in metal settings that are attached to the pieces (tables 1 and 2). The two pedestal-based objects are comparatively large, 37 cm and 55 cm high, respectively, and difficult to handle under a microscope. The settings of the stones as well as the fragility of the pieces themselves inhibit the use of a refractometer. To avoid any damage or contamination to those parts made of silver, all of the investigators wore cotton gloves.

For the microscopic examination, we used a Leica Stereozoom Binocular Microscope with a fiber-optic light source. The microscope was equipped with a camera enabling us to take photomicrographs with magnifications from 10× to 50×.

A handheld OPL spectroscope was used in connection with a fiber-optic light to analyze the blue stones that looked like a cobalt glass. Because the objects were so bulky, chemical analysis was not possible.

Conclusive identifications were made by taking Raman spectra of each of the "stones" in both objects and comparing the spectra to those in our reference data file. The spectra were obtained using a Renishaw Raman System 1000 equipped with a Peltier-cooled CCD detector, together with a 25 mW air-cooled argon ion laser (Spectra Physics; 514 nm) The laser beam was focused onto the sample, and the scattering was collected with an Olympus BH series microscope equipped with 10×, 20×, and 50× MSPlan objectives. Because most minerals have their characteristic Raman peaks between 100 and 1800 cm^{-1}, we measured spectra from 100 to 1900 cm^{-1} using the "extended scanning" facility (again, see Box A). A standard personal computer with GRAMS/386 software was used to collect and store

Figure 4. Four of the stones tested were found (by microscopy and Raman analysis) to be doublets with quartz tops and a layer of red cement. This stone, in the Reliquary cross, measures 10.7 × 8.6 mm.

the Raman spectra, as well as to analyze the data and compare the collected spectra to reference spectra stored in electronic files (Schubnel, 1992; Hänni et al., 1997).

The metals in the two objects were not analyzed, but the white metal is believed to be silver and the yellow appears to be gold-plated silver.

RESULTS
Description of the Objects. With few exceptions, the faceted "stones" in both objects are cut in sym-

Figure 5. Red pigment is seen here mixed in the cement of the doublet in figure 4. Magnified 60×

metrical shapes (e.g., oval or octagonal). The style of cutting usually uses a slightly domed table and one step of parallel facets on the crown. In most cases, the cutting style could be identified only on the crown side; because the stones are held in closed-back settings, any fashioning of the pavilion generally was not visible. In some doublets, the pavilion was completely invisible from above because of the decomposed cement layer. For the most part, those "stones" that were not faceted—including turquoise, sapphire, spinel, and garnet—were cabochons.

The Reliquary Cross. The partially gold-plated Reliquary cross (again, see figure 1) is in the Gothic style. The design of the mold-made crucifix and the stamped evangelical medallions on the reverse of the quatrefoil (four-lobed decorative motif) that terminates each arm of the cross has many similarities to comparable crucifixes of the same era. However, the use of rock crystal in the arms of the crucifix is unusual, if not singular. The presence of gem materials on the front of the cross gives the impression that this was a cherished object. On the back, at the intersection of the arms, a rock crystal capsule contains the relics of St. Catherine and St. Jacob, which can be seen through the transparent quartz window.

The Dorothy Monstrance. Crockets (in Gothic architecture, a crocket is an ornament that resembles an outward-curving leaf) frame the almond-shaped vessel like tongues of flame (again, see figure 2). The base, which consists of an eight-lobed foot, a smooth shaft, and a knob that resembles bundled rods, is more soberly treated.

A red niello coat of arms riveted to the door of the rear opening suggests that the monstrance was a gift from master craftsman Henmann Offenburg, of the Saffron guild of Basel. Restrained gilding on the front of this slender object creates a charming effect. The embossed figure of St. Dorothy in lavishly draped garments, hand-in-hand with the naked Christ child, appears to float within the mandorla (an almond-shaped halo of light enclosing the whole of a sacred figure). The preciousness of the object is enhanced by the fashioned stones and other ornamental materials set around the saint and by the cameo at her feet.

Identification of the Ornamental Materials. Tables 1 and 2 list the results of our testing on the stones in the Reliquary cross and Dorothy monstrance, respectively.
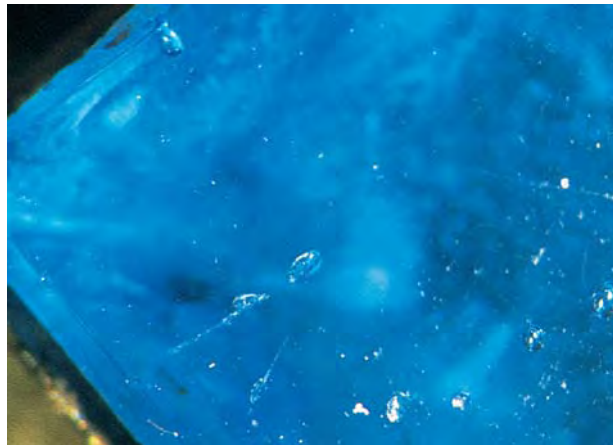
Figure 6. This piece of fashioned blue glass in the Reliquary cross showed the air bubbles typical of glass. Magnified 40×.

Figure 7. This yellow stone, set in the Reliquary cross, contains fluid and two-phase (fluid and gas) inclusions that are typical of crystalline quartz, in this case citrine. Magnified approximately 60×

Optical Microscopy. We identified many doublets (figure 4) and glass imitations in the Reliquary cross. Because all the gem materials are mounted in closed-back settings, in most cases we could not identify the pavilion material of the doublets. In some cases, however, gas bubbles were visible with magnification. The red doublets were found by microscopy to have quartz tops, with a cement layer that showed a red pigment mixed into the adhesive (figure 5). Probably due to their age, the cement layers in most of the doublets appeared to have dried out or shrunk, where air had entered the joining plane. The blue glasses showed air bubbles, either round or elongated (figure 6), that are typical of glass; with the spectroscope, we observed a weak cobalt spectrum.

Among the natural stones found, amethyst, citrine, and colorless quartz contained typical fluid and two-phase (fluid and gas) inclusions (figure 7). The turquoise cabochon (subsequently identified by Raman analysis) has a slightly greenish color that is typical of many turquoises seen today.

The Dorothy monstrance also contains a number of glass imitations (table 2), but it has some interesting natural stones as well. We identified peridot (figure 8), blue sapphire, red garnet, pink spinel (figure 9), and amethyst. A carnelian finely engraved with a goat (figure 10) suggests an interesting link to Greek art (Gray, 1983). An agate is engraved with the profile of a woman's head (figure

Figure 8. Raman analysis identified this 10.7 × 9.3 mm stone in the Dorothy monstrance as peridot.

Figure 9. Blue sapphire, red garnet, and pink spinel were identified in the Dorothy monstrance. The center stone (garnet) is approximately 6 mm in longest dimension.

Figure 10. This intaglio engraved with the figure of a goat was found to be carnelian. From the Dorothy monstrance, it is approximately 11 × 12 mm.

Figure 11. This cameo, also part of the Dorothy monstrance, was fashioned from agate. It is approximately 21.5 × 13.5 mm.

11). Four colorless to slightly yellow quartz doublets with heavily decomposed cement layers are particularly interesting (figure 12).

Raman Analysis. For the most part, the Raman spectra simply confirmed the microscopic observations. Figure 13 shows typical spectra from samples of the quartz varieties (rock crystal, amethyst, citrine) that were present in the Reliquary cross and the Dorothy monstrance. These spectra do not differ greatly from one another, but the quartz spectrum itself is very distinct from other materials. Figure 14, in comparison, shows the Raman spectrum taken at the porous surface of a black cabochon (stone no. 11 of the Dorothy monstrance). In addition to a small peak at 461 cm^{-1}, the spectrum shows two broad peaks at 1355 and 1605 cm^{-1}. On the basis of the peak at 461 cm^{-1}, the stone was identified as chalcedony. The peak at 1605 cm^{-1} is seen in epoxy resins, such as those used for emerald treatments. To protect the pieces, a layer of varnish was applied to them around 1970; museum personnel removed this layer with acetone prior to these analyses. Because of the porous nature of the chalcedony, it is likely that the protective varnish was not completely removed by the cleaning process, which resulted in the peak at 1605 cm^{-1}. The broad peak at 1355 cm^{-1} is possibly due to carbon, present as the coloring agent.

Good spectra were also obtained from peridot, garnet (figure 15), and sapphire mounted in the

Dorothy monstrance; whereas glass gives a relatively nonspecific spectrum, with broad bands varying from sample to sample. The spectrum of the spinel in the Dorothy monstrance (figure 16) and that of

Figure 12. A decomposed layer of cement is evident in this approximately 11.1 × 8.6 mm quartz doublet from the Dorothy monstrance.
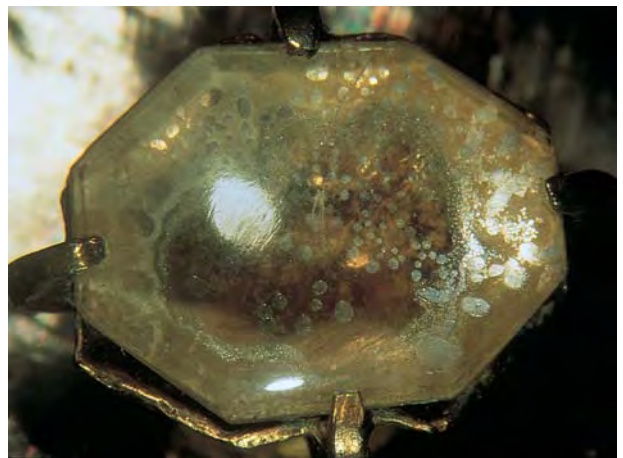
the turquoise in the Reliquary cross showed high fluorescence and small, but characteristic, peaks.

In the pedestal to the Dorothy monstrance, the ends of the bundled rods are adorned with red and green enamel inlay (again, see figure 2). Although more precise characterization of this enamel is possible with Raman analysis, as recently demonstrated by Menu (1996), we did not pursue this because we were not equipped with reference data for enamel and its pigments.

DISCUSSION

We were surprised to find so many imitations, such as glass and doublets, in a historic piece of art with outstanding metal work. We cannot evaluate the significance of these imitations that today we call fakes. Blue (cobalt?) glass (figure 6) seems to have been a common substitute for sapphire. Red doublets (figure 4) might have been selected to mimic ruby. We believe that the near-colorless quartz and glass doublets once contained colored cement, but that the color faded over the centuries because of the organic dyes used at that time. Given that colorless glass and quartz usually exist in fairly large pieces, this seems to be the only explanation for such assemblages. In those cases where the cement layer still exhibited color, such as in the red stone A4 (figure 4) of the Reliquary cross, we recognized pigment powder.

Among the natural gemstones encountered, varieties of quartz (rock crystal, amethyst, citrine, smoky quartz, and chalcedony) were the most common. In central Europe, a few occurrences of such stones have been known for centuries. The spinel and sapphire, however, show inclusions and growth zoning that suggest a Sri Lankan origin (Hänni, 1994). Although many occurrences of red garnets in Europe have been known since ancient times, there was only very limited use of this material.

The turquoise and peridot probably originated from Near East deposits (Khorassan, Persia; and Zabargad, Egypt, respectively), since the pieces predate the discovery of America. Regarding the engraved carnelian and agate, we consider a Greek or Roman origin, dating from the classical age, as most probable, inasmuch as engraved gemstones from the classical Greek and Roman period were frequently recycled in the Gothic era. However, it is also possible that they were fashioned at approximately the same time as the objects themselves, because there was a resurgence of interest in engraved gems in the 15th century (Gray, 1983).
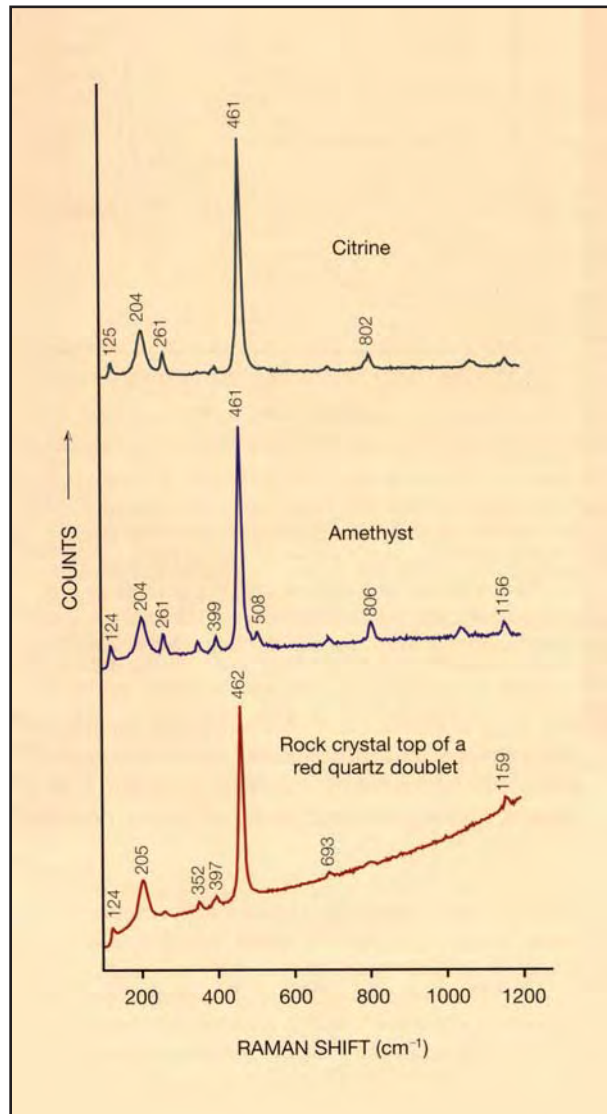
Figure 13. Note the similarities in the Raman spectra of the rock crystal top of a red quartz doublet (bottom), amethyst (middle), and citrine (top) set in the Reliquary cross. The most distinctive peak for quartz is at 461 ($\pm$2) cm^{-1}. Additional characteristic peaks are at 124, 204, and 261 cm^{-1}. Other peaks are less distinct and occur in different intensities, depending on the crystallographic orientation of the gem.

CONCLUSION

Our investigations of the Reliquary cross and Dorothy monstrance provided a great deal of information both on the gem materials used in these two 15th century religious objects and on the viability of Raman analysis for the characterization of
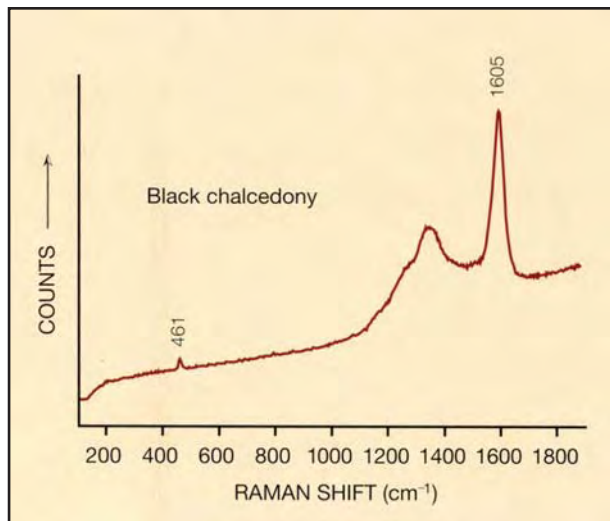
Figure 14. On the basis of the 461 cm⁻¹ Raman peak, we identified this black opaque stone in the Dorothy monstrance as chalcedony. The peak at 1605 cm⁻¹ is derived from residue of the varnish; whereas the broad peak at 1355 cm⁻¹ may be due to the presence of carbon, which is the typical coloring agent for black chalcedony.
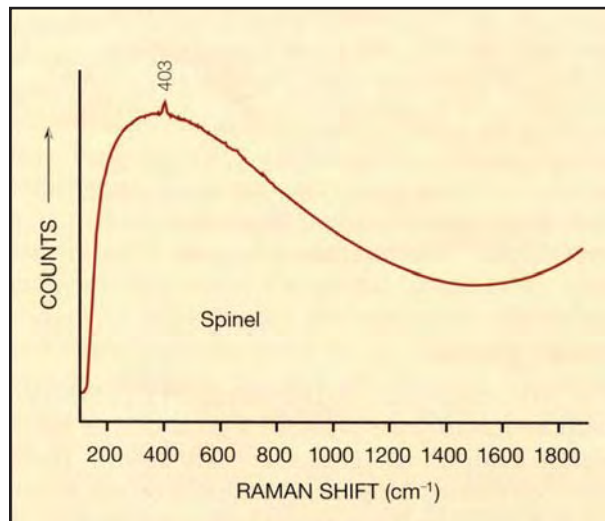
Figure 15. The Raman spectrum of a garnet set in the Dorothy monstrance shows its strongest peak at 913 cm⁻¹, with peaks of lower intensity at 341, 496, 862, and 1039 cm⁻¹. If we compare this spectrum with our reference spectra for garnet, the stone appears to be garnet with a high percentage of almandine.

such unique *objets d'art*. Although the metalwork appears to be quite fine, many of the "stones" in both pieces are actually colorless materials with a pigment backing, colored glass, or quartz doublets

with a (presumably dyed) cement layer. Nevertheless, there are also some attractive natural gems, such as peridot, sapphire, garnet, spinel, and turquoise, as well as varieties of quartz. Raman analysis provided a manageable, relatively quick method for identifying these materials without any damage to either the gems themselves or the metal in which they were set.

Figure 16. Spinel generally shows a high Raman fluorescence at low wavenumbers, which is overlain by its distinct peaks at 403, 308, 663, and 765 cm⁻¹. The intensity of the peaks depends on the color of the spinel. In this Raman spectrum of a pink spinel set in the Dorothy monstrance, only the peak at 403 cm⁻¹ is clearly visible.

REFERENCES

Barth U. (1990) *Erlesenes aus dem Basler Münsterschatz (Masterpieces from the Basel Münster Treasure).* Historisches Museum Basel, Basel, Switzerland.

Bouquillon A., Querré G., Poirot J-P. (1995) Pierres naturelles et matières synthétiques utilisées dans la joaillerie égyptienne. *Revue Française de Gemmologie*, Vol. 124, pp. 17–22.

Burckhardt R.F. (1933) *Die Kunstdenkmäler des Kantons Basel-Stadt, Vol. II: Der Basler Münsterschatz.* E. Birkhäuser Verlag and Cie., Basel, pp. 194–199 (Dorothy monstrance), pp. 238–241 (Reliquary cross).

CISGEM (1986) *Analisi gemmologica del Tresoro del Duomo di Milano.* CISGEM, Milan, Italy.

Delé-Dubois M.-L., Dhamelincourt P., Schubnel H.-J. (1980) Étude par spectrométrie Raman d'inclusions dans les diamants, saphirs et émeraudes. *Revue de Gemmologie*, No. 63, pp. 11–14, and No. 64, pp. 13–14.

Dhamelincourt P., Schubnel H.-J. (1977) La microsonde moleculaire à laser et son application dans la minéralogie et la gemmologie. *Revue de Gemmologie*, No. 52, pp. 11–14.

Gray F. (1983) Engraved gems: A historical perspective. *Gems & Gemology*, Vol. 19, No. 4, pp. 191–201.

Griffith W.P. (1987) Advances in the Raman and infrared spectroscopy of minerals. In R.J.H. Clark and R.E. Hester, Eds., *Spectroscopy of Inorganic-Based Materials*, Wiley & Sons, New York, Chap. 2, pp. 119–186.

Hänni H.A. (1994) Origin determinations for gemstones: Possibilities, restrictions and reliability. *Journal of Gemmology*, Vol. 24, No. 3, pp. 139–148.

Hänni H.A., Kiefert L., Chalain J-P., Wilcock I.C. (1997) A Raman microscope in the gemmological laboratory: First experiences of application. *Journal of Gemmology*, Vol. 25, No. 6, pp. 394–406.

Johnson M.L., Koivula J.I. (1996) Gem news: International conference on Raman spectroscopy and geology. *Gems & Gemology*, Vol. 32, No. 4, pp. 290–291.

Kiefert L., Hänni H.A., Chalain J-P. (1996) Various applications of a Raman microscope in a gemmological laboratory. In *Proceedings of the 2nd Australian Conference on Vibrational Spectroscopy*, 2–4 October 1996, Queensland University of Technology, Brisbane, Australia, pp. 202–203.

Köseoglu K. (1987) *The Topkapi Seray Museum: The Treasury*. Little, Brown and Co., Boston.

Lasnier B. (1995) Utilisation de la spectrométrie Raman en gemmologie. *Analusis Magazine*, Vol. 23, No. 1, pp. 16–18.

Malézieux J.-M. (1990) Contribution of Raman microspectrometry to the study of minerals. In A. Montana and F. Barragato, Eds., *Absorption Spectrometry in Mineralogy*, Chap. 2, Elsevier Science Publishers, Amsterdam.

McMillan P.F. (1989) Raman spectroscopy in mineralogy and geochemistry. *Annual Review of Earth and Planetary Sciences*, Vol. 17, pp. 255–283.

McMillan P.F., Hofmeister A.F. (1988) Infrared and Raman spectroscopy. In F. C. Hawthorne, Ed., *Spectroscopic Methods in Mineralogy and Geology*, Mineralogical Society of America, *Reviews in Mineralogy*, Vol. 18, Chap. 4, pp. 99–159.

Meixner H. (1952) Die Steine und Fassungen von Ring und Anhänger der hl.Hemma aus dem Dome zu Gurk in Kaernten: 1. Teil, Die Steine. *Carinthia II*, Vol. 142, No. 62, pp. 81–84.

Menu A.C. (1996) Les minéraux dans les enluminures. Thesis in Gemology, University of Nantes, France.

Ostertag T. (1996) Special application of Raman spectroscopy in the areas of mineralogy, petrology, and gemology. Diploma thesis, Albert-Ludwigs University, Freiburg, Germany.

Pinet M., Smith D., Lasnier B. (1992) Utilité de la microsonde Raman pour l'identification non destructive des gemmes. In *La Microsonde Raman en Gemmologie*, special issue of *Revue de Gemmologie*, pp. 11–61.

Querré G., Bouquillon A., Calligaro T., Dubus M., Salomon J. (1996) PIXE analysis of jewels from an Achaemenid tomb (IVth century BC). *Nuclear Instruments and Methods in Physics Research B*, Vol. 109/110, pp. 686–689.

Querré G., Bouquillon A., Calligaro T., Salomon J. (1995) Analyses de gemmes par faisceaux d'ions. *Analusis Magazine*, Vol. 23, No. 1, pp. 25–28.

Scarratt K. (1998) *The Crown Jewels.* C. Blair, Ed., The Stationery Office, London.

Schubnel H.-J. (1992) Une méthode moderne d'identification et d'authentification des gemmes. In *La Microsonde Raman en Gemmologie*, special issue of *Revue de Gemmologie*, pp. 5–10.

Smith D.C. (1987) The Raman spectroscopy of natural and synthetic minerals: A review. *Terra Cognita*, Vol. 7, pp. 20–21.

TOPAZ, AQUAMARINE, AND OTHER BERYLS FROM KLEIN SPITZKOPPE, NAMIBIA

By Bruce Cairncross, Ian C. Campbell, and Jan Marten Huizenga

This article presents, for the first time, both gemological and geologic information on topaz, aquamarine, and other beryls from miarolitic pegmatites at Namibia's historic Klein Spitzkoppe mineral locality. Topaz from Klein Spitzkoppe was first reported more than 100 years ago, in 1889. Many fine specimens have been collected since then, and thousands of carats have been faceted from colorless, transparent "silver" topaz. Gemological investigations of the topaz reveal refractive index values that are somewhat lower, and specific gravity values that are slightly higher, than those of topaz from similar deposits. In fact, these values are more appropriate to topaz from rhyolitic deposits than from pegmatites, and apparently correspond to a high fluorine content. The gemological properties of the aquamarine are consistent with known parameters.

The perfectly formed, transparent-to-translucent gem crystals from Klein Spitzkoppe, a granitic mountain in western Namibia, are in great demand by mineral collectors. For many years now, gems cut from some of these crystals—topaz, aquama-rine, and other beryls—have also been entering the trade (figure 1). The senior author (BC) visited Klein Spitzkoppe in 1975 and 1988 to study the geology of the deposit and obtain specimens, some of which were photographed and used for gemological testing. This article presents the results of this investigation, along with a discussion of the history of these famous deposits and the geology of the region.

LOCATION AND ACCESS
Klein Spitzkoppe ("small pointed hill") is located in southern Damaraland, northeast of the coastal harbor town of Swakopmund (figure 2). This granite inselberg has an elevation of 1,580 m above sea level and forms a prominent topographic landmark above the Namib Desert (figure 3). Inselbergs (derived from the German word meaning "island mountain") are common geologic features in southern African deserts; they are steep-sided, isolated

ABOUT THE AUTHORS

Dr. Cairncross (bc@na.rau.ac.za) is associate professor, and Dr. Huizenga is a lecturer, in the Department of Geology, Rand Afrikaans University, Johannesburg, South Africa. Mr. Campbell is an independent gemologist (FGA) and director of the Independent Coloured Stones Laboratory, Johannesburg, as well as an active consultant to the Jewelry Council of South Africa Diamond Grading and Coloured Stones Laboratory, Johannesburg.

Please see acknowledgments at end of article.

Figure 1. Both the 23 ct aquamarine and the 43 ct "silver" topaz were faceted from material found at Klein Spitzkoppe. Courtesy of Martha Rossouw; photo © Bruce Cairncross.

hills or mountains—formed by erosion—that rise abruptly from broad, flat plains. Much of the surrounding desert surface is covered with calcrete, a conglomerate composed of sand and gravel that has been cemented and hardened by calcium carbonate. Approximately 12 km east-northeast of Klein Spitzkoppe is another granite inselberg, Gross Spitzkoppe, which rises 1,750 m above sea level; no gems have been recovered from this area. *Spitzkoppe* has been spelled several ways in the literature, such as *Spitzkopje* (Heidtke and Schneider, 1976; Leithner, 1984) and *Spitzkop* (Mathias, 1962). The spelling used here is the one used on official geologic maps of the region.

Access to Klein Spitzkoppe is relatively straightforward, and the deposits can be reached using a conventional motor vehicle. The main highway (B2) that connects the coastal town of Swakopmund with Okhandja passes south of Klein Spitzkoppe. About 110 km northeast of Swakopmund, a road leads northwest from B2 back toward the coastal village of Henties Bay. About 30 km from the B2 turn-off, this road passes a few kilometers south of the topaz and aquamarine deposits at Klein Spitzkoppe, with the granite inselberg readily visible from the road. Large portions of the diggings are on public land. However, entry to privately owned granite quarries in the area is prohibited. Collecting of specimens by local people is carried out year-round, and a visitor to the site will always be met by these diggers offering specimens for sale.

HISTORY

The Klein Spitzkoppe deposits were first described in the late 19th century German literature (Hintze, 1889). At the time, the locality was known as *Keins-Berge,* although the Dutch name, *Spitskopjes,* was already used for several steep-sided inselbergs and isolated mountains in the Damaraland region.

Figure 2. Klein Spitzkoppe is located in central Namibia, about 200 km northwest of the capital city of Windhoek.
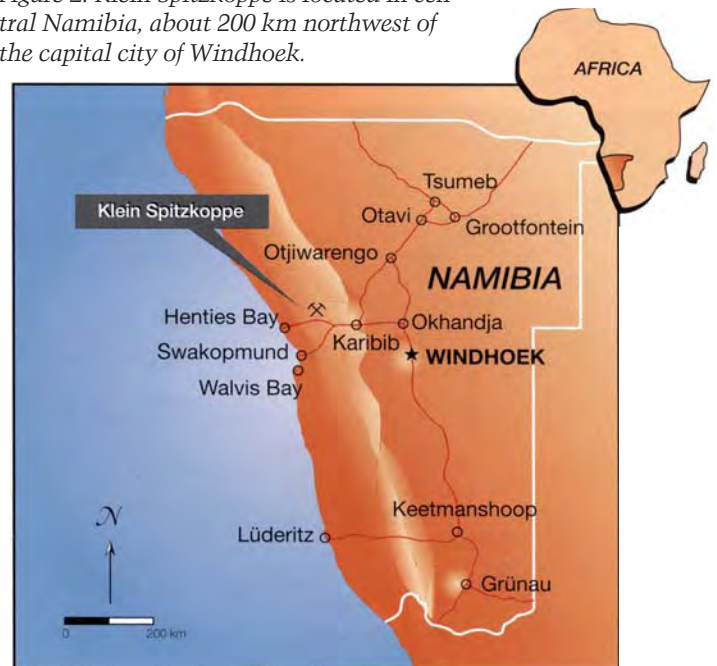
Figure 3. Klein Spitzkoppe mountain is surrounded by the arid plains of the Namib Desert. Photo by Horst Windisch.

For the initial description of the crystal morphology of the topaz from this region, Hintze used crystals that Baron von Steinäcker had originally collected at Klein Spitzkoppe. Hintze (1889) stated that the Namibian specimens were reminiscent of crystals from Russia, as they had a similar morphology and were "water clear."

Figure 4. A Damara woman digs for topaz in a highly weathered, soil-filled cavity in a gem-bearing pegmatite at Klein Spitzkoppe. Wind-blown sand and soil obscure the pegmatite. Photo by Horst Windisch.

It has been reported that 34.5 kg of facet-quality topaz was collected in Namibia, mostly from the Klein Spitzkoppe deposits, during 1930–1938 (Schneider and Seeger, 1992). More recent production figures are not available. Most topaz mining is carried out informally by local Damara diggers (figure 4), who usually sell their wares to tourists and local dealers. Aquamarine is also extracted, but it is less commonly encountered than topaz. Although no production figures are available, many hundreds of carats of aquamarine have been cut from material collected at Klein Spitzkoppe (see, e.g., figure 1). Yellow beryl is also infrequently recovered from the pegmatites, and some fine gems have been cut from this material as well.

Whereas gemstone mining is small-scale and informal at Klein Spitzkoppe, granite is quarried on a large scale. African Granite Co. (Pty) Ltd extracts a yellow granite, known colloquially as "Tropical Sun," which is exported primarily to Germany and Japan (ASSORE, 1996). Topaz crystals are frequently found during these quarrying operations and are collected by the local workers. Aquamarine is found less commonly in the quarries.

REGIONAL AND LOCAL GEOLOGY

Previous Work. The two Spitzkoppe mountains appear on a geologic map (scale 1:1,000,000) of central Namibia (then South West Africa) by Reuning (1923), which is one of the oldest geologic maps of the region. The regional geology was systematically

mapped during 1928, revised in 1937, and the combined results published several years later (Frommurze et al., 1942), accompanied by a more detailed geologic map (scale 1:125,000). In their report, Frommurze et al. briefly described the topaz occurrences at Klein Spitzkoppe and provided a map of the localities where topaz had been found.

Geology. Gem-quality topaz and beryl are derived from cavities within pegmatites that intrude the Klein Spitzkoppe granite. This granite is one of several alkali granites in the area that are Late Jurassic to Early Cretaceous in age (approximately 135 million years old; Miller, 1992). Such granites comprise part of the late- to post-Karoo intrusives that occur over a wide area of Namibia (Haughton et al., 1939; Botha et al., 1979). Other, somewhat similar granites in the area contain economic deposits of tin, rare-earth elements, tungsten, copper, fluorite, tourmaline, and apatite (Miller, 1992). The Klein Spitzkoppe granite is medium- to coarse-grained, light yellow to light brown, and consists predominantly of quartz, plagioclase, and microcline, with accessory magnetite, hematite, and limonite.

Menzies (1995) classified the pegmatites at Klein Spitzkoppe as "syngenetic," because they lie within the parent granite. (Ramdohr [1940] refers to these pegmatites as "greisens.") The pegmatites seldom exceed 1 m in width and 200 m along the strike. At least two occur on the eastern and southwestern slopes of Klein Spitzkoppe (Frommurze et al., 1942; Schneider and Seeger, 1992; figure 5). One of these pegmatites was mined via an underground shaft at the so-called Hassellund's Camp (see Sinkankas, 1981, p. 5, for a photo). The pegmatites pinch and swell in thickness; where there is sufficient space, cavities may be found that are lined with euhedral crystals of quartz, microcline feldspar, fluorite, and, locally, topaz and beryl. Some vugs contain euhedral biotite. The topaz and beryl tend to be more abundant when they occur with a quartz-feldspar assemblage, rather than with biotite. Frommurze et al. (1942, p. 121) also report that the beryl crystals are well formed and "invariably very clear and transparent. The colour varies from pale-green to dark sea-green and the bluish-green of precious aquamarine. Occasionally very deep-green varieties approaching emerald, and yellowish varieties known as heliodor are found." Besides topaz and beryl, 24 other minerals have been identified in the pegmatites (table 1), of which approximately a dozen occur as collectable specimens.
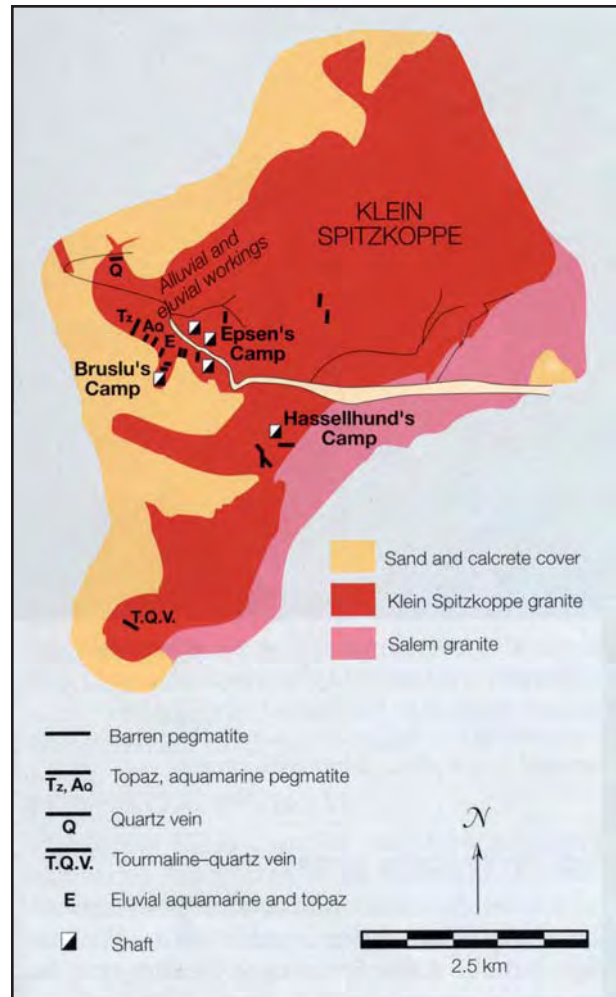
Figure 5. Topaz and aquamarine are mined from alluvial and eluvial deposits derived from miarolitic pegmatites intruding the Klein Spitzkoppe granite. Bruslu's, Epsen's and Hassellhund's camps are historical claims named after their respective discoverers. Redrawn after Frommurze et al. (1942).

MODERN QUARRYING AND MINING

Presently there is relatively little formal mining activity at Klein Spitzkoppe. One company is mining the granite for building stone. Most, if not all, of the topaz, aquamarine, and other gem or collectable minerals are extracted by local workers. They either dig randomly in the weathered granite outcrops, where it is relatively easy to pry crystals loose from their matrix, or they collect (by hand) topaz and beryl from the alluvium (again see figure 4). These alluvial crystals are usually abraded and are more suited for faceting than as mineral specimens.

Figure 6. This 3.8 cm crystal shows the remarkable transparency and complex habit typical of some topaz specimens from Klein Spitzkoppe. The crystal is attached to a feldspathic matrix. Courtesy of Desmond Sacco; photo © Bruce Cairncross.

KLEIN SPITZKOPPE TOPAZ

The worldwide occurrences of topaz were recently the subject of an in-depth publication (Menzies, 1995), but the Klein Spitzkoppe locality received only a brief mention in this article. Very little has been published on the Klein Spitzkoppe deposits, and even less has been written on the topaz per se. The notable exceptions are the few articles that have appeared in German publications, such as Leithner (1984).

Topaz has been found in several localities in Namibia (Schneider and Seeger, 1992), but the first recorded discovery of topaz there was Hintze's (1889) report on Klein Spitzkoppe. Topaz is probably the best-known gem species from Klein Spitzkoppe. Crystals over 10 cm long are well known, and Ramdohr (1940) reported on one specimen measuring $15 \times 12 \times 8$ cm and weighing over 2 kg. Because most of the topaz is found in alluvial and eluvial deposits, matrix specimens are rare (figure 6). Loose colorless crystals 1–2 cm long are abundant; in the past, bags full of this material were collected (Bürg, 1942; "South-West Africa's gem production," 1946). Not all crystals are gem quality, as internal fractures, cleavages, and macroscopic inclusions are fairly common. However, transparent crystals have

been cut into fine gems (figure 7). Typically they range from 0.5 to 5 ct, although stones up to 60 ct have been cut.

The topaz crystals are usually colorless, referred to as "silver" topaz, although pale blue (figure 8) and pale yellow (figure 9) crystals also occur (Beyer, 1980); brown topaz is not recorded from Klein Spitzkoppe. The blue and yellow colors are produced by color centers activated by radiation, either natural or artificial (Hoover, 1992). Blue usually results from electron or neutron bombardment (D. Burt, pers. comm., 1997). The less valuable yellow or brown hues can be removed by heating. They are also destroyed by prolonged exposure to sunlight, which may explain why most of the Klein Spitzkoppe topaz that is collected from exposed or weathered surfaces is colorless.

Several generations of topaz are found in the peg-

TABLE 1. Minerals from Klein Spitzkoppe.[a]	
Mineral	Composition
Albite	$NaAlSi_3O_8$
Axinite	$(Ca,Mn^{+2},Fe^{+2},Mg)_3Al_2BSi_4O_{15}(OH)$
Bertrandite	$Be_4Si_2O_7(OH)_2$
Beryl	$Be_3Al_2Si_6O_{18}$
Biotite	$K(Mg,Fe^{+2})_3(Al,Fe^{+3})Si_3O_{10}(OH,F)_2$
Bixbyite	$(Mn^{+3},Fe^{+3})_2O_3$
Chabazite	$CaAl_2Si_4O_{12} \cdot 6H_2O$
Columbite	$(Fe^{+2},Mn^{+2})(Nb,Ta)_2O_6$
Euclase	$BeAlSiO_4(OH)$
Euxenite-(Y)	$(Y,Ca,Ce,U,Th)(Nb,Ta,Ti)_2O_6$
Fluorite	CaF_2
Gibbsite	$Al(OH)_3$
Goethite	$\alpha\text{-}Fe^{+3}O(OH)$
Microcline	$KAlSi_3O_8$
Molybdenite	MoS_2
Muscovite	$KAl_2(Si_3Al)O_{10}(OH,F)_2$
Phenakite	Be_2SiO_4
Pyrophyllite	$Al_2Si_4O_{10}(OH)_2$
Quartz	SiO_2
Rutile	TiO_2
Scheelite	$CaWO_4$
Schorl	$NaFe_3^{+2}Al_6(BO_3)_3Si_6O_{18}(OH)_4$
Siderite	$Fe^{+2}CO_3$
Topaz	$Al_2SiO_4(F,OH)_2$
Wolframite	$(Fe^{+2},Mn^{+2})WO_4$
Zircon	$ZrSiO_4$

[a]*After Ramdohr, 1940; Frommurze et al., 1942; and Beyer, 1980.*

Figure 7. Faceted, colorless topaz from Klein Spitzkoppe is commonly marketed as "silver" topaz.The emerald-cut stone in the left foreground is 1.4 cm long, and the stones average about 5–6 ct. Courtesy of Rob Smith; photo © Bruce Cairncross.

matite cavities, in five commonly occurring crystallographic forms (Beyer, 1980):

Type I: Simple forms; usually colorless (figure 10).
Type II: Complex habits; usually colorless, (again, see figure 6).
Type III: Complex prismatic, stubby crystals; yellow (again, see figure 9).
Type IV: Simple prismatic forms; yellow; associated with unaltered microcline.
Type V: Long, thin prismatic crystals; yellow.

Types I and III are always transparent with highly lustrous crystal faces. These occur in vugs with microcline, and occasionally with black tourmaline (schorl). Type V is the last form to crystallize, and it is always associated with needle-like crystals of aquamarine and highly corroded microcline. Types I and II are associated with large quartz crystals, biotite, light green fluorite, tourmaline, and rutile.

Outstanding specimens of gem-quality, euhedral topaz crystals perched on, or partially overgrown by, highly lustrous smoky quartz are among the most sought-after collector pieces. Also desirable are matrix specimens consisting of topaz on white or pale yellow feldspar (again, see figure 6). In rare instances, topaz and green fluorite are found together. The value of mineral specimens is well recognized by the local diggers, as is evident from the availability of some fake specimens of topaz fashioned from locally mined pale green fluorite. The crystallographic configuration of the topaz is easily recognized and very well copied by the local diggers. (Fake specimens of aquamarine are also known

from Klein Spitzkoppe—see figure 12 in Dunn et al., 1981.) Detailed crystallographic descriptions of Spitzkoppe topaz are published elsewhere (Hintze, 1889; Ramdohr, 1940; Beyer, 1980).

KLEIN SPITZKOPPE BERYL

Beryl (figure 11) is found in miarolitic cavities in pegmatites associated with microcline, smoky quartz, topaz, bertrandite, phenakite, and fluorite (De Kock, 1935; Frommurze et al., 1942; Schneider and Seeger, 1992). Aquamarine forms elongate hexagonal prisms with flat or bipyramidal terminations; the semitransparent crystals commonly

Figure 8. This pale blue topaz, 2.8 cm long, displays unusual, multiple terminations. Photo © Bruce Cairncross.

Figure 9. The topaz at Klein Spitzkoppe may be pale yellow as well as pale blue or colorless. This 1.4 cm high yellow topaz crystal has a complex termination. Photo © Bruce Cairncross.

attain sizes up to 6 cm long and 1 cm in diameter (Leithner, 1984). The largest documented aquamarine from Klein Spitzkoppe measured 12 cm long and 5 cm in diameter (Ramdohr, 1940). Faceted aquamarine over 20 ct is common (again, see figure 1).

Figure 10. Most of the topaz specimens are broken off their host rock, as it is extremely difficult to remove specimens from the vugs intact. The crystal on the right is 5 cm. Photo © Bruce Cairncross.

Other varieties of gem beryl include hexagonal, prism-etched, transparent-to-translucent green and yellow varieties up to 6 cm long (Heidtke and Schneider, 1976). One crystal described by Beyer (1980, p. 16) measured 2 cm, and was colorless with a "rose" pink ("rosaroten") core! Yellow beryl (heliodor) is usually associated with fluorite and finely crystalline mica, or is intergrown with orthoclase (Heidtke and Schneider, 1976; Strunz, 1980; Schneider and Seeger, 1992). Heliodor was originally described from a pegmatite situated close to Rössing, located about 70 km northeast of Swakopmund (Kaiser, 1912), and it was described further by Hauser and Herzfeld (1914). Klein Spitzkoppe heliodor ranges from deep "golden" yellow to light yellow to yellow-green (figures 12 and 13). Crystals up to 12 cm long and 5 cm in diameter, some of which are transparent, have been recovered. Some heliodor crystals display naturally etched crystal faces, the most common feature being hook-shaped patterns on the *c* faces (Leithner, 1984).

MATERIALS AND METHODS

Gemological properties were obtained on five topaz (figure 14) and four aquamarine (figures 11 and 15) crystals from Klein Spitzkoppe. All of the topaz crystals and two of the aquamarines were obtained by two of the authors (IC and BC) from reliable dealers; the other two aquamarine crystals were loaned by Bill Larson of Pala International, Fallbrook, California. Although we were able to obtain cut stones for photography, we were not able to keep them long enough to perform gemological testing.

Refractive indices were determined using a Rayner Dialdex refractometer with a sodium light source. We obtained good readings from crystal faces and spot readings from cleavage surfaces on the crystals that did not have original crystal faces. One of us (IC) has performed R.I. measurements on gem rough for decades using this method, with reliable results. Luminescence tests were done in complete darkness, using a Raytech LS-7 long- and short-wave UV source. We determined specific gravity by the hydrostatic method. Distilled water softened with detergent was used to reduce surface tension.

Absorption spectra were observed with a calibrated Beck desk-model type spectroscope. We used an SAS2000 spectrophotometer with a dual-channel dedicated system, PC based, with a fiber-optic coupling in the visible to near-infrared range (380–850 nm), to obtain transmitted-light spectra.

Pleochroism was observed using a Rayner (calcite) dichroscope with a rotating eyepiece, in conjunction with fiber optics and a Mitchell stand with a rotating platform. Optic character was observed with a Rayner polariscope. The Chelsea filter reaction was determined in conjunction with a variable-power 150 watt fiber-optic tungsten light. All of the crystals were examined with a Wild Heerbrugg gemological binocular microscope under 10×, 24×, and 60× magnification.

The two aquamarine crystals loaned by Bill Larson were examined by Brendan Laurs at GIA in Carlsbad, California, with the following methods. Refractive indices were measured on a GIA Gem Instruments Duplex II refractometer, using a monochromatic sodium-equivalent light source. Pleochroism was observed with a calcite-type dichroscope. Fluorescence to short- and long-wave UV radiation was tested with a GIA Gem Instruments 5 watt UV source, in conjunction with a viewing cabinet, in a darkened room. Internal characteristics were examined with a standard gemological microscope, a Leica Stereozoom with 10×–60× magnification. Absorption spectra were observed with a Beck spectroscope.

RESULTS

Topaz. *Visual Appearance.* The topaz crystals (5.2 to 28.5 ct) were all colorless, except for one extremely light blue specimen. Light brown iron-oxide minerals (e.g., limonite) caused a brown discoloration to some of the crystal faces. All of the crystals were somewhat stubby, displaying short, prismatic forms with wedge-shaped terminations.

Microscopic Examination. One crystal contained partially healed fractures, as irregular planes ("fingerprints") of fluid and two-phase (fluid-gas) inclusions. We also observed isolated two-phase (fluid-gas) inclusions (figure 16). Acicular greenish blue crystals of tourmaline (identified optically) were seen slightly below the crystal faces in two of the specimens; some of these penetrated the surface of the host crystal (figure 17).

Gemological Properties. The results of the gemological testing are summarized in table 2. The R.I. values of the topaz were 1.610 and 1.620, although one specimen had a slightly lower maximum value of 1.616; birefringence was constant (0.010) for the other four samples. All the specimens appeared yel-

Figure 11. These aquamarine crystals, part of the test sample for this study, show the typical color and crystal form of specimens from Klein Spitzkoppe. The standing crystal measures 1.0 × 4.8 cm. Courtesy of William Larson; photo © Harold & Erica Van Pelt.

low-green through the Chelsea filter and were also inert to short- and long-wave UV. The specific gravity for all samples was 3.56. No spectral characteristics could be resolved with a desk-model spectroscope. All samples showed similar transmittance spectra with the spectrophotometer (figure 18): A steady increase in transmittance occurs from approximately 380 nm, at the violet end of the spectrum, to 600 nm, with a more gradual increase from 600 to 850 nm. There were no unusual features in the spectra that could be used to identify material as coming from this locality.

Figure 12. In addition to aquamarine, the deposit also produces fine crystals of yellow beryl, like this 3.4 cm specimen. Johannesburg Geological Museum specimen no. 65/116; photo © Bruce Cairncross.

Aquamarine. *Visual Appearance.* The samples studied were light greenish blue prismatic crystals of faceting quality. The two crystals studied by the authors (figure 15) weighed 5.5 ct and 8.6 ct, with smooth, shiny prism faces and etched terminations. The crystals studied at GIA weighed 90.3 and 158.9 ct, and were color zoned—light greenish blue with near-colorless terminations. Most of the prism faces were striated parallel to the c-axis, and the terminations were sharp and unetched.

Figure 13. Large stones have been faceted from the yellow beryl. The largest, a Portuguese-cut specimen at the top, weighs 42 ct. Courtesy of Desmond Sacco; photo © Bruce Cairncross.

Microscopic Examination. "Fingerprints" consisting of irregular planes of fluid and fluid-gas inclusions were the most common internal feature. Fractures were also common, and were iron-stained where they reached the surface. Hollow or fluid-and-gas-filled growth tubes were noted in the crystals examined at GIA; these tubes were oriented parallel to the c-axis. Large (up to 3 mm), angular cavities were also noted in these crystals. Both the growth tubes and the cavities locally contained colorless daughter minerals.

One specimen examined by the authors had brightly reflecting pinpoint inclusions of an unidentified material; these could be fluid inclusions. At 60↔ magnification, we saw radial stress fractures surrounding the inclusions. We saw similar pinpoint inclusions, but without the fractures, in another crystal. A feather-like, partially healed fluid inclusion extended from the base of this crystal to halfway up its length.

Gemological Properties. The R.I. values were 1.561–1.562 (n_ε) and 1.569–1.570 (n_ω), and the birefringence was 0.007–0.009. Dichroism was strong, colorless to greenish blue. The specific gravity was 2.68–2.69. All of the aquamarine samples appeared yellow-green through the Chelsea filter, and all were also inert to both short- and long-wave UV radiation. No spectral characteristics were resolved by the authors using the desk-model type spectroscope; at GIA, a faint line was seen at 430 nm in

Figure 14. The test sample included these five topaz crystals, which weigh, clockwise from top left: 13.7 ct, 5.2 ct, 28.5 ct, 15.4 ct, and 6.6 ct. The largest crystal (top right) is 21 mm along its longest axis. Photo © Bruce Cairncross.

both samples. The spectrophotometer results were identical for the authors' two specimens (figure 19): a small minimum at 425 nm, with a transmittance maximum at about 500 nm, and generally decreasing transmittance at higher wavelengths.

DISCUSSION

Topaz. The gemological results obtained from the Klein Spitzkoppe topaz are interesting for several reasons. The R.I. values (1.610 and 1.620) are relatively low compared to pegmatitic topaz from other localities (typically 1.614 to 1.635; Hoover, 1992). These R.I. values are similar to those of topaz from rhyolitic deposits, such as at the Thomas Range (Utah) and at San Luis Potosí, Mexico (Hoover, 1992); however, no rhyolites occur at Klein Spitzkoppe. The R.I. values of the Klein Spitzkoppe topaz are significantly lower than those for topaz from hydrothermal deposits, such as Ouro Preto, Brazil (1.630–1.638; Sauer et al., 1996), and Katlang, Pakistan (1.629–1.643; Gübelin et al., 1986). The variation in R.I. is caused by substitution of the hydroxyl (OH) component by fluorine in the topaz $[Al_2SiO_4(F,OH)_2]$ structure (Ribbe and Rosenberg, 1971). The Klein Spitzkoppe topaz is fluorine rich with nearly the maximum amount possible (about 20.3 wt.% F), similar to rhyolite-hosted topaz from the Thomas Range (Ribbe and Rosenberg (1971; as reproduced in Webster and Read, 1994).

Hoover (1992) and Webster and Read (1994) both state that the birefringence for colorless (and blue) topaz is 0.010, which is identical to the birefringence determined for the Klein Spitzkoppe material. The birefringence of hydrothermal topaz from Ouro

Figure 15. These two aquamarine crystals were also characterized for this study. The longest crystal is 22 mm. Photo © Bruce Cairncross.

Preto is somewhat lower, 0.008 (Keller, 1983), which is in agreement with similar values quoted for brown and pink topaz (Hoover, 1992). It is interesting to note that the pink topaz from Pakistan also has a birefringence of 0.010 (Gübelin et al., 1986).

The 3.56 S.G. for Klein Spitzkoppe topaz is identical to the value obtained for colorless and light blue topaz from localities in Russia, Germany, and the United States (Webster and Read, 1994). This is somewhat higher than the S.G. values (3.51–3.54) for pink and orange topaz from Pakistan (Gübelin et al., 1986) and Ouro Preto (Sauer et al., 1996). Like R.I., the S.G. values of topaz also vary with fluorine content; that is, they rise with increasing fluorine (Ribbe and Rosenberg, 1971). This relatively high

Figure 16. Fluid and two-phase (fluid and gas) inclusions such as these were seen in a topaz from Klein Spitzkoppe. Photo © Bruce Cairncross; magnified 24×.

Figure 17. Dark greenish blue tourmaline crystals, up to 0.8 mm long, form conspicuous inclusions near the surface of a topaz crystal from Klein Spitzkoppe. Photo © Bruce Cairncross.
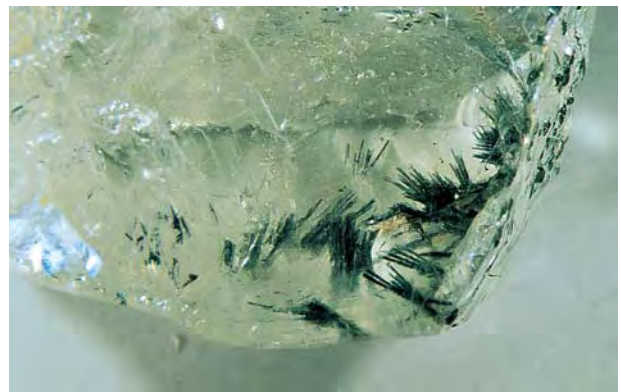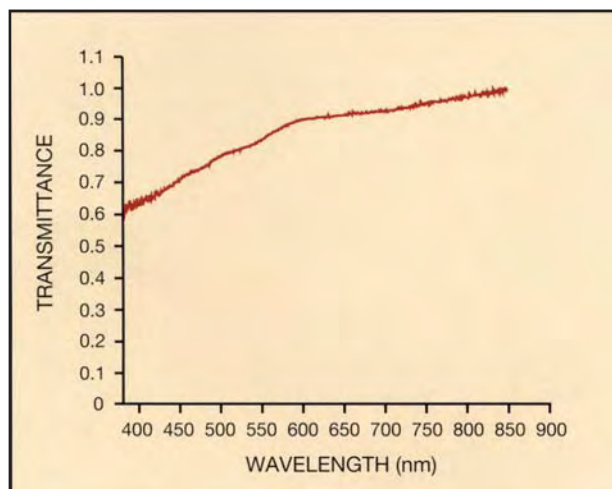
Figure 18. This transmittance spectrum is typical of the spectra recorded on the topaz specimens from Klein Spitzkoppe. A gradual increase in transmittance is seen over the entire range measured.
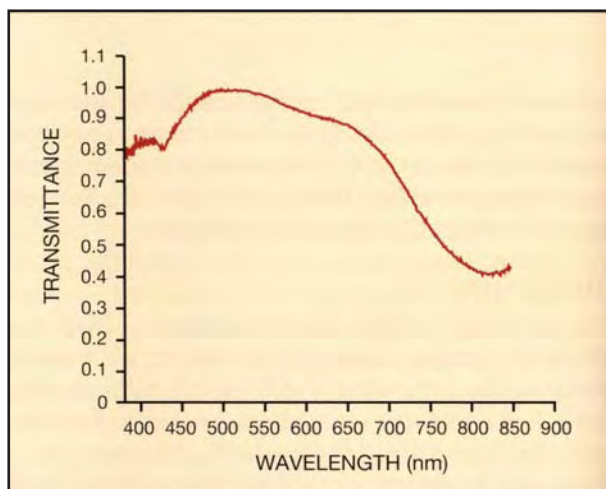
Figure 19. This transmittance spectrum is typical of the aquamarines examined from Klein Spitzkoppe, and shows a small minimum at 425 nm, a transmittance maximum at about 500 nm, and generally decreasing transmittance at higher wavelengths.

S.G. of Klein Spitzkoppe topaz is consistent with its low R.I. values and high inferred fluorine content.

The Klein Spitzkoppe topaz samples we examined had few inclusions compared to topaz from other localities. Some exceptions are the specimen

illustrated in figure 16, which contains well-developed fluid and fluid-and-gas inclusions, and the one shown in figure 17, which encloses small, greenish blue tourmaline needles. However, there are no inclusions, fluid or solid, that could be used to distinguish Klein Spitzkoppe topaz crystals from those of other deposits.

We do not know of any published data on the effects of irradiation or heat treatment on Klein Spitzkoppe topaz.

Beryl. For the most part, the results obtained from the aquamarines tested were typical for the species. The R.I. values (n_ε=1.561–1.562, n_ω=1.569–1.570) are low compared to typical values (n_ε=1.567–1.583, n_ω=1.572–1.590; Webster and Read, 1994), but low R.I. values are characteristic of beryl that contains little or no alkali impurities (Černý and Hawthorne, 1976). The birefringence (0.007–0.009) is relatively high for aquamarines with low R.I. values (typically 0.005; Webster and Read, 1994). However, the S.G. (2.68–2.69) is typical for aquamarines with low concentrations of alkalis (Webster and Read, 1994). The growth tubes and fluid inclusions also are typical of beryl from other pegmatitic deposits (see, e.g., Lahti and Kinnunen, 1993).

Webster and Read (1994) reported that some of the yellow beryls from Klein Spitzkoppe show radioactivity due to the presence of uranium oxide. To check this, we tested three crystals of yellow beryl using an Eberline ion chamber, but no radioactivity was detected.

TABLE 2. Summary of the gemological properties of topaz and beryl (aquamarine) from Klein Spitzkoppe, Namibia.

Property	Topaz	Aquamarine
Color	Colorless ("silver") to very light blue	Light greenish blue
Refractive indices		
Lower	n_α=1.610	n_ε=1.561–1.562
Upper	n_γ=1.620[a]	n_ω=1.569–1.570
Birefringence	0.010[a]	0.007–0.009
Optic character	Biaxial (+)	Uniaxial (–)
Luminescence (SW and LW UV)	Inert	Inert
Specific gravity	3.56	2.68–2.69
Dichroism	None	Pale blue to colorless
Chelsea filter	Yellow-green	Yellow-green
Absorption spectrum	No features noted with the spectroscope; increasing transmittance from 380–850 nm noted with the spectrophotometer	Faint line at 430 nm, or no features noted with the spectroscope; small minimum at 425 nm, and maximum at 500 nm, with the spectrophotometer
Inclusions	"Fingerprints," two-phase inclusions, tourmaline crystals	"Fingerprints," fractures, growth tubes, two- and three-phase inclusions

[a]*For one topaz specimen, R.I. values were 1.610–1.616 (birefringence 0.006), which is slightly outside the range reported here.*

FUTURE POTENTIAL

Topaz and, to a lesser degree, aquamarine have been found at Klein Spitzkoppe for more than 100 years. Local diggers collect most of the gems from weathered miarolitic pegmatites and alluvium. The quarrying of granite for building stone also yields some specimens and gems. The supply of gem-quality material, as well as specimen-grade crystals, will most likely continue for some time.

REFERENCES

ASSORE (1996) *The Associated Ore & Metal Corporation Limited Annual Report 1996*, Associated Ore & Metal Corporation (ASSORE), Parktown, Johannesburg.

Beyer H. (1980) Mineral-Beobachtungen an der Kleinen Spitzkopje (SW-Afrika). *Der Aufschluss*, Vol. 31, No. 1, pp. 4–32.

Botha B.J.V., Botha P.J., Beukes G.J. (1979) Na-Karoovulkanisme wes van Spitzkoppe, Suidwes-Afrika. *Annals of the Geological Survey of South Africa*, Pretoria, Vol. 13, pp. 97–107.

Bürg G. (1942) Die nutzbaren Minerallagerstätten von Deutsch-Südwesrafrika. *Mitteilungen der Gruppe deutscher koloniale wirtschaftlicher Unternehmungen*, Vol. 7, Walter deGruyter and Co., Berlin.

Černý P., Hawthorne F.C. (1976) Refractive indices versus alkali contents in beryl: General limitations and application to some pegmatitic types. *Canadian Mineralogist*, Vol. 14, pp. 491–497.

De Kock W.P. (1935) Beryl in SWA. *Open File Report, Geological Survey of Namibia*, Eg 056.

Dunn P.J., Bentley R.E., Wilson W.E. (1981) Mineral fakes. *Mineralogical Record*, Vol. 12, No. 4, pp. 197–219.

Frommurze H.F., Gevers T.W., Rossouw P.J. (1942) The geology and mineral deposits of the Karibib area, South West Africa. *Geological Survey of South Africa, Explanation of Sheet No. 79 (Karibib, S.W.A.)*, Pretoria.

Gübelin E., Graziani G., Kazmi A.H. (1986) Pink topaz from Pakistan. *Gems & Gemology*, Vol. 22, No. 3, pp. 140–151.

Haughton S.H., Frommurze H.F., Gevers T.W., Schwellnus C.M., Rossouw P.J. (1939) The geology and mineral deposits of the Omaruru area, South West Africa. *Geological Survey of South Africa, Explanation of Sheet No. 71 (Omaruru, S.W.A.)*, Pretoria.

Hauser O., Herzfeld H. (1914) Die "Heliodore" aus Südwest-Afrika. *Chemikerzeitung*, Vol. 66, pp. 694–695.

Heidtke U., Schneider W. (1976) Mineralien von der Kleinen Spitzkopje. *Namib und Meer*, Vol. 7, pp. 25–27.

Hintze C. (1889) Ueber Topas aus Südwest-Afrika. *Zeitschrift für Krystallographie*, Vol. 15, pp. 505–509.

Hoover D.B. (1992) *Topaz.* Butterworth-Heinemann Gem Books, Oxford, England.

Kaiser E. (1912) Ein neues Beryll (Aquamarin) Vorkommen in Deutsch Südwest-Afrika. *Zentralblatt für Mineralogie, Geologie, und Paläontologie*, Vol. 13, pp. 385–390.

Keller P.C. (1983) The Capão topaz deposit, Ouro Preto, Minas Gerais, Brazil. *Gems & Gemology*, Vol. 19, No. 1, pp. 12–20.

Lahti S.I., Kinnunen K.A. (1993) A new gem beryl locality: Luumäki, Finland. *Gems & Gemology*, Vol. 29, No. 1, pp. 30–37.

Leithner H. (1984) Topas und Beryll aus Namibia (Südwestafrika). *Lapis*, Vol. 9, No. 9, pp. 24–29.

Mathias M. (1962) A disharmonious granite; the Spitzkop granite, South West Africa. *Transactions of the Geological Society of South Africa*, Vol. 65, Part 1, pp. 281–292.

Menzies M.A. (1995) The mineralogy, geology and occurrence of topaz. *Mineralogical Record*, Vol. 26, pp. 5–53.

Miller R. McG. (1992) Stratigraphy. In *The Mineral Resources of Namibia*, 1st ed., Geological Survey, Ministry of Mines and Energy, Windhoek, Namibia, pp. 1.2-1–1.2-4.

Ramdohr P. (1940) Eine Fundstelle von Beryllium-Mineralien im Gebiet der Kleinen Spitzkopje, Südwestafrika, und ihre Paragenese. *Neues Jahrbuch für Mineralogie, Geologie, und Paläontologie*, Vol. A, No. 76, pp. 1–35.

Reuning E. (1923) Geologische Uebersichtskarte des mittleren Teils von Südwestafrika. (1:1,000,000 Geological Map of Central Namibia). Scharfes Druckereien, Wetzlar.

Ribbe P.H., Rosenberg P.E. (1971) Optical and X-ray determinative methods for fluorine in topaz. *American Mineralogist*, Vol. 56, pp. 1812–1821.

Sauer D.A., Keller A.S., McClure S.F. (1996) An update on imperial topaz from the Capão Mine, Minas Gerais, Brazil. *Gems & Gemology*, Vol. 32, No. 4, pp. 232–241.

Schneider G.I.C., Seeger K.G. (1992) Semi-precious stones. In *The Mineral Resources of Namibia*, 1st ed., Ministry of Mines and Energy, Geological Survey, Windhoek, Namibia, pp. 5.2-1–5.2-16.

Sinkankas J. (1981) *Emerald and other Beryls.* Chilton Book Co., Radnor, PA.

South-West Africa's gem production (1946) *South African Mining and Engineering Journal*, Vol. 57, Part 1, No. 2780, p. 305.

Strunz H. (1980) Plattentektoniek, Pegmatite und Edelsteine in Ost und West des Südatlantik. *Nova acta Leopoldina*, Vol. 50, No. 237, pp. 107–112.

Webster R., Read P.G. (1994) *Gems: Their Sources, Descriptions and Identification*, 5th ed. Butterworth-Heinemann Gem Books, Oxford, England.

G I A   G E M   T R A D E   LAB NOTES

CALCITE, Colored by Inclusions

A rare-mineral dealer from Colorado sent the 10.45 ct orange-red cabochon shown in figure 1 to the West Coast laboratory for identification last summer. He stated that the material was found at the site of an old copper mine in his local area. The dealer knew that the material was a carbonate, but he was unsure whether it was an unusual color of rhodochrosite or another carbonate mineral colored by inclusions.

Refractive indices of 1.49 and about 1.65 were obtained by the spot method, with a weak but clear birefringence blink. When we examined the cabochon with magnification, we

Figure 1. This 10.45 ct orange-red calcite is colored by inclusions of chalcotrichite, a fibrous variety of cuprite.

saw strong doubling and pock marks on the surface, with frequent undercutting, which implies a low hardness. A small drop of dilute hydrochloric acid caused the material to effervesce strongly, thus confirming that it was a carbonate. Two hydrostatic determinations of the specific gravity yielded a value of 2.73. Although rhodochrosite is also soft and effervesces to HCl, we identified the bulk material as calcite on the basis of specific gravity together with the refractive indices.

Magnification also revealed numerous orange and red reflective needles, as well as clusters of transparent-to-translucent purplish red crystals. Using diffused light, we observed that the body of the cabochon was quite pale, and the overall color was due to these inclusions. The cabochon fluoresced weak red to long-wave UV radiation and weak, moderately chalky reddish orange to short-wave UV. Lines at 500, 590, and 610 nm were visible in a desk-model spectroscope. From their habit and color, as well as from the reported provenance of the cabochon, we believe that the inclusions are chalcotrichite, a fibrous variety of cuprite.

The appearance of these inclusions and the overall color of the material reminded us of some bright red quartz from Zacatecas, Mexico, reported in the Spring 1993 Gem

News section (pp. 59–60). That material was also found in an old copper mine, and EDXRF of those inclusions showed them to be rich in copper and almost free of iron. The color is quite distinct from the more brownish red of the iron-rich inclusions, such as goethite and lepidocrocite, that are found in "strawberry" quartz from Russia (Gem News, Spring 1995, p. 63).   *IR and CYW*

CORUNDUM, Diffusion Treated

For some time now, laboratories on both coasts have been receiving large lots of rubies and sapphires for identification, which includes a determination of whether the stones have been subjected to any type of enhancement. One such parcel recently submitted to the West Coast lab contained small, attractive red stones, with one oval mixed cut that stood out visually from the rest because it was much darker in tone. (A closer inspection also revealed that this stone had a poor polish, unlike the rest of the parcel.) The client believed that they were all rubies and sent

them to the lab out of concern about heat treatment.

Ruby has a characteristic spectrum—with chromium lines at about 694 nm, 668 nm, and 659 nm, and another pair of lines at 476 nm and 468 nm—that conclusively distinguishes it from other red gems such as garnet and spinel, or from imitations such as glass. Consequently, we began our examination with a desk-model spectroscope to verify quickly whether all the stones in the parcel were ruby. We found this spectrum for all the stones except the darker-toned oval, which showed only a single strong absorption line in the red end of the visible spectrum.

Next we turned to the refractometer, but we experienced some difficulties obtaining the R.I. for this stone. The table gave an indistinct reading over the limits of the refractometer, whereas one small area of the pavilion yielded a vague reading of 1.7. The polariscope, however, revealed that the stone was doubly refractive, with a clear uniaxial figure. The specific gravity was measured hydrostatically at 4.00. This combination of properties proved that the stone was indeed corundum.

We turned next to observation with the microscope, and saw clearly why the refractive index reading of this oval was difficult to obtain and rather vague. The stone was heavily scratched on all sides and showed a very thin, crazed surface layer similar in appearance to that seen in Lechleitner synthetic emerald overgrowth on beryl. However, this oval mixed cut did not have any inclusions except for a tiny "fingerprint," which was too small to indicate whether the stone was of natural or synthetic origin. (Magnification revealed evidence of heat treatment in the rest of the stones in the parcel.)

Examination in diffused light showed that the purplish red color of this stone was irregularly distributed and concentrated at the facet junctions. These features indicate diffusion treatment. When we immersed the stone in methylene iodide, the dif-

Figure 2. When immersed in methylene iodide and placed over diffused transmitted light, this 0.69 ct oval mixed-cut corundum showed both the color concentrations on facet junctions and the spots devoid of color that indicate that it was colored by diffusion treatment.

fusion layer became quite prominent, as illustrated in figure 2. This figure also reveals some areas that did not have the red diffusion layer, probably due to recutting or polishing. On the basis of these results, the laboratory identified the stone as a diffusion-treated corundum and included a comment stating that its natural or synthetic origin is currently undeterminable.   *KH*

DIAMOND

Colored by Pink Coating

In the second edition of his book *Gemstone Enhancement* (Butterworth-Heinemann, 1994), Dr. Kurt Nassau references Benvenuto Cellini's *Treatise on Goldsmithing*, published in Venice in 1568, about gemstone treatment. Specifically, he cites Cellini's discussion of a variety of coatings and elaborate backings that were used to enhance diamonds primarily, as it was against the law to coat emerald, ruby, and sapphire. Not only does Cellini mention the blue dye—indigo—that was used to coat yellow diamonds, but he also states that "smoky colors" were the most desirable and describes the several steps required to achieve them.

Over the years, most coated diamonds that we have encountered in

the laboratories have been light yellow to near colorless, with the net result of the treatment being that the stones appear less colored, or "whiter." In some instances, we have seen diamonds that were "painted" to imitate fancy colors. The most notable in recent memory was a 10.88 ct light yellow emerald cut that had been coated pink with fingernail polish (reported in Gem Trade Lab Notes, Summer 1983, pp. 112–113).

The 5.75 ct brownish purple-pink marquise brilliant shown in figure 3 is the most recent example of a coated diamond that simulates a color that rarely occurs naturally in diamonds. In fact, the color reminded us of some of the first diamond crystals we saw from Russia in the early 1970s, which were given to one of the editors by Robert Webster. At the time, we were under the impression that this color would be representative of the production from Russia, but since then we have seen very few diamonds (from Russia or elsewhere) in this color range.

The first thing we saw with magnification was that the stone did not have the characteristic colored glide planes that are usually present in diamonds in this hue range. Identification was rather straightforward when we viewed the stone with a microscope using darkfield illumination and a white diffuser plate between the light source and the diamond: The speckled surface color typical of a coating was readily visible (figure 4). Although we were unable to identify the exact nature of the coating sub-

Figure 3. The brownish purple-pink color of this 5.75 ct marquise diamond was the result of a surface coating.
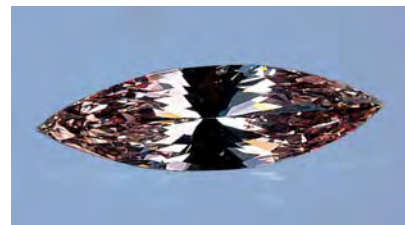
Figure 4. The spotty surface coating on the diamond shown in figure 3 was revealed with magnification (here, 63×) and a diffuse light source.

stance, it appeared to have been sputtered onto the entire stone and was most visible as small concentrated spots on the pavilion.

GRC and TM

With Different Color Appearances Depending on Viewing Position

From our discussions with members of the diamond trade, we are aware that they move colored diamonds through a number of positions when assessing the color. While this can be helpful in making manufacturing decisions, it has been our experience that consistent, repeatable results for color grading are best obtained by limiting the color appearance variables and, especially, controlling the viewing environment. With colored diamonds, the face-up position best accounts for the influence of cutting style on color appearance and is also the angle from which the diamonds will be viewed when worn in jewelry (see, e.g., King et al., *Gems & Gemology*, Winter 1994, p. 225). For these reasons, the laboratory color grades *colored* diamonds in the face-up position only.

A 2.67 ct emerald-cut diamond that was recently submitted to the East Coast laboratory provided an interesting example of the potential confusion that can arise if the stone is placed in more than one position for grading. Following GIA GTL's standard color-grading methodology, the diamond was described as Fancy

Deep Brown-Yellow (figure 5). Later, during the diamond's examination for origin determination, it was viewed through the pavilion and a noticeably different brown-orange bodycolor was observed (figure 6). A grader attempting to reconcile these two appearances might reach a color description that was not directly observed from either viewing angle. Examination of the stone face-up, though, results in the most consistent description of the diamond's characteristic color.

John King

Manufactured GLASS, Represented as "Green Obsidian"

It is usually a straightforward exercise to distinguish between glass imitations and the natural materials that are being imitated (see, for instance, "Glass Imitations of Various Gems," by Nicholas DelRe, in the Summer 1992 Lab Notes, pp. 125–126). Among the features that can be diagnostic for glass are its singly refractive optic character, low refractive index, and low specific gravity; also, swirled growth bands and (spherical or stretched) gas bubbles may be visible with magnification. Of course, the presence of any "mold marks" on the surface of a suspect gem or object is another factor that should always be taken into consideration. However, it is much more difficult to distinguish

between a natural glass, such as obsidian or moldavite, and a manufactured glass.

The six modified triangular brilliants shown in figure 7 were represented as natural green obsidian from Tunduru, Tanzania. They ranged in size from 9.06 × 9.46 × 6.11 mm (2.05 ct) to 12.03 × 12.21 × 8.18 mm (4.93 ct), and in color from yellowish green to green. They had the following gemological properties: color distribution—even; diaphaneity—transparent; optic character—singly refractive with weak anomalous double refraction; R.I.—1.518 to 1.530; S.G.—2.50 to 2.52; inert, faint yellow, or weak-to-medium green to short-wave ultraviolet radiation, and inert to long-wave UV; no obvious lines in the spectrum seen with a handheld spectroscope, but dark in the blue and in the red (above 650 nm) regions. This was enough information to confirm that these samples were glass, but not to identify whether they were of natural or manufactured origin.

With magnification, we saw a few perfectly spherical gas bubbles and swirl lines with weak-to-moderate curvature. These inclusions did not resemble those in natural glasses with which we are familiar: Obsidian, for example, usually contains tiny crystalline inclusions, and the swirls and bubbles in moldavite are often quite contorted (see, for instance, A. de Goutière, "Photogenic Inclusions in

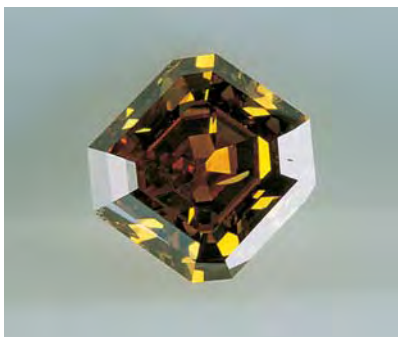*Figure 5. The face-up color of this 2.67 ct emerald-cut diamond received a grade of Fancy Deep Brown-Yellow.*

Figure 6. The bodycolor of the diamond in figure 5 appears to be much more orange when it is viewed through the pavilion.

Figure 7. These six modified triangular brilliants (2.05–4.93 ct) were represented as natural "green obsidian," but they proved to be manufactured glass.

Moldavite," *Journal of Gemmology*, Vol. 24, No. 6, pp. 415–419). The inclusions in these six triangular brilliants were strong—but not conclusive—indications that the glass was manufactured rather than natural. To be certain of the identification, we went to advanced testing procedures.

Three samples—one of each intensity of green—were examined by Fourier-transform infrared (FTIR) spectroscopy. We have analyzed several natural and manufactured glasses over the past few years; most samples, from both categories, are opaque below about 2100 cm⁻¹ (this edge shifts depending on the nature and size of the sample). Most obsidians show a saturated "hump" that rises sharply at about 3700 cm⁻¹ and tails off to lower wavenumbers (to about 3200 cm⁻¹, but this is quite variable). There are sometimes two weak, broad features centered around 3900 and 4500 cm⁻¹ as well. Moldavite and Libyan Desert glass also have distinctive spectra.

Although not all manufactured glasses have the same infrared spectra, many show a common pattern— which we have not seen in natural glasses—that consists of a broad plateau from about 3600 cm⁻¹ to the 2100 cm⁻¹ (or so) absorption edge, with superimposed broad peaks at 2830 cm⁻¹ and about 3520 cm⁻¹. (For example, brown glass beer bottles have this spectrum.) The three samples we examined also had this "manufactured glass" infrared spectrum. EDXRF analysis on one sample found major Si; minor Ca, Al, and Na; and trace amounts of K, Ti, Cr, Fe, Cu, Pb, Sr, and Zr. We concluded that this material was manufactured glass; in fact, we cannot recall seeing an example of transparent "green obsidian" that has ever proved to be a natural glass.

MLJ, IR, and Philip Owens

PEARLS

Cultured, with Dolomite Beads

Although commercial pearl culturing is nearly a century old, from time to time we still see examples of innovation in this field. For example, we reported on pearls cultured with dyed green beads made from powdered oyster shell and a polymer in the Fall 1990 Lab Notes section (pp. 222–223). Earlier this year, the West Coast labo- ratory received nine loose, undrilled pearls for identification, along with some beads used in their culturing that were represented to be dolomite (figure 8).

The beads, about 8 mm in diameter, were white and translucent. They had an aggregate structure, but the surfaces were poorly polished and the refractometer showed only a birefringence blink. They fluoresced a weak white to both long- and short-wave UV radiation, and a weak pinkish orange to X-rays. The specific gravity was measured hydrostatically at 2.84. These properties are consistent with dolomite, but without a refractive index reading they do not conclusively identify the material.

We next turned to several methods of advanced testing to gain additional information on the beads. EDXRF analysis showed the presence of both calcium and magnesium, which is also consistent with dolomite. The Raman spectrum matched our reference spectrum for dolomite, but the Raman spectra for dolomite and magnesite are very similar. An X-ray diffraction pattern confirmed the identification as dolomite.

The client was able to share some information regarding the dolomite beads and the pearls cultured on them. The beads are fashioned in South Korea, but our client did not know the source of the dolomite rock itself. These nine pearls were cultured in Japan to test whether dolomite works well as a bead nucleus for cultured pearls; during this test, it was found that the overall yield was about the same as for pearl culturing using freshwater shell beads. Dolomite is of interest for pearl nuclei because it is quite easy to obtain in sizes large enough to fashion beads up to 20 mm in diameter, whereas the traditional freshwater shell used for culturing rarely grows to such a thickness.

The nine samples ranged in size from 10.75 × 10.30 mm to 7.90 × 7.35 mm, and in color from white to gray to light yellow. On exposure to X-rays, they fluoresced a very weak orange; as is the case with other cul-

Figure 8. The pearls on the left, which range from 10.75 × 10.30 mm to 7.90 × 7.35 mm, were cultured on white dolomite beads similar to the ones shown on the right.

Figure 9. In this X-radiograph, the pearls cultured on dolomite beads have a very different appearance from the Tahitian black cultured pearl placed in the center as a reference.

tured pearls, this X-ray luminescence comes from the bead nucleus. The X-radiograph showed all nine to be cultured pearls, but the nuclei in these pearls looked distinctly different from the shell beads typically used to culture pearls, as illustrated in figure 9. The dolomite nuclei appeared darker (more transparent to the X-rays), and some of them had a mottled appearance. One sample showed a thick dark layer of conchiolin at the surface of the bead, which gave a silvery appearance to the pearl overall.

CYW and IR

Cultured, with Treated Black Color

The strand of fairly large black pearls shown in figure 10 was brought to the West Coast lab for identification. The strand consisted of 34 "circled" drop-shaped and oval pearls, ranging from approximately 13 × 10 mm to 10 × 9 mm, which were predominantly bluish black. However, some of the pearls also showed distinct green, and even violet, overtones. Because the pearls had the "metallic" appearance that is usually associated with irradiated freshwater tissue-nucleated cultured pearls (see Winter 1988 Lab Notes, p. 244), the client suspected that the color had been enhanced through irradiation.

X-radiography confirmed that the pearls were cultured. Visual examina-tion of the pearl surface with 20× binocular magnification revealed that the color was not uniform or evenly distributed, but rather it was concentrated in dark reddish brown "spots" that gave the cultured pearls a peculiar speckled appearance (figure 11). This type of color distribution typically results not from irradiation, but from dyeing, which is commonly done with a silver nitrate solution. EDXRF analysis of the pearls revealed silver, which proved that these cul-tured pearls owed their black color to dye, not radiation.

KH

**QUARTZITE,
Dyed to Imitate Sugilite**

The 1.12 ct purple cabochon shown in figure 12 was one of a group of five submitted to the West Coast lab for identification. The purple color was variegated and within the range seen commonly for sugilite (see J. Shigley

Figure 10. The client suspected that this strand of black cultured pearls was colored by irradiation.

et al., "The Occurrence and Gemological Properties of Wessels Mine Sugilite," *Gems & Gemology*, Summer 1987, pp. 78–89). However, this cabochon served as a reminder that the gemologist must examine all the properties and make sure they form a consistent picture to arrive at a correct result.

The material appeared translucent and showed an aggregate structure. We obtained a spot refractive index reading of 1.55. While the R.I. reported for sugilite is 1.607–1.610, the aforementioned article and the *Gem Reference Guide* (GIA, 1990, p. 235) warn that because gem-quality sugilite may contain quartz impurities, the refractive index reading can be around 1.54. The desk-model spectroscope showed a broad band from 540 to 580 nm. Purple sugilite has a characteristic spectrum—with lines at 411, 420, 437, and 445 nm, and a band at 550 nm—but Webster's *Gems* (4th ed., Butterworths, 1983, p. 359) states that these lines in the violet end are difficult to see without using a very bright light and a blue filter. However, the specific gravity, measured hydrostatically, was 2.64. This value is identical to that expected for quartz, but is quite low for sugilite, which is normally 2.74 even if it contains some quartz.

The combination of refractive index and specific gravity indicated a

Figure 12. This 1.12 ct purple cabochon looks very much like sugilite.

Figure 13. Closer examination of the cabochon shown in figure 12 revealed the characteristic appearance of a dyed aggregate material, in this case quartzite. Magnified 30×.

quartz aggregate. Examination with magnification revealed that this color was concentrated around and between the grains of the aggregate, which is diagnostic for dyed material (figure 13). Quartz (like sugilite) is usually inert to both long- and short-wave UV, but this cabochon fluoresced a weak greenish yellow, with a somewhat stronger reaction to long-wave UV. This fluorescence may well have been due to the purple dye.

This material looks like "purple onyx," also a dyed purple quartzite, which we discussed in the Winter 1990 Gem News section (p. 309). However, the particular shade of purple is different (this one is more reddish), as are the fluorescence and spectrum. Also in Gem News (Summer 1991, pp. 122–123), we described dyed purple quartzite that imitated dyed lavender jadeite.

IR and MLJ

An Unusual SAPPHIRINE

Not long ago, a client told us about an 8 ct "idocrase" from the new alluvial gem deposits in Tunduru, Tanzania. We could not recall seeing idocrase from that area, so we readily accepted the opportunity to examine the stone shown in figure 14.

The 8.64 ct cushion mixed cut was a moderately dark brownish orangy red. Microscopic examination revealed several long, thin needles scattered throughout the stone and a plane of crystals at one end. We

measured refractive indices of 1.700–1.707, giving a birefringence of 0.007, and we saw a biaxial figure in the polariscope. The specific gravity was 3.43, measured by the hydrostatic method. The stone was inert to long-wave UV and weakly fluoresced a chalky green color to short-wave UV. The refractive index and specific gravity were consistent with idocrase, but idocrase is uniaxial (although rarely it is anomalously biaxial).

However, the stone also displayed strong trichroism: brownish red, light orange, and colorless. Idocrase usually displays only weak pleochroism (and only two colors would be expected). Examination with a desk-model spectroscope did not reveal the band at 461 nm typical

Figure 14. This 8.64 ct brownish orangy red cushion mixed cut from Tunduru, Tanzania, turned out to be the largest sapphirine ever seen at the GIA Gem Trade Laboratory.

Figure 11. Examination with magnification of the cultured pearls in figure 10 revealed the spotty color distribution that is characteristic of dyed black pearls. Magnified 20×.
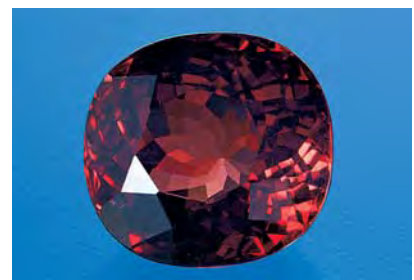
for idocrase (described in Webster's *Gems*, 4th ed., Butterworths, 1983, pp. 329–330), but instead it showed sharp lines in the red portion of the spectrum. The spectroscope lamp also revealed moderate red transmission (red fluorescence to visible light), a property shown by many gems that are colored by chromium.

It was apparent that further investigation was necessary, so we turned to the Raman microspectrometer. We were quite surprised when the spectrum obtained perfectly matched our reference spectrum for sapphirine. We had fallen into one of the oldest traps in gem identification: We had not considered this possibility because the stone was almost three times the size of the largest faceted sapphirine we had ever heard of. We were also not aware of any chrome-bearing sapphirine, or one of this color. An X-ray diffraction analysis confirmed the stone's identity. Since it was such an unusual stone, we also examined the chemistry by EDXRF. As expected from the formula $[(Mg,Al)_8(Al,SiO)_6O_{20}]$ for sapphirine, Mg, Al, and Si were present as major elements; minor amounts of Cr, Ca, Ti, Fe, Ni, and Ga were found as well. Because idocrase is a calcium-magnesium aluminosilicate, the EDXRF result alone would not have identified this gem.

Thirteen years ago, we encountered another sapphirine that was similar in some respects to the current stone (Fall 1985 Lab Notes, pp. 176–177). That stone was described as purplish pink and weighed 1.54 ct. It had nearly identical optical properties, which are at the low end of the reported ranges for this mineral. To the best of our knowledge, this 8.64 ct sapphirine is the largest sapphirine that has been reported to date. It is also the only one we know of that has been reported from Tunduru.   *SFM*

GEM N·E·W·S

DIAMONDS

Diamond exploration in Alberta, Canada . . . So far, more than 200 kimberlites (most of them without diamonds or subeconomic) have been found in Canada's Northwest Territories, writes Professor A. A. Levinson of the University of Calgary, Alberta. Just south of the Northwest Territories, the province of Alberta is becom-

Figure 1. A new kimberlite district has been identified in the Buffalo Hills area of north-central Alberta, south of the future Ekati and Diavik mines in the Northwest Territories. Most of Alberta had been staked for diamond exploration (shaded in yellow) as of March 1998. Map modified from "Alberta Diamond and Mineral Exploration Activity Map," April 1998, by EnerSource, Calgary, Alberta.
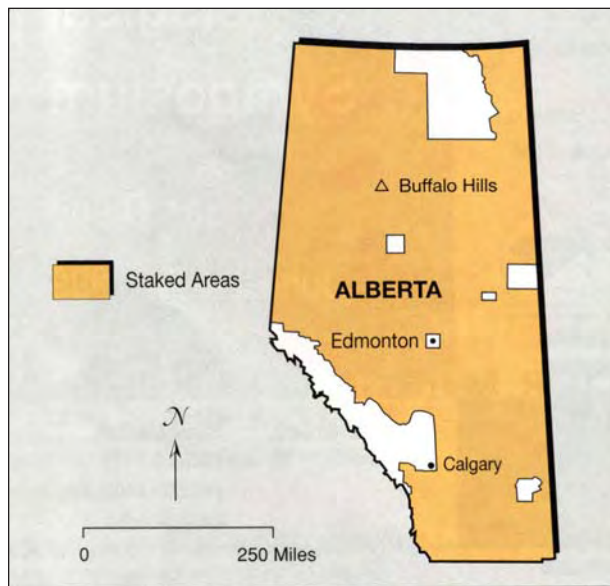
ing a hotbed of diamond exploration (figure 1). More than 80% of the stakable land in the Texas-size province has been staked for diamonds by at least 30 companies, including De Beers (operating as Monopros). Geologically, Archean-age rocks underlie much of the province, which is favorable for the occurrence of diamond-bearing kimberlites.

Although De Beers has been exploring in northern Alberta with varying degrees of intensity since the mid-1970s, no significant results were ever announced. Since 1996, however, more than 20 kimberlites have been discovered, many containing diamonds. Most of these were found by a consortium led by Ashton Mining of Canada that includes the Alberta Energy Company and Pure Gold Minerals. Many of the kimberlites are in the Buffalo Hills area of north-central Alberta (figure 2), which is now recognized as a distinct kimberlite province. The largest diamond recovered thus far weighed 1.31 ct, which suggests that there may be an economic population of jewelry-size stones.

Compared to the harsh conditions at remote sites in the Northwest Territories, diamond exploration in Alberta is both easier and more economical. Alberta has an excellent network of roads and many available services. The kimberlites are covered only by shallow till deposits (with some even visible as surface outcrops); they are not found under lakes as they frequently are in the Northwest Territories. Geophysical exploration has identified many anomalies that remain to be evaluated, any of which might represent a near-surface kimberlite pipe. Thus, there is "guarded optimism" (in Professor Levinson's words) that a mineable diamond deposit will be found and developed in Alberta. However, it will take several years before the true potential of this region can be determined.

. . . and anticipated production in the Northwest Territories. Professor Levinson also noted that this year

will "mark a milestone in the annals of the world production of rough diamonds," because the Ekati mine in the Lac de Gras region of the Northwest Territories (NWT) will begin operation this fall. The estimated production of about 4.2 Mct (million carats) per year would make Canada the sixth largest diamond producer (by volume) in the world. Another mine is at an advanced stage of development: At the Diavik project, about 16 miles (26 km) southeast of Ekati, a production of 6.5 Mct per year is anticipated beginning in 2002. If these production expectations are met, Canada will produce more diamonds annually than South Africa.

Cooperation among the mining companies, indigenous peoples, and the government of NWT is essential for a successful mining venture. In addition to various environmental safeguards, the government of NWT had requested "value-added activities"—that is, that the Territories would not merely be exporting raw materials, but might also be involved with the later processing steps (such as sorting, cutting, and polishing) that add value to the diamonds produced. In this regard, the government of NWT has come to an understanding with BHP Diamonds Inc. and Dia Met Minerals Ltd., the major-share partners in the development of the Ekati mine. BHP Diamonds Inc. (the operating company) will establish a diamond valuation facility that will be used at first for training, basic sorting, and government valuation; more-detailed sorting may follow as the work force gains more skills and expertise. BHP will also facilitate the sale of rough diamonds (for cutting and polishing) to qualified northern manufacturers at competitive prices, while the government will have primary responsibility for attracting and retaining those manufacturers. Both parties will work together to ensure that potential manufacturers have the necessary qualifications and a valid business plan.

International Rough Diamond Conference in Israel. Throughout 1998, Israelis are celebrating the 50th anniversary of the founding of the State of Israel. In honor of this anniversary, the diamond industry distinguished itself with a fascinating conference titled "Israel's Tribute to the Rough Diamond Producers—International Rough Diamond Conference," held June 23–24 in Tel Aviv. Professor A. A. Levinson provided the following report from this conference.

Israel is the world's largest cutting center for gem-quality diamonds (as distinct from the near-gems cut in India). The purpose of this conference was to acknowledge the contributions of the world's rough diamond producers to the success and prosperity of the Israeli cutting industry.

Approximately 200 foreign delegates and 300 members of the Israeli diamond industry attended the two-day conference. Renowned diamond journalist Chaim Even-Zohar was the moderator. The list of speakers included executives of companies that play major roles in dia-

Figure 2. Diamond-bearing kimberlite was discovered in this natural clearing in the heavily wooded Buffalo Hills area of Alberta. Petroleum exploration geologists had been using the clearing as a natural helicopter landing pad for several decades before the outcropping was identified as kimberlite. Photo courtesy of Ashton Mining of Canada.

mond mining, exploration, manufacturing, and financing, as well as government decision makers from several countries. One objective of the conference was to inaugurate the new Rough Diamond Trading Floor at the Israel Diamond Exchange in Ramat Gan. This was done on the first day by Prime Minister Benjamin Netanyahu, who noted that a free market for rough diamonds was being created, and encouraged rough suppliers to trade in Israel. The ceremony was followed by a forum with presentations by two senior Israeli government officials and the presidents of the two Exchanges, as well as the president of the Israel Diamond Manufacturers Association and the director of the (research-oriented) Israel Diamond Institute. Several of these speakers noted the positive role the Israeli government has played by virtue of its policies of minimum regulation and enlightened taxation with respect to the diamond industry (for instance, taxes generally are assessed at 1% of turnover, regardless of profit).

The second day of the conference featured 15 talks by presenters from the world diamond industry. De Beers was represented by three officials from the CSO (A. Oppenheimer, T. Capon, and S. Lussier), who covered topics ranging from the historic relationship between the CSO and Palestine (later Israel) since 1940, through projected polished diamond consumption into the next century, to the controversial concept of branded "De Beers Diamonds," which are currently being test marketed in England. High-ranking officials from the major producing countries of Botswana (B. Marole), Russia (S. Oulin), and Angola (J. D. Dias) discussed various aspects of the diamond industry as it relates to their economies, including the advantages of marketing some or all of their rough production through the CSO. Other speakers, representing smaller producers (D. M. Hoogenhout and L. Leviev),

Figure 3. These two agates from Botswana, 71.62 and 93.85 ct, show structures but not the colors that resemble the flames of candles. Photo by Maha DeMaggio.

explained their mining operations and why they find it advantageous to market independently.

New exploration ventures, particularly in Canada, attracted much attention. Rio Tinto (G. Sage), which operates the Argyle mine in Australia, is also developing the Diavik mine in Canada (scheduled to open in 2001); this will insure that Rio Tinto will be a major force in rough diamonds well into the future. The exploration activities on four continents of Ashton Mining (a minority stakeholder in the Argyle mine) were reviewed by R. J. Robinson. Some of the most notable future producers attended not as speakers but rather as delegates to familiarize themselves with the cutting industry. These included BHP Diamonds President J. Bothwell, whose Canadian Ekati mine will start producing this October.

Figure 4. These two "flame agates" are from Villa Ahumada, Mexico, the classic locality for such agates. The larger of the two weighs 51.95 ct. Photo by Maha DeMaggio.

Financial aspects were covered by P. K. Gross of the Belgian bank ABN-AMRO, a major lender to the diamond industry. Mr. Gross outlined methods of "risk analysis." At present, the total bank indebtedness of the four main diamond-cutting centers (Antwerp, Mumbai, Tel Aviv, and New York) is at an almost record level of US$4.5 billion. Even more worrisome is the industry's debt to capital ratio, now about 1 to 1.5. Evaluation of the inherent share value, and near-term potential, of publicly traded rough-diamond producers in South Africa and Canada was discussed by South African mining analyst D. Kilalea, who reported that the current picture is not bright.

The program was rounded out by an overview of world rough diamond production in relation to polished demand by Mr. Even-Zohar, a discussion of the cooperation between rough suppliers and their customers by Y. Hausman, and a colorful presentation by M. Rapaport on the relationship between rough and polished prices. Overall, the conference provided an excellent opportunity for dialogue between the world's rough diamond producers and their customers (particularly the Israeli diamond manufacturers). However, the topics covered have ramifications for the entire industry. In particular, there appeared to be a general concern that the diamond industry is currently in a less-than-satisfactory condition, which most speakers attributed primarily to the economic conditions in Southeast Asia and Japan, as well as to the strong U.S. dollar. Without doubt, the International Rough Diamond Conference was a great success.

COLORED STONES AND ORGANIC MATERIALS

"Flame agate": What's in a name? *Agate*, like the names of other chalcedony varieties, is often subject to misun-

Figure 5. It does not take much imagination to see why the name flame agate was applied to Mexican stones displaying colorful patterns, like the one shown here. Photomicrograph by John I. Koivula; magnified 5×.

derstanding, misuse, and/or misinterpretation. This results at least in part from the fact that there is no international body that decides how a particular agate or chalcedony should be named. *Flame agate* is a case in point. Should such agates be red to orange or yellowish orange, like the color of flames, or is any coloration, such as brown, acceptable? Is structural pattern a required criterion, or is it the only requirement? Dr. H. G. Macpherson, in the book *Agates* (British Museum of Natural History, 1989), used the term *flame agate* to refer to agate of any color in which the pattern resembles a candle flame. Based on Macpherson's use of the term, the two inexpensive, tumble-polished Botswana agates shown in figure 3, would qualify as flame agates.

A much earlier and more specific use of the term *flame agate* can be found in the classic 1959 reference *Gemstones of North America*, by John Sinkankas. In this work, Sinkankas describes a very specific highly translucent, colorless agate with few typical agate bands, but rather containing long streaks or "flames" of a bright red color. This material came from Chihuahua, Mexico, west of Villa Ahumada, and has been well established among agate collectors as "flame agate." Two excellent cabochons of Mexican "flame agate" are shown in figure 4, while a magnified image of the typical flame pattern is shown in figure 5. Lelande Quick, in *The Book of Agates* (1963), also refers to this Mexican agate as "flame agate," and agrees with the Sinkankas reference for the use of the term. When we compare the Mexican agates to the tumble-polished Botswana agates in figure 3 (or to the so-called flame agate image in Macpherson's book), it is easy to see why the descriptive name *flame agate* was first applied to the Mexican material. It is also easy to see how the term has become less focused and much more broadly used.

In short, no one governs the use of such descriptive terms in gemology. As a result, their original meaning may be lost through general usage. With respect to *flame agate*, it is suggested that both color and pattern are important, and that the name should be applied appropriately.

Update on benitoite mining. Benitoite was the subject of a feature article in the Fall 1997 issue of *Gems & Gemology* (B. Laurs et al., "Benitoite from the New Idria District, San Benito County, California," pp. 166–187). Since that time, the only commercial deposit of gem benitoite, the Benitoite Gem mine, has been placed under a 14-month option for evaluation by AZCO Mining Inc., of Vancouver, British Columbia, Canada. This option extends to February 1, 1999, at which time AZCO may elect to purchase the mine for $1.5 million.

In a press release dated May 7, AZCO supplied the 1998 production figures for the Benitoite Gem mine. In a mining season that ran just over one month, about 900 tons of alluvial material were processed by the present owners, producing 522 grams of "gem-quality" benitoite

Figure 6. This photo shows a portion of a spectacular benitoite specimen that was recovered last year. The white natrolite has been partially removed to expose the benitoite crystals. The entire specimen measures about 40 × 40 cm, and also contains neptunite and joaquinite crystals (not shown here); the benitoite crystals range up to about 4 cm in their longest dimension. Courtesy of the Collector's Edge; photo © Geoffrey Wheeler Photography.

rough. AZCO is nearing the completion of its bulk sampling and drilling of the deposit, and is engaged in geologic reconnaissance of the district.

Earlier this year, a spectacular benitoite specimen was meticulously prepared and then sold to a private collector by the Collector's Edge of Golden, Colorado. This specimen (figure 6) was recovered from a boulder that was discovered at the Benitoite Gem mine in spring 1997 (see figure 8, p. 173, of the Laurs et al. article for a photo of the original boulder).

Beryl from Madagascar: Aquamarine . . . The island republic of Madagascar is unusually rich in many kinds of gems, including sapphires, emeralds, tourmalines, and garnets, all of which have been profiled in the pages of *Gems & Gemology*. At the Tucson show this year, Tom Cushman of Allerton Cushman & Co., Sun Valley, Idaho, also showed the Gem News editors a large faceted aquamarine (figure 7) from Farafangana in southern Madagascar. It appears that this stone had not been heated, as the long axis had a greenish blue pleochroic color. The rough was reportedly mined about two years ago.

. . . and trapiche beryl. A light grayish green six-sided "trapiche" beryl (figure 8) was shown by Sunil Tholia, president of Universal Point, Forest Hills, New York, to GIA GTL (New York) gemologist Nick DelRe in Tucson. This stone was one of several Mr. Tholia had that reportedly came from the mining area surrounding Mananjary,

Figure 7. The crystal from which this 20.48 ct aquamarine was cut was mined in southern Madagascar. Stone courtesy of Allerton Cushman & Co.; photo by Maha DeMaggio.

Madagascar. The specimen measured 15.15 × 14.65 × 10.85 mm and weighed 13.74 ct. The refractive index (spot) was about 1.58, and the specific gravity was about 2.64, measured by the hydrostatic method. These properties are consistent with what we expect in such stones. The trapiche structure was most obvious in transmitted light (figure 8, right). We detected no evidence of clarity enhancement in the stone.

"Almost blue" Sri Lankan color-change garnets. In the Spring 1996 Gem News section (p. 53), we described a 3.29 ct color-change garnet that had the bluest color (in daylight-equivalent fluorescent light) we had seen up to that time; this color was described as bluish green. In the past few months, some very dark, desaturated color-change garnets (made available to the Gem News editors in Carlsbad and to contributing editor Emmanuel Fritsch in Nantes, France) also appeared to be somewhat blue with fluorescent illumination.

The 0.99 ct cushion mixed cut shown in figure 9 was loaned to the Gem News editors by Barry Schenk of M. M. Schenk Jeweler, Chattanooga, Tennessee. This stone had been purchased in Sri Lanka in 1997. Dr. Fritsch examined two stones, 0.48 and 0.59 ct, loaned by John Bachman, a colored-stone dealer in Boulder, Colorado, who stated that they came from Athiliwewa, Sri Lanka (see the Winter 1996 Gem News, pp. 285–286, for more on garnets from this locality). Because the possible existence of blue garnets continues to intrigue many gemologists, we characterized these stones in detail.

The gemological properties for the three stones are summarized in table 1. Although there is some variation in the specific properties, on the whole they are consistent with those for pyrope-spessartine garnets. The samples also contained similar inclusions, although more information was gained from those in France, as the GIA in Carlsbad had not acquired its laser Raman microspectrometer at the time of examination. Prominent in the 0.99 ct stone were oriented needles (figure 10), some of which showed stress or partially healed fractures in polarized light. The two smaller stones contained similar needles, identified as rutile by Raman analysis (with a Jobin Yvon T6400 spectrometer). These two stones also contained large, transparent, birefringent crystals, rounded or angular, that were proved by Raman analysis to be a carbonate, probably dolomite (figure 11); large, flat stacks of black hexagonal plates (probably graphite or hematite); and a small transparent inclusion that showed a Raman spectrum typical of spinel.

Because the chemical analyses of the stones examined in France showed no detectable chromium, Dr. Fritsch speculates that the combination of Mn^{2+} and V^{3+} absorptions was responsible for the color change in stones in which Cr^{3+} was absent, and contributed to the color change even in stones where Cr^{3+} was present.

Cat's-eye opal from Tanzania. Hussain Rezayee, an independent gem dealer based in Los Angeles, California, recently brought several parcels of this material to the

Figure 8. This 13.74 ct trapiche beryl crystal was found near Mananjary, Madagascar. In transmitted light (right), the spoke-like structure typical of trapiche emerald or beryl is evident. Courtesy of Universal Point, Inc.; photos by Nick DelRe.

Figure 9. This 0.99 ct pyrope-spessartine garnet from Sri Lanka changed color from dark grayish greenish blue in daylight-equivalent fluorescent light (left) to dark grayish violet in incandescent light (right). Stone courtesy of Barry Schenk; photos by Maha DeMaggio.

attention of the *Gems & Gemology* editors. The opal was found as nodules weathered in place in a field near Kasulu in Tanzania, near the border with Burundi. Mr. Rezayee's associates have collected "a few tons" of the rough opal since late 1995, and they report that the easily worked surface deposits are now nearly depleted. Only

about 1% can be fashioned into cat's-eye stones, and to date, about 30,000 carats have been cut. Mr. Rezayee sorts the material into 18 color categories; the five oval cabochons in figure 12, with sizes between 10.92 × 9.63 × 7.48 mm (4.04 ct) and 13.49 × 10.45 × 8.40 mm (6.71 ct), were representative of the range of colors in the material we saw. All five showed sharp eyes.

The gemological properties of these five stones were as follows: color—yellow, orange, brownish orange, and orangy brown; color distribution—even in all but the darkest stone, which showed brown color zones; diaphaneity—translucent to semi-translucent; optic character—isotropic with anomalous double refraction; (Chelsea) color filter reaction—none; refractive index—1.44 (spot reading); specific gravity—2.03–2.11; fluorescence—inert to both long- and short-wave UV radiation; spectroscope spectrum—none seen in the yellow and orangy brown stones, low-wavelength cutoff at about 400–500 nm in the orange and brownish orange stones. Using a microscope, we saw: red-brown staining along fractures, resembling dendrites, in the yellow stone; red-brown needle-like inclusions and brown breadcrumb-like inclusions; and patchy "clouds," sometimes elongated transverse to the chatoyant band. The acicular inclusions, when visible as distinct needles, were also parallel to the overall mass of much finer needles that caused the chatoyancy, but these masses of much smaller needles

TABLE 1. Gemological properties of three grayish greenish blue color-change garnets.

Property	Carlsbad sample	Nantes samples
Weight	0.99 ct	0.48 and 0.59 ct
Color in daylight	Dark grayish greenish blue (fluorescent light)	Grayish greenish blue (daylight)
Color in incandescent light	Dark grayish violet	Purple
Optic character	Singly refractive with weak anomalous double refraction	Singly refractive with weak anomalous double refraction
Color filter reaction	Orange	Orange
Refractive index	1.760	1.77
Specific gravity	3.88	About 3.91
Fluorescence to LW and SWUV	Inert	Inert
Luminescence to visible light	None	None
Absorption spectrum	400–450 nm cutoff, weak absorption at 450–470 nm, diffuse bands at 480–490 nm, 504 and 520 nm, and 560–580 nm	435 nm cutoff; 460, 480, 504, and 520 nm lines; and wide band at 573 nm
Inclusions	Oriented needles, some showing stress	Rutile needles, carbonate, graphite(?), spinel
Chemical analysis	EDXRF	SEM-EDS (0.48 ct)
Major elements	Mg, Al, Si, Mn	Mg, Al, Si, Mn
Minor to trace elements	Fe, Ca, V, Cr, Zn, Y, Zr	Fe, Ca, V
UV-visible spectrum	Absorption minimum (transmission maximum) at 475 nm; weak absorption peaks at 504 and 525 nm superimposed on a strong broad peak centered at 573 nm; and a strong peak centered at 685 nm	UV cutoff at about 430 nm; weak band at 483 nm; and a broad, slightly asymmetric band with apparent maximum at 580 nm

Figure 10. The 0.99 ct color-change garnet in figure 9 contained oriented parallel arrays of needles, as are commonly seen in garnets. Photomicrograph by John I. Koivula; magnified 17×.
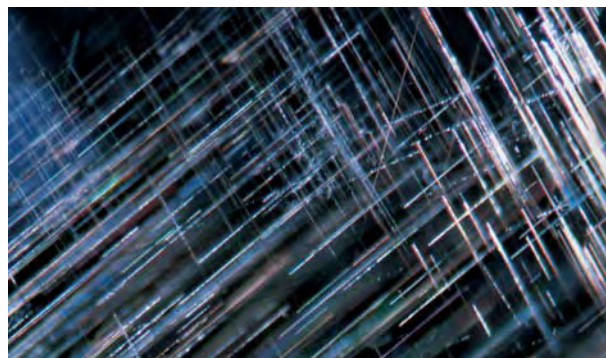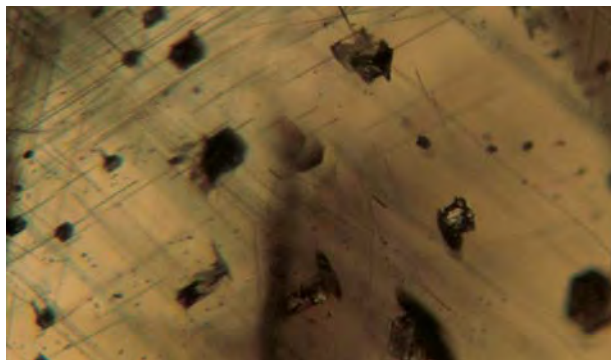
Figure 11. In addition to rutile needles, this 0.59 ct color-change garnet contained carbonate crystals, probably dolomite. Photomicrograph by Emmanuel Fritsch; magnified 25×.

were not obvious at 63× magnification. Some crazing was visible, but for the most part these curved fractures were iron stained, which indicates that they existed prior to the cutting of the stones. This suggests that the cutting did not damage the stones; that is, they were relatively stable at the time they were mined.

Additional testing yielded the following information. For all five stones, FTIR spectroscopy revealed a typical natural opal spectrum between 1000 and 6000 cm^{-1}, with no evidence of polymer impregnation. EDXRF analysis showed silicon as a major element (expected for opal), and minor iron and calcium. Three stones (one orange, two orangy brown) contained traces of zinc; the two orangy brown stones also contained traces of manganese.

Figure 12. These five cat's-eye opals (4.04–6.71 ct) from southern Tanzania show the range of colors examined by the editors. Photo by Maha DeMaggio.

Of rubies and rubles. A new find of rubies in Russia has quickly attracted the interest of mineral and gem collectors worldwide. The rough material is being recovered from the Rais mine, located in the Polar Urals in Siberia. Samples of these rubies, in their host matrix, were provided for examination by the Mineral Department of The World of Science, Rochester, New York, through a loan arranged by William Pinch of Pittsford, New York. The crystals are dark slightly brownish red; they occur as well-formed hexagonal prisms with sharp interfacial angles.

The ruby crystals are contained in a matrix consisting primarily of white feldspar and greenish brown mica, as identified in GIA's Research Department by laser Raman microspectrometry. Some of the rubies have pinacoidal terminations, while others, like the one shown in figure 13, are terminated by parting planes that result from excessive lamellar twinning. Detailed microscopic examination of the matrix also revealed the presence of ruby microcrystals.

The gem potential of this deposit is unknown at the current time. As reserves are established and mining continues, more details will become available. Mr. Pinch stated that the crystals seen thus far make excellent mineral specimens. Some of the material is cabochon quality, although lamellar twinning could cause problems with parting during the fashioning process.

Star sapphire from Madagascar. Star and trapiche blue sapphires are being recovered from a new alluvial deposit in northern Madagascar, according to Randy Wiese, of Michael Couch and Associates, Fort Wayne, Indiana. The stones are found in northeast Madagascar, about 120 km south of the island's northern tip, near the east coast. (The mine was recently shut down, however, after an endangered species was discovered living in the area—see, e.g., *ICA Gazette*, May-June 1998, pp. 6–7.) Blue sapphires from southern Madagascar were described in a comprehensive Summer 1996 article by D. Schwarz et al. ("Sapphires from the Andranondambo Region, Madagascar," *Gems & Gemology*, pp. 80–99) and a Fall 1996 Gem News update (pp. 217–218).

We examined five representative stones, weighing 1.37 to 6.88 ct (figure 14). All five showed good stars. Their gemological properties were quite uniform: color—dark blue; color distribution—uneven with hexagonal banding; diaphaneity—semi-transparent to semi-translucent; refractive indices—1.762–1.770 (spot measurements); specific gravity—4.00–4.01; fluorescence—inert to both long- and short-wave UV radiation. All five showed the same absorption spectrum through the handheld spectroscope: bands at 450, 460, and 470 nm. When viewed through the microscope, all showed straight growth banding oriented in hexagonal patterns, "fingerprint" inclusions, and clouds of "silk." One stone showed iron stains, and another had a surface-breaking opaque reddish brown inclusion that Raman analysis

Figure 13. Mined in Siberia, this 20 × 14 mm ruby is contained in a matrix of feldspar and mica. The large crystal "face" is actually a parting plane that parallels the lamellar twinning. Photo by Maha DeMaggio.

Figure 14. These star sapphires, which weigh 1.37 to 6.88 ct, are from northern Madagascar. Photo by Maha DeMaggio.

proved to be columbite. These stones could be mistaken for synthetic star sapphires (so-called "Linde stars") if the straight growth banding was interpreted as curved banding due to the curvature of the cabochon surface.

TREATMENTS

Jadeite boulder fakes. Although various treatments (i.e., dyeing and polymer impregnation) are used to improve the apparent color of fashioned jadeite, most buyers do not suspect that rough jadeite can also be altered. Larry Gray of the Mines Group, Boise, Idaho, submitted one such faked boulder to the Gem News editors for examination. The rough boulder was apparently still covered with its alteration crust, or rind, with a few "windows" (figure 15, left) polished into it. However, when the boulder was sawn, the "windows" were found to be thin slices of better-color green jadeite that had been placed under a fabricated crust (figure 15, right).

The sawn boulder measured 96.30 × 84.60 × 34.10 mm, with a weight of 422 grams. The core of the boulder was a dark mottled grayish green, with more saturated green "windows," and the crust was a mottled dark brown. By shining a strong light through the edge of one "window," we were able to observe an absorption spectrum with the handheld spectroscope: This showed a line at 437 nm, but no detectable "chromium lines." (Chromium lines would be expected in a piece of jadeite with as intense a green color as the windows suggested.) Only two features—besides the appearance where the boulder had been sawn—provided any suggestion that the quality of this piece had been falsified. First, weak yellow fluorescence to long-wave UV radiation was seen in areas of the crust surrounding the "windows" (probably caused by the binding material). Second, the crust in many places—not just by the windows—reacted when it was approached by a hot point. This latter observation suggests that much of the crust, not just that covering the edges of the "windows," may have been made of ground rock plus an organic binding material.

A similar fake was reported on the Canadian Institute of Gemmology's Web site (http://www.cigem.ca/357.html) after the 1997 Tucson show. This boulder had been

Figure 15. Left: this "window" (about 1.5 cm long) in a jadeite boulder suggests that the boulder is of reasonably good quality. Right: when the boulder was sawn, the owner found that the "windows" were thin slices of jadeite that had been placed under a fabricated crust. Photos by Maha DeMaggio.

Figure 16. A plasma-deposited titanium coating creates the iridescent, high-luster surfaces in this 24-mm-long pendant-set cabochon and the two free-form cabochons. Pendant courtesy of Maxam Magnata; photo © GIA and Tino Hammid.

sliced into three pieces, hollowed out, and filled with a "leaf-to-emerald green jelly" that enhanced the appearance of a "window" polished on the surface. Again, the fraud was not obvious until the boulder was sawn.

Titanium- and gold-coated drusy materials in jewelry.
The appearance of a material can be substantially changed by altering its luster as well as its color. To this end, very thin layers of metals and oxides are used to create lustrous (but still transparent) materials with unusual colors. Examples include blue "Aqua Aura"-coated quartz (Gem News, Winter 1988, p. 251; Fall 1990, pp. 234–235) and the many colors of coated quartz that we reported in the Fall 1996 Gem News (pp. 220–221). As these layers are very thin, the coated material is generally not appropriate for many jewelry purposes.

However, the techniques for applying these coatings—among them, plasma deposition and sputtering—can also be used to apply thicker metallic coatings with better durability. Because the metals are opaque, though, all but the thinnest coatings tend to be opaque as well. One of the more spectacular metals used for such coatings is titanium, since it reacts with oxygen or oxidizers to form titanium oxide layers with bright "interference" colors and a metallic to submetallic luster. Among the

colors reported by J. B. Ward ("The Colouring and Working of the Refractory Metals Titanium, Niobium, and Tantalum for Jewellery and Allied Application," *Worshipful Company of Goldsmiths [London] Technical Advisory Committee Project Report* No. 34/1, 1978) are: "gray, pale amber, dark amber, brown, purple, maroon, navy blue, sky blue, rich purple, bottle green, lime green, peacock blue, and gray brown." Over the past few years, we have seen many items––from quartz crystals to arrowheads––that had such coatings. Few, though, would be considered gem materials.

Recently, Maxam Magnata, of Fairfield, California, began selling drusy gem materials with this thicker plasma-deposited coating (see, e.g., figure 16). Mr. Magnata and his partner, Abigail Harris, are marketing these materials as "Titania Gemstones." Although they do not specify the type of drusy material that has been coated, a similar piece of unknown provenance that was examined in the Gem Trade Laboratory proved to be drusy quartz and chalcedony (resembling a section of a geode). Durability, although much improved, continues to be a concern, and Ms. Harris and Mr. Magnata caution that their "Titania Gemstones" should be cleaned with a soft toothbrush and water or mildly acid solutions (not detergent). Such coatings should not be buffed or polished.

This year at Tucson, Mr. Magnata also showed us fashioned pieces that had been coated with "hardened" 23K gold (figure 17). He explained that these coatings are applied to drusy quartz using vacuum deposition (sputtering); in some cases, an iridium-rich layer is added for hardening. For "black drusy"—on a base composed of quartz and manganese oxide (psilomelane)—an additional layer of transparent silica is added for protection. The

Figure 17. From left to right, these three free-form cabochons are "gold drusy," psilomelane drusy partially covered with 23K gold, and psilomelane drusy; the last measures 19 × 26 mm. Photo by Robert Weldon; courtesy of Maxam Magnata.

gold coatings can be applied with a mask, so only part of the piece is coated. The same cautions apply for this material as for the "Titania Gemstones," and ultrasonic cleaning should not be used.

Surface-treated topaz. Gemstone treaters are constantly looking for new ways to add color to otherwise colorless gem materials. When simple heat treatment is not sufficient, other methods (such as irradiation or chemical diffusion) are often attempted. Following the success of diffusion treatment of corundum, the process has been tried on many other gem materials. Some of these attempts have resulted in surface coatings (e.g., quartz coated with blue cobalt glass, Summer 1994 Gem Trade Lab Notes, pp. 118–119), but we are not aware of any that have produced actual diffusion.

Last year we were told of several new colorless topaz treatments which have produced pink, orange, red, and bluish green colors. All these treatments have been represented as diffusion. We had the opportunity to examine specimens of all of these colors and determined that two different treatment processes are actually being used.

The pink, orange, and red colors have been treated by what appears to be a sputter-coating process, which produces a spotty surface coloration. This coating is not permanent; it can be scratched off easily with a needle or any other sharp object (figure 18). Indeed, at the Tucson show this year, several large parcels of the red material showed obvious paper wear on the facet junctions. This is clearly not a surface-diffusion process.

The bluish green material, however, is different. A parcel of approximately 30 stones was supplied to us for study by the inventor of the process, Richard Pollak of United Radiant Applications in Del Mar, California, and

Figure 19. These two stones represent the range of color seen in the bluish green to greenish blue surface-treated topaz supplied for this study. Photo by Maha DeMaggio.

the distributor, Gene Dente of Serengeti Company, San Diego, California. Although Mr. Pollak believes that the material is diffusion treated, and the treatment process is similar to that used for diffusion, Mr. Pollak confesses that he does not completely understand the exact mechanism taking place. A patent on this process is currently pending.

We examined six samples from the parcel in detail. These samples represented the range of color present in that parcel (bluish green to greenish blue; figure 19) and weighed from 5.64 to 6.36 ct. The gemological properties were as follows: refractive indices—1.610–1.611 for the low index and 1.620 for the high; diaphaneity—transparent; pleochroism—weak, green and bluish green; optic character—biaxial positive; (Chelsea) color-filter reaction—pink to red; fluorescence—inert to both long- and short-wave UV radiation; absorption spectrum using a desk-model spectroscope—three bands centered at 545, 585, and 640 nm.

When these samples were examined with a microscope, the bluish green color revealed a spotty appearance (figure 20), similar to that seen on the surface of the other colors of coated topaz described above. Many of the stones had chips on the keel line of the pavilion or elsewhere on the stone. All of these chips penetrated the colored layer and revealed the colorless material beneath (again, see figure 20). Penetration of the colored layer into the topaz could not be seen, even with magnification as high as 210×. Two of the stones showed blue concentrations at the point where some fractures reached the surface (figure 21). It first appeared that this might be similar to the "bleeding" we have observed in some diffusion-treated sapphires, but on closer inspection we could find no penetration of the color into the fractures themselves. With reflected light, we saw irregularities at these blue concentrations that made the surface look as if it had

Figure 18. The pink surface coating on this topaz was easily scratched with a pin, as seen here in reflected light. Photomicrograph by Shane F. McClure; magnified 23×.
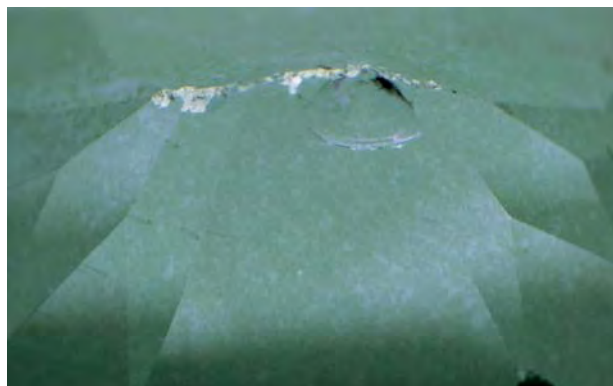
Figure 20. Spotty surface coloration is clearly visible on this treated topaz. Notice also the small chips at the culet that break through to the colorless material underneath. The large chip at the culet must have been present before the stone was treated, as it is covered by the treatment. Photomicrograph by Shane F. McClure; magnified 23×.
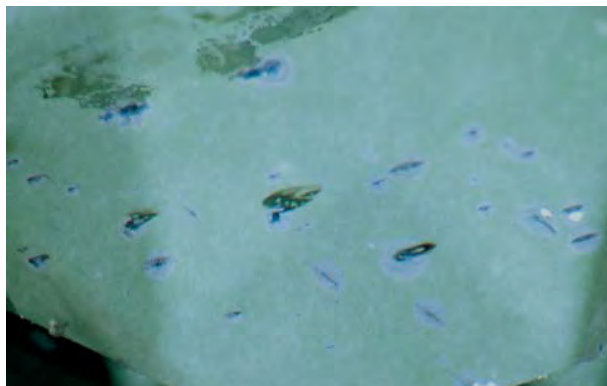

Figure 21. Blue color concentrations can be seen around several minute fractures on the table of this surface-treated topaz. Photomicrograph by Shane F. McClure; magnified 23×.

been melted. Again, the blue color was confined to the surface, at least at the magnifications available to us.

The chemistry of each of the six samples was determined by EDXRF. High concentrations of cobalt were detected, which is consistent with the color of the material, its absorption spectrum, and its reaction in the Chelsea filter.

We also attempted to determine the hardness of the bluish green/greenish blue color layer. To our surprise, we could not scratch it with a needle or with a Mohs 7 hardness point. It was only when we used a Mohs 8 hardness point (i.e., topaz) that we were finally able to scratch the treated surface. We also put half of one stone in a solar simulator for 164 hours to test the stability of this treatment to light. No fading of the color was observed in comparison to the other half of the stone, which we kept in the stone paper as a control.

Further investigation is necessary to understand the physical mechanisms taking place during this treatment process. Given the hardness of the color layer, it is clear that we are not dealing with a typical applied coating. It is also possible that there is some penetration of the color into the stone.

INSTRUMENTATION

New faceting machine. Development engineer Nick Michailidis has designed a new faceting machine, which he recently demonstrated to GIA staff. The "Diamante" (figure 22) can facet both diamonds and colored stones, and can do so in manual and automatic modes. The cutter can perform all the operations that turn a sawed and bruted diamond into a fashioned gem, such as blocking, polishing crown and pavilion mains, brillianteering, table polishing, and girdle polishing. These operations can also be performed on colored stones.

The major features of the "Diamante" include: a portable benchmount (the machine has overall dimensions of $30 \times 56 \times 35.5$ cm high), low vibration and noise levels, easy conversion between diamond and colored stone faceting, specially formulated cast-iron laps for diamond cutting (although it uses commercial 8 inch [20 cm] laps for colored stone polishing), a high-torque reversible motor with variable speed control, and a special fixture for re-facing cast-iron laps. The precision quill head enables quick inspection of the stone without losing the stone orientation, and it can position facet angles to 0.1°. Other diamond holders and colored stone dops are available.

In addition to the spatial advantages that result from use of a single instrument for all steps in diamond

Figure 22. This new faceting machine, Imperial Gem Instruments' "Diamante," can be used to perform all steps in faceting both diamonds and colored stones. Photo by Nick Michailidis.

faceting, Mr. Michailidis notes a personnel advantage for small factories, as it is easier to train employees to proficiency on one machine rather than require that they learn to use several machines. He is marketing this machine through his company, Imperial Gem Instruments of Santa Monica, California.

ANNOUNCEMENTS

AGTA Announces Tanzanian Miners' Relief Effort. At the JCK Las Vegas Show in June, the American Gem Trade Association (AGTA) announced its Merelani Miners Relief program. This fund-raising drive comes in response to a recent catastrophe at the tanzanite mines in Merelani, Tanzania. In addition to the press release from the AGTA, we have some information from gem dealer Michael Nemeth of San Diego, California, who visited the region soon after the disaster (and who previously reported on conditions at Merelani in the Summer 1996 Gem News section, pp. 135–136).

In early April of this year (April 8, according to Mr. Nemeth), heavy rains led to the flash-flooding of several pits in Block B at Merelani, down to 1,000 feet (about 330 m). Although the disaster occurred during a holiday, 14 mines were being worked during the cool weather of the night and early morning. In addition, some workers were in the mines seeking shelter because of crude or nonexistent facilities on the surface. An early estimate of the loss of life was approximately 200 people, with 65 bodies recovered as of May 21, when AGTA representatives Philip Zahm and Jeff Schneider visited the area.

Ironically, the disaster came just as tanzanite production in Block B showed signs of increasing after a year-long dearth of stones. Mining was halted immediately after the disaster but has since resumed in some areas. Nevertheless, the task of cleaning out the flooded chambers (figure 23) will take months.

The tragedy has prompted the Tanzanian government and the mine owners to improve the primitive conditions at Merelani, where most of the mining is done by hand. The government has already dug a new drainage canal to redirect rain runoff away from the mines. AGTA's goal is to raise $100,000, which will be used to construct a multi-purpose building on-site for the miners, as well as to train and equip a basic emergency medical team and a basic mine-rescue team. AGTA has already obtained pledges from medical and rescue trainers to volunteer their time and expertise. Anyone interested in contributing to the relief program should contact AGTA headquarters at 181 World Trade Center, 2050 Stemmons Freeway, Dallas, TX 75207 (Phone: toll-free in the U.S., 800-972-1162; outside the U.S., 214-742-4367).

Birthstone Exhibit at the Carnegie Museum. A collection of birthstones will be displayed at the Carnegie Museum of Natural History in Pittsburgh, Pennsylvania, through September 6. The exhibit features 127 specimens of rough and cut gems and crystals based on AGTA's offi-

Figure 23. These Tanzanian miners are using a rudimentary rope-and-bucket system to remove dirt and debris from the flooded mine shaft. Photo by Jeff Schneider.

cial lexicon of birthstones, including a collection of natural fancy-color diamonds, a 17th-century diamond and ruby necklace, a wide range of pearls, and a 15 ct emerald. For more information, call (412) 622-3131, or visit the Carnegie's Web site at http://www.clpgh.org/cmnh.

Ninth annual conference of the Canadian Gemmological Association. On October 24 and 25, 1998, the Canadian Gemmological Association will hold its annual conference in Montreal, Quebec, at the Montreal Board of Trade, 5 Place Ville Marie. Although other subjects will be explored—including Canadian diamonds and Tahitian cultured pearls—the main topic will be emeralds, including production, cutting, marketing, and treatments. Among the guest speakers will be M. Boucher (on diamonds); M. Coeroli (on pearls); J.-P. Riendeau (on light sources); and K. Scarratt, A. Groom, contributing editor H. Hänni, and J.-C. Michelou (on emeralds). There will also be workshops on emerald treatments, to be held in both French and English. For conference reservations or additional information, please contact François Longère at (514) 844-3873.

Thank You, Donors

The Treasured Gifts Council, chaired by Jeanne Larson in 1997 and now chaired by Richard Greenwood, was established to encourage individual and corporate gifts-in-kind of stones, library materials, and other non-cash assets that can be used directly in GIA's educational and research activities. Gifts-in-kind help GIA serve the gem and jewelry industry worldwide while offering donors significant philanthropic and tax benefits. Treasured Gifts Awards are presented to those who have given gifts valued at $10,000 or more. We extend a sincere thank you to all those who contributed to the Treasured Gifts Council in 1997.

$100,000 or more
American Pearl Company
Stephen & Eileen Silver
Touraine Family Qtip Trust

$50,000 to $99,999
Chatham Created Gems
Ramsey Gem Imports, Inc.
Zvi & Rachel Wertheimer

$10,000 to $49,999
Kazanjian Bros., Inc.
Kenneth McCauley
Oro America
Martin and Juliette Smilo
Strategem
The Bell Group, Inc.
David I. Warren

$5,000 to $9,999
Fortunoff Fine Jewelry
Susan G. Goldstein, G.G.
Mrs. Lelia L. Larson
Tahiti Perles

$1,000 to $4,999
Bremer Jewelry
Donald Clary, Gemologist
Color Masters Gem Corporation
J. Mark Ebert, G.G.
Bob Flower
Heath Wind
The Home Shopping Network
Komatsu Diamond Industry Ltd.
M.B. Gems
Manufacturing Jewelers & Silversmiths of America
Betsy Ross Marcinkus
Morgana's
NorthStar Gems, Corp.
Benjamin Pecherer
Service Merchandise
Sherri Gourley Skuble
T.Q. Diamonds
Mr. & Mrs. Francis T. Tomlinson
United States Pearl Co., Ltd.
August O. Weilbach
Barbara Anne Zinker

$500 to $999
William E. Boyajian, G.G., C.G.
Michael A. Cheatham
Columbia Gem House, Inc.
Cooper Jewelers
Crescent Jewelers, Inc.
Martin B. de Silva, G.G.
James Avery Craftsman

Roberts & Son Co.
Linda Koenig
Christopher LaVarco
Mayor's Jewelers
O & D Bush Jewelers, Inc.
Sara Gem Corp.
Harriet S. Shane, M.F.A., G.G.
Norman & Noreen Shmagin
Edward R. Swoboda

$250 to $499
Henry F. Baldwin
Peter & Virginia Bancroft
Cabnet Goldsmiths
Margaret C. Canganelli, G.G.
Cumberland Diamond Exchange
David B. Dubinsky Gemstones
Gray & Company Fine Jewelers, Inc.
Lauren Gunning Ansorge
Kristopher R. Hernandez
Jeffrey Kaphan
Gail B. Levine, G.G.
J.S. Lizzadro, Ltd.
Joseph Mayer, G.J.G.
McCoy Jewelers
Michael's Jewelry
Penn Gem International
Kelly J. Rapp
Theresa M. Rezzarday
Robert Solomon
Star Ring, Inc.
Thomas A. Davis Jewelers
Tryon Mercantile, Inc.

$100 to $249
A.M. DePrisco Inc.
Gary Alfieri
Assured Loan Company
Aucoin-Hart Jewelers
Back Cove Resources

Concord Manufacturing Company
D & J Rare Gems Ltd.
Guy J. De Leon
Diamonds Plus
Patricia A. Doolittle
Exclusive Merchandisers, Inc.
John E. Fitzgerald, G.G.
Foremost Fine Jewelry Corp.
Gordon Brothers Partners, Inc.
Maggi R. Gunn
Hayman Jewelers
Deborah Hiss-Odell, G.G.
Dale Holland
Abdulhakim I. Hussein
Robert E. Kane, G.G.
Karl's Jewelry Inc.
H. Oliver Keerins
L. Morgan Jewelers
Roger G. Larson
Diane J. Lindley
Loren Industries, Inc.
Thaïs Anne Lumpp, G.G.
Lynn's Jewelry
M. R. Lava
Merchant's Oceanic Ent.
Kenneth L. Moyer, Gemologist
Moyer Jewelers, Inc.
Nagi's Jewelers
Bernard H. Norris, Gemologist
R. Goldworks Co.
Rock Craft by Yttri
Rottermond Custom Jewelers
Susan Sadler
Mark H. Smith
Sutherlands'
William Crow Jewelry Inc.

Under $100
Georgia Allen
Joel E. Arem, Inc.

Byron Austin
B. Miller Siegel
Katherine T. Beasley, G.G.
Theresa Beltrani, G.G.
Berthet Jewelers
Bess Friedheim Jewelry, Inc.
Mary Jane Bloomingdale
Carolyn J. Bomberger, G.G.
John A. Bondick
Michael Christie
Chevis D. Clark, Jr.
Brian C. Cook
Crosby's Jewelry
Gerald R. Dawson, Jr.
Kathryn De Long, G.G.
Mary T. Denewellis, G.G.
Dorado Co.
Luella W. Dykhuis, G.G.
Edizioni Gold SRL
Fantasy Gems
Jeffrey Foster
Jann Garitty
Gem and Mineral Exploration Company
Gemming International Co.
Golay Buchel Japan K.K.
The Golden Swann Jewelery & Collectible Gallery
Diane C. Goodrich
Robert S. Harris
Heather's Neste Antiques
Alice L. Hildreth
Darrell Hillhouse
Solon R. Holt, Jr., G.G.
Ingeborgs Stenar AB
Carolyn S. Jacoby, G.G.
Jewel Tunnel Imports
Mary L. Johnson, Ph.D.
Susan B. Johnson, G.G., C.G.
Joseph's Jewelers
Kathleen Kibler, G.G.

Robert J. Kivett-Cantero, G.J.G.
Richard M. Knox
Merle S. Koblenz, G.G.
Kunzelman Brothers
Brendan M. Laurs, G.G.
Donald B. Lee
Donald Lie
Arthur & Anni Lipper
Ruth May
Metro Gem Consultants
The Milagro Goldworks Studios
Mojave Blue Chalcedony
Rodrigo Moncada
Jim Morey
Kathy Newcomb
Nikolai's
Patricia M. Oakes
Harold A. Oates, G.G., F.G.A.
Charles F. Peterson, G.G.
Phoebe's Fine Jewelry
Prompt Gem
Maurice D. Quam, G.G., F.G.A.
R. Hoppe Jewelers and Gifts
Timothy A. Rector
Richter and Phillips Co.
Nicholas and Marsha Rochester
Edmond Root
Royal Gemms
Schatzley's Gems Unlimited, Inc.
Scheherazade Jewelers
Henri-Jean Schubnel
Andy Scott
Seagem
Kathy B. Shipp
Silver & Gold Shop
Lewis & Alice Silverberg
Skyline Diamond Setters, Inc.
Dr. Iouliia P. Solodova
Sonya Pearls and Corals
Srinath Group
Sheryl Suko, G.J.G.
Suzanne's Source
Terry Tasich, G.G.
Tiffany & Co.
Geraldine A. Towns, G.G.
Starla E. Turner, G.G.
Stephen R. Turner, G.G.
Howard Vaughan
Village Goldworks, Ltd.
Ottaviano Violati Tescari, G.G.
Brian L. Walters
Warwick Jewelers
Gregory J. Washer
Deborah A. Welker

In its efforts to serve the gem and jewelry industry, GIA can use a wide variety of gifts. These include natural untreated, treated, and created stones, media resources for the Richard T. Liddicoat Library and Information Center, and equipment and instruments for ongoing research support. If you are interested in making a donation, and receiving tax deduction information, please call Associate Campaign Director Anna Lisa Johnston at (800) 421-7250, ext. 4125. From outside the U.S. call (760) 603-4125, fax her at (760) 603-4199, or e-mail ajohnsto@gia.edu. Every effort has been made to avoid errors in this listing. If we have accidentally omitted or misprinted your name, please notify us at one of the above numbers.

Book Reviews

Susan B. Johnson and Jana E. Miyahira, Editors

THE PEARL BOOK: THE DEFINITIVE BUYING GUIDE—How to Select, Buy, Care for & Enjoy Pearls

By Antoinette L. Matlins, 198 pp., illus., publ. by GemStone Press, Woodstock, VT, 1996. US$19.95*

As the subtitle suggests, this book describes the "how-to's" of selecting, buying, caring for, and enjoying pearls. Although targeted for the pearl consumer, the information presented is useful for trade professionals as well.

The Pearl Guide opens with some history and lore, and then moves on to explain how pearls form. Because today's consumer can choose from a variety of pearls (saltwater Japanese, South Sea, and Tahitian—and freshwater Chinese and American—cultured pearls, among others), the author describes and compares the different types. Next is a discussion of the six factors that affect the quality and value of pearls: (1) luster and orient, (2) nacre thickness and quality, (3) color, (4) surface perfection, (5) shape, and (6) size. This section, which also offers some pricing guidelines, is perhaps the most useful to consumers. It is followed by a section that presents commentary from industry experts.

Wear, care, and consumer protection advice are included in the next two sections. *The Pearl Guide* concludes with referrals to appraisal organizations and independent laboratories. There is a section of color photos, in the center of the book, that features some magnificent pieces of jewelry. Missing, however, are color photos of the different quality factors.

Pearls are enjoying a surge in popularity today, and Ms. Matlins' book is an interesting buying guide.

DIANE SAITO
Gemological Institute of America
Carlsbad, California

GEMSTONES OF BRAZIL: GEOLOGY AND OCCURRENCES

By Patrick J. V. Delaney, 125 pp., illus., publ. by Revista Escola de Minas, Ouro Preto, Brazil, 1996. US$23.80

In the preface to this thin volume, the author states his intent to pull together, from various sources and for the first time, what is known of the geology of Brazilian gemstone deposits. Dr. Delaney is well qualified, having spent his professional career as a geologist in Brazil. His sources, largely from Brazilian literature, are well documented and make the reference list valuable for gemologists interested in Brazil. Unfortunately, poor editing and proofreading detract considerably from the book's overall value.

Chapter 1 covers (in 22 pages) the 12 principal diamond-producing districts. Each is discussed separately, except for the Pardo (Bahia) district, a brief description of which is included in the section on the Chapada Diamantina district. Dr. Delaney indicates that he combined these two districts because the diamond-bearing formations are correlative. However, the diamond-bearing Tombador-Lavras Formation in the Chapada Diamantina area is Middle Proterozoic, while the Salobro Formation at Pardo is Late Proterozoic, or possibly Cambrian in age.

The descriptions of each district include some historical aspects and the geologic settings. The names of the sedimentary or meta-sedimentary formations in which the diamonds occur are noted, but because there is no section describing the general geology, this information is lost on readers who are not familiar with Brazilian stratigraphy. On the important Diamantina-Jequitinhonha district, Dr. Delaney writes that "Conventional wisdom tells us that the further downstream diamonds are found in the Jequitin-

honha River basin, the *poorer* [italics added] the quality and the smaller the size." Since fluvial transport actually increases the general quality of diamonds, this error appears to be a glaring example of the poor editing given this book.

Chapter 2 covers the 12 principal emerald deposits in 19 pages, with the greatest emphasis on Carnaíba and the Santa Terezinha deposits. The format is similar to that of the diamond chapter. The Socotó deposit, near Carnaíba, is placed incorrectly both on the map (figure 11) and in the text; its actual location is about 25 km north-northeast, not 15 km east, of Campo Formoso.

The remaining chapters cover aquamarine and other beryl, chrysoberyl, Imperial and other topaz, tourmaline, opals, quartz, and other gemstones. The format changes in these chapters, with interesting bits of information on history and gems from the various mines. Discussion of the geology of individual mines or districts is limited because of their sheer number.

Three appendices follow: a list of localities for gems not discussed, a section with suggestions for field trips to Brazil, and a glossary. The glossary gives both geologic and gemological terms, which suggests that the intended audience is the lay public.

Although this book contains much information of interest to gemologists, the author has tried to cover too much material in too few pages. This lack of depth, coupled with poor editing, limits the book's usefulness.

D. B. HOOVER
Consulting Gemologist
Springfield, Missouri

ENCYCLOPEDIA OF MINERAL NAMES

By William H. Blackburn and William H. Dennen, illus., edited by Robert F. Martin, 360 pp., illus., publ. by the Mineralogical Association of Canada, Ottawa, Ontario, 1997. US$40.00

With this book, the Mineralogical Association of Canada introduces its *Special Publication* series. In the words of the editor, the intent is "to provide reference books of broad interest to all involved in the study of minerals." This encyclopedia is indeed a worthy first offering.

The authors begin with an intriguing and illuminating introduction to mineral nomenclature that includes a discussion of the development and evolution of European languages. The core of the book is an alphabetical compilation of all 3,800-plus minerals officially accepted by the International Mineralogical Association (IMA) through the end of 1996. Also presented here are important mineral group and series names and a few mineral names in common usage that are not currently accepted by the IMA. Each entry includes the etymology of the name and the mineral's chemical formula, original source (type locality), and crystallographic space group, plus relevant literature references and information about relationships to other minerals.

One's first reaction might be that at least some of the information provided is superfluous to the specific subject, but the authors have actually planned their presentation well. The information they have chosen to include relates to the most common origins for mineral names: locations, chemical constituents, crystal symmetry, relationships to other minerals, and (most commonly) people. The careful research and editing that went into this work is obvious from the quality and accuracy of the content and the effectiveness of the presentation. I noted only a few minor typographical and informational errors. The 32 excellent black-and-white mineral drawings by Peter Russell, while not a significant source of information, contribute polish and aesthetics. This is a book that I can recommend virtually without reservation to anyone interested in minerals.

Still, I must also mention a shortcoming that will certainly affect the usefulness of this book for those primarily interested in gems. Most of the names in common usage in the gem world are mineral variety names and, as such, are not considered "official" names for minerals. Very few variety names (e.g., *emerald, ruby,* and *sapphire*) are included in the *Encyclopedia.* The only such names I found were *adularia, agate, alexandrite, amazonite, amethyst, aquamarine,* and *jade.* It seems odd that of the few variety names included, all but one (*jade*) begin with the letter A. I can only guess that the authors started to include the variety names and subsequently changed their minds. The *Encyclopedia* would have been of greater interest to a broader audience if mineral variety names had been included.

The authors have promised annual updates in the Mineralogical Association of Canada's scientific journal, the *Canadian Mineralogist.* I hope they decide to add variety names and to make the updates available as separate supplemental publications, or—better yet—as a second edition a few years down the line.

ANTHONY R. KAMPF
*Natural History Museum
of Los Angeles County*

PROCEEDINGS OF THE SIXTH INTERNATIONAL KIMBERLITE CONFERENCE

Edited by N. V. Sobolev and R. H. Mitchell, 619 pp. in two volumes, illus., publ. by Allerton Press, New York, 1997. US$95.00 (individuals), US$225.00 (institutions)

Since the First International Kimberlite Conference was held in Cape Town, South Africa, in 1973, the world's leading authorities on the earth's upper mantle and the formation of natural diamonds have gathered every four or five years in various parts of the world (USA, 1977; France, 1982; Australia, 1986; Brazil, 1991) to present the results of their research. In August 1995, they met in Novosibirsk, Russia, for the sixth conference. This was a milestone not only because it marked the first time the conference had been held in Russia, but also because it was the first opportunity for many in the international scientific community to see various aspects of the Russian diamond industry, including mines and research centers. This two-volume set is an excellent English publication of 47 papers that are representative of the 268 oral and poster presentations at the conference. Only about 40% of the papers in this *Proceedings* are concerned strictly with Russian localities or minerals.

Volume 1—*Kimberlites, Related Rocks and Mantle Xenoliths*—contains 24 papers describing these rocks in Canada, Botswana, Namibia, Tanzania, Australia, Vietnam, Brazil, the Czech Republic, and various parts of Russia. Volume 2—*Diamonds: Characterization, Genesis and Exploration*—contains 23 papers covering a wide range of topics, such as inclusions in diamonds, physical and chemical characteristics of diamonds from numerous localities, characteristics of indicator minerals, and upper-mantle studies of kimberlite areas in Yakutia (Russia), Canada, and elsewhere. In general, the papers show that substantial progress has been made in the understanding of the mineralogy and petrology of kimberlites and lamproites, and in the study of diamond genesis by various techniques (e.g., cathodoluminescence).

There is plenty in these volumes to bewilder the average gemologist, as the papers are written at a very advanced technical level. Nevertheless, there is much to interest and challenge experts in the physical and chemical aspects of diamonds, kimberlites, and the upper mantle, as well as those individuals who are seriously involved in diamond exploration.

A. A. LEVINSON
*University of Calgary
Calgary, Alberta, Canada*

Gemological

ABSTRACTS

COLORED STONES AND ORGANIC MATERIALS

The ABCs of pearl processing. D. Federman, *Modern Jeweler*, Vol. 97, No. 3, March 1998, pp. 53–57.

With supply and demand for South Sea pearls at an all-time high, the South Sea Pearl Consortium is trying to raise awareness to the fact that some pearls are enhanced by any one of several methods before reaching jewelers. There is a spirited debate in the trade as to which enhancements require disclosure.

Once out of the shell, pearls are usually cleaned by various chemical and buffing techniques. Whether this step qualifies as a treatment and merits disclosure remains to be decided. Pearls are also bleached (with hydrogen peroxide or other chemicals) for tone consistency in pearl strands, but since bleaching is used almost exclusively to remove rather than add color, some argue that there is no need for its disclosure. Natural pinkish pearls are often dipped in solutions with organic pigments to enhance their appearance; these "pinked" pearls may be recognized by small deposits around the drill hole.

Disclosure is less discretionary with Akoya gray pearls, because in some the color is natural, whereas in others it results from irradiation. Some Akoya pearls are dyed by immersion in silver nitrate salts to resemble Tahitian black pearls; disclosure of dyeing in this case is common practice and does not seem to hurt sales. The same pattern of disclosure generally is not followed with

---

solution-treated fancy yellow and golden pearls. Because there is no way to detect this enhancement, dealers fear that producers are remaining silent about it. The GIA Gem Trade Laboratory is working on treatment detection through spectrophotometry and other advanced techniques.

Luster is highly valued in pearls, and pearl processors have used a combination of techniques, such as tumbling and buffing, to attain the best polish. While these are perfectly acceptable finishing processes, a new wave of polymer coatings is being used to give dull pearls sheen and luster. However, detection of such coatings is fairly easy for laboratories.   *MD*

Emerald stirs many passions. *Jewellery International*, No. 43, March/April 1998, pp. 43–46.
Famous jewelers from Cartier to Harry Winston have used emeralds in their most spectacular creations. Their designers look to the source countries of Colombia, Brazil, and Zambia—or to distributors in New York, Paris, and Israel—in search of the perfect stone. Most emeralds are enhanced with treatments that vary from oils to resins. While some in the industry insist that enhancement is a routine part of the cutting and polishing of emeralds, a need for disclosure is becoming evident.

The American Gem Trade Association has recently released the *Consumer Guide to Emeralds*, a pamphlet designed to educate the consumer on possible emerald treatments. While oiling long has been accepted by the trade as a means to enhance emeralds, some consider the use of resins to be "unnatural." The industry must decide which of the multitude of treatments used worldwide should be deemed acceptable, and which must be disclosed.   *MD*

La géologie des gisements de saphirs (On the geology of sapphire deposits). C. Simonet, *Revue de Gemmologie*, No. 132, 1997, pp. 21–23.
On the basis of a literature survey, the author has classified corundum deposits into three types according to their geologic origin.

1. *Volcanic (primary) deposits*. Corundum in this category is brought to the surface by magma from sources at depth. The large deposits in Australia, China, and Southeast Asia—as well as the deposits in Rwanda, northern Kenya, and Nigeria—belong to this category.
2. *Metamorphic (primary) deposits.* Corundum in metamorphic rocks is found in formations high in aluminum and low in silicon. Two subtypes are recognized: (1) isochemical (i.e., the bulk chemical composition of the host rock does not change during metamorphism); and (2) metasomatic (i.e., during metamorphism, the chemical composition of the host rock changes due to chemical reactions with the neighboring rock formations or fluids). Examples of corundum localities of the first subtype are Sri Lanka, Russia (Ural Mountains), Afghanistan, Pakistan (Kashmir ruby), and

Tanzania (Longido). Important examples of the second subtype are found in Pakistan (Kashmir sapphire), Madagascar, Tanzania (Umba Valley), Sri Lanka, Myanmar, and Kenya.
3. *Sedimentary (secondary) deposits*. Most of this corundum is retrieved from alluvial and eluvial deposits; no further details are supplied.

Application of this classification to exploration for corundum is briefly discussed.   *PRB*

A miscellany of organics. G. Brown, *Australian Gemmologist*, Vol. 19, No. 12, October-December 1997, pp. 503–506.
This compilation of the identifying features (most as viewed with a 10× hand lens), augmented by interesting facts, of rare and common organic gem materials is based on laboratory reports prepared by the author over the last decade. *Dyed walrus ivory* shows a "rice bubble" pattern. Hawaiian *kukui* nuts display either a gleaming ebony color or a rare mottled brown-black *kalaloa* hue. *Oxblood colored precious coral* is frequently imitated by red-dyed, plastic-impregnated, common reef-building coral, which can be identified by the presence of round bubbles within the plastic. *Apple coral*, the basis of a large export industry for inexpensive coral jewelry centered at Zamboanga, Mindanao, Philippines, is frequently encountered as fragments joined by a colored plastic adhesive. A "*Colombian amber*" specimen was found to be a copal resin; this material can be identified by its solubility in volatile organic solvents such as ether, chloroform, or alcohol. *Black pearls* purchased in the Philippines at bargain prices have proved to be ground and polished segments of black shell, such as that of the black-lipped pearl oysters, and are easily identified with magnification.   *MD*

Present situation and prospects of China freshwater pearl breeding. Y. Feng, *China Gems*, Vol. 6, No. 4, 1997, pp. 35–37 [in Chinese with English abstract].
The culturing of freshwater pearls in China began in 1972. By the end of the 1970s, China was exporting about 11 tons of pearls annually, which earned about US$18 million. During the 1980s, the freshwater cultured pearl industry developed rapidly, and both production and exports multiplied. Overproduction in the 1990s has pushed prices down to the level of the early 1980s. Today, the freshwater pearl culturing industry in China faces serious challenges that can be overcome only by improving the quality and size of the pearls and limiting the amount of production.   *Yan Liu*

Red beryl mine finds new investors. M. Lurie, *Colored Stone*, Vol. 10, No. 6, November/December 1997, pp. 26, 28.
Gemstone Mining Inc. (GMI) has acquired a one-year option to study the feasibility of mining red beryl from the Ruby Violet mine in Beaver County, Utah. This is the only known occurrence of gem-quality red beryl in the

world, and it has been mined only on a small scale. Amelia Investments Ltd., the parent company of GMI, paid $1 million to extend an option previously held by Kennecott Exploration Co. Subsequently, Neary Resources Corp. of Vancouver, British Columbia, purchased a 60% interest in GMI for $3 million. This was expected to fund operating costs and completion of the feasibility study by year's end. *[Editor's note: In a news release dated June 9, 1998, Neary announced the completion of the feasibility study, and that it was investigating various financing opportunities to fund the project.]*

The agreement includes the Cedar City (Utah) pilot plant, built by Kennecott to process the stones, and some properties adjoining the main mining claims. All cut and rough stones from the property, along with production records and marketing data, were also acquired by Amelia, which formed GMI to administer, evaluate, and operate the property. GMI hopes for an initial annual production of 25,000 carats of finished goods. MVI Marketing, of Beverly Hills, California, has been hired to devise a marketing campaign for the red beryl. *MD*

Research on texture type of Burmese jadeite Y. Ao and R. Wu, *China Gems*, Vol. 6, No. 4, 1997, pp. 118–121 [in Chinese, no English abstract].

Jadeite from Burma (Myanmar) formed in rocks that were subjected to regional metamorphism involving deep burial with high pressures but with relatively low temperatures. The different jadeite textures that have been observed (with a polarizing microscope) can be explained by variations in the geologic conditions under which jadeites form and to which they are subsequently subjected. In this article, Burmese jadeite is classified into eight different "primary" or "secondary" textures.

Four primary textures form during the crystallization stage of jadeite: granular, cylindrical, fibrous, and "spotlike." Four secondary textures form subsequently: plastically deformed, fractured, "solid solution," and recrystallized. Photomicrographs featuring characteristics of the various textures are presented.

Yan Liu and Taijin Lu

DIAMONDS

The applications and properties of MONOCRYSTAL. P. R. de Heus, *Industrial Diamond Review*, Vol. 57, No. 572, January 1997, pp. 15–18.

The properties of synthetic single-crystal diamonds, called Monocrystal, are outlined. De Beers produces these synthetic diamonds for industrial uses. Compared to a natural diamond, which has an octahedral shape, Monocrystal products are cut from cube-shaped crystals. The sawn plates are available with a thickness of up to 2 mm and a maximum edge length of 8 mm. Each face lies in the {100} (or 4-point) plane, so in theory each has four machining directions.

Because these synthetic diamonds grow so rapidly,

there is very little nitrogen migration within the lattice. Instead, the nitrogen is randomly distributed throughout the lattice (type Ib diamond), giving the crystals (1) a typically golden color and (2) exceptional thermal conductivity. Monocrystal is, therefore, generally superior to natural diamond (which is usually type Ia) for high-quality diamond tools, because the high thermal conductivity ensures rapid removal of heat. Practical industrial applications are discussed. *RAH*

CIS supplement. *Supplement to Mining Journal, London*, Vol. 329, No. 8455, November 14, 1997, 32 pp.

The Commonwealth of Independent States (CIS) consists of the nations of the former Soviet Union, with the exceptions of Estonia, Latvia, and Lithuania. In Russia, changes in government policies in the last few years have affected mineral exports. For example, in August 1996, Roskomdragmet (the Russian Federation Committee for Precious Metals and Stones) was dissolved; this committee formerly determined the conditions for exporting diamonds, a function that is now under the control of the Russian Ministry of Economics. Russia exports almost all (97%) of its cut diamonds. The Russian gem industry reported $1 billion in sales of cut and polished diamonds in 1996, the same as 1995. Furthermore, Russia has the capacity to cut $1.3 billion worth of diamonds annually.

For a brief period in 1995, the Russian government permitted the publication of mining statistics, including production statistics on diamonds; however, in November 1995 information on remaining diamond (and precious metal) reserves was reclassified as a state secret. Nevertheless, it is known that diamond reserves in the CIS grew 21% in 1996 compared to 1995.

More than 98% of all diamonds produced in Russia were mined by Almazy Rosii-Sakha (Alrosa) in the Yakut/Sakha Republic. In 1996, the value of exported rough diamonds increased by 3% [to US$1.42 billion] over 1995 values. The new mill at Yubileinaya went into operation, and a new diamond pipe, Nyurbinskaya, was discovered. If Alrosa can get the large capital investments it desires, it plans to increase diamond output by 25% over the next three years.

The Lomonosov diamond deposit in the Arkhangelsk region was discovered in 1980, with exploration continuing until 1987. Joint stock company SeverAlmaz was formed to exploit this deposit; however, the legal basis for this company is still uncertain. Another difficulty in attracting foreign investments is that all data on the Lomonosov deposit is a Russian state secret. Other mining areas to the north and east of Archangelsk also look promising, including Verkhotinskaya, Tovskaya, and Ust-Pinega.

Additional diamond information is provided for other CIS nations. Diamond-bearing kimberlites have been discovered in the Ukraine, along a 250-km-long stretch of the coast of the Sea of Azov (in southeastern Donetsk), and along the Dnipro and Buh Rivers. Belarus has no nat-

ural diamond deposits, but has large diamond cutting and synthetic diamond manufacturing industries. In October 1996, the cutting and polishing plant Kristall in Homvel (formerly Gomel), Belarus, was reportedly at a near stand-still; however, Belarus refused an offer of 150,000 carats of gem and 350,000 carats of industrial diamonds from Alrosa, as the cost was too high.   *MLJ*

Diamond mine economics. *Mining Journal, London,* Vol. 329, No. 8459, December 12, 1997, p. 483.

An economic analysis of hard-rock diamond mining to determine profitability under various production and pricing scenarios was undertaken based on data for 38 mines (pipes and dikes) and prospects. Operating costs per ton of ore (in 1996 US dollars) are: $18–$30 per ton for large open pits (>3 hectares [ha] and >5 million tons [Mton] per year milled); $25–$32 per ton for small- to medium-sized open pits (1–3 ha and <5 Mton/year milled); $17–$20 per ton for block-caving operations (3–5 Mton/year milled); and $25–$30 per ton for stoping operations (1 Mton/year milled). About 70% of the 38 properties are profitable using the criterion of a rate of return greater than 20%; some mines are "obscenely" profitable. The small (<1 ha) Internationalnaya pipe in Russia, for example, has ore worth an estimated $400/ton. Pipes in expensive locations (many in Siberia, also Canada) and several small operations in Africa (with very low operating costs) were not considered in this analysis.

Four production-pricing scenarios were considered: (1) present production and pricing; (2) a 50% fall in rough diamond prices; (3) a 2% annual increase in demand over a 10 year period from a 1996 (base level) 10 Mct [million carats] current oversupply, with five major new mines coming on line, and static rough prices; and (4) the third scenario with a 5% annual price decrease in rough. Under the first scenario, there are three "really great" mines: Jwaneng (56 ha), Udachnaya (20 ha), and Venetia (18 ha). If prices fall 50% (scenario 2), four of the 38 mines remain very profitable—the best two being Jwaneng and Venetia—and six others are still profitable; however, the major mines Orapa, Udachnaya, and Argyle are no longer profitable. In the third scenario, supply and demand remain in balance; but in the fourth scenario, significant shortfalls quickly develop. It is suggested that if De Beers were to flood the market with small and lower-quality stones for any significant amount of time, its competitors Argyle and Udachnaya would be quite resilient to falling prices, but some of its own mines, including Orapa, would have to close. The effect of new production is also likely to threaten the market position of small and low-quality diamonds.   *MLJ*

Marine diamond mining comes of age. D. Clifford, *Mining Magazine*, Vol. 177, No. 6, December 1997, pp. 337, 339–340.

Namco has a new seabed crawler—a dredge that travels along the ocean floor—for mining off Namibia's coast.

The NamSSol is a machine 6 m high, 8 m long, and 5 m wide that weighs 120 tons; it cost about £6 million to develop. It has an articulated (i.e., jointed) suction boom, with a powerful dredge pump that sucks gravels off the seafloor, and two other pumps to locally agitate the gravels for removal. The gravels are mixed into slurry (about 18% solids; in contrast to the 3%–5% solids achieved by airlifts) for transportation to the mining ship. The boom can also rotate through 270°, so that the dredge unit does not need to be moved as often; and it can thump on the ocean floor, with a force of about 20 tons, to break up the sandstone crust that commonly overlies the diamond-bearing gravels in the area.

The NamSSol is operated from the mining vessel *MV Kovambo*. The slurry is brought aboard the ship in 450-mm-diameter flexible hoses, where it is wet-screened and the 2–12 mm size fraction retained. The gravels are scrubbed in a ball mill, and then coated with ferrosilicon; the fractions with densities less than 3.1 g/cm^3 are separated by a cyclone and then discarded. The remainder is sorted first by fluorescence to X-rays and then by hand.

The NamSSol is planned for immediate service in features 19 and 20 of Namco's Koichab prospect, off Luderitz Bay. These features are expected to be the most productive part of the Koichab prospect, with inferred resources of 626,000 and 775,000 carats, respectively (in water depths of 65 to 85 m; of the 1.874 Mct inferred for Koichab features 11, 18, 19, and 20). Given earlier recoveries, the stones should average about 0.36 ct. With 300 days of mining per year anticipated, Namco targets an average recovery rate of 150,000 carats/year for this ship.

This article also contains a short history of seafloor mining in Namibia. "Local legend" Sam Collins first dredged off the southern Namibian coast in the early 1960s, recovering about 788,000 carats. After much exploration, De Beers began dredging operations in 1991. Offshore production (by various operators) grew from 29,000 carats in 1990 to more than 650,000 carats in 1996, and some insiders anticipate annual productions of over 2 Mct by the turn of the millennium. The diamond-bearing gravels extend along 1,400 km of coastline, including southern Namibia and northern South Africa, and contain an estimated 3,000 Mct of diamonds.

                    MLJ

Mink's Mali macros. *Mining Journal, London*, Vol. 329, No. 8457, November 28, 1997, p. 440.

Five "macrodiamonds" have been found at three separate areas in the Kenieba prospect in Mali; the two largest stones, weighing 1.0 and 0.5 ct, were the first diamonds ever found in the Faraba district.   *MLJ*

A new view on the mechanism of diamond polishing. F. M. van Bouwelen, L. M. Brown, and J. E. Field, *Industrial Diamond Review*, Vol. 57, No. 572, January 1997, pp. 21–25.

A new model is proposed to explain the well-known high-

ly anisotropic behavior of diamond during friction and polishing: Diamond hardness varies with crystallographic direction, and the rate of polishing also varies with the direction of the polishing surface relative to the rotation of the scaife. For many years, a micro-cleavage theory was used to describe the removal of material from the surface during polishing, but this new model proposes instead a local graphitization at the diamond surface. This model rests on the observations that friction measurements and polishing produce similar wear tracks and similar debris [so-called "black powder"], and that the surface of a polished diamond shows loss of crystallinity and damage to the upper atomic layers.   *RAH*

GEM LOCALITIES

Uruguay: Untapped potential. *Supplement to Mining Journal, London*, Vol. 329, No. 8455, November 14, 1997, 16 pp.

Uruguay is best known to gemologists as a major source of amethyst and agate; however, the country appears to have potential for diamonds as well. The regional geology consists of Precambrian basement rocks covered by younger sediments and flood basalts. Preliminary exploration by Rea Gold and SouthernEra Resources (following traces of diamond indicator G9 and G10 garnets in streambeds) has uncovered 11 diatremes in the Rio Arapey region. The two main target areas lie west and northeast of Tacuarembo.

Agate and amethyst are found in geodes in Cretaceous lavas in the northwest of the country, near Artigas. Only one "phase" of lava flows is significantly mineralized; it is mined by both open-pit and underground operations. The geodes, which measure up to 2 m across, are commonly found in clusters; they are removed using jack hammers and blasting. Ground-penetrating radar is being studied as a means to prospect for geodes underground. In 1996, 70 tons of amethyst and 154 tons of agate were mined; however, production could easily grow with higher demand.   *MLJ*

INSTRUMENTS AND TECHNIQUES

A combined spectroscopic method for non-destructive gem identification. L. I. Tretyakova, N. B. Reshetnyak, and Yu. V. Tretyakova, *Journal of Gemmology*, Vol. 25, No. 8, October 1997, pp. 532–539.

The authors propose that no single analytical instrument or technique can provide conclusive, nondestructive identification of all gems. They point out the specific limitations of what they consider the three most viable methods—Raman laser spectroscopy, "mirror" infrared reflection spectroscopy, and UV-Vis-NIR (ultraviolet-visible-near infrared) diffuse reflection spectroscopy—and show how these three are mutually complementary. By using one or more of these methods—as determined by the type of gem, its mounting, size, and the like—an unknown sample can be identified unequivocally. At first this article may seem of use only to practitioners of instrumental analysis, but the warnings of the potential hazards and limitations of the various methods also may inform gemologists in search of high-tech assistance as to which ones to avoid.   *CMS*

Praktische Analytik für Sammler: Mineralbestimmung per REM und EDX-Analyse (Practical analytical methods for collectors: Mineral identification with SEM and EDX analysis). Th. Raber, *Lapis*, Vol. 21, No. 12, 1996, pp. 21–25 and 58.

Readers of the mineralogical and gemological literature are familiar with such terms as SEM [scanning electron microscopy] and EDX [energy-dispersive X-ray] analysis, but many of those who have not been educated in the sciences probably do not know the theory behind these techniques and their capabilities. This article explains in simple language: (1) the development and use of scanning electron microscopes, (2) how SEM pictures and EDX spectra are generated and the information they contain, (3) how samples (as small as a period) are prepared and handled, and (4) what types of data can and cannot be gathered from the samples. The article, which is written in German, requires only basic scientific knowledge.
                    RT

JEWELRY HISTORY

Fool's gold? . . . The use of marcasite and pyrite from ancient times. L. Bartlett, *Journal of Gemmology*, Vol. 25, No. 8, October 1997, pp. 517–531.

The material known in the trade as "marcasite" is, in fact, cut and polished pyrite, the cubic form of iron disulfide (FeS_2). In mineralogy, the term marcasite refers to the orthorhombic form of FeS_2. According to the author of this interesting and readable article, this confusing use of the name "has existed for hundreds of years," with the terms pyrite and marcasite being used interchangeably until the 19th century, when the new science of crystallography established the definitions. Since at least the 16th century, however, it was known that various forms and colors of FeS_2 existed.

This article focuses on pyrite, beginning with a brief description and quickly moving on to its use throughout history. Because pyrite is the world's most commonly occurring sulfide, it has been used since prehistoric times in both the Old and New Worlds. Its use with flint to start fire is at least 14,000 years old and led to its use in firearms in the 16th century. Almost as old is its use to create vitriol, an important black dye, from before the time of Christ through the Industrial Revolution.

As an ornamental material, pyrite again dates to prehistoric times. In the Middle East, beads and crystals have been found in archeological sites and graves. The early cultures of Middle and South America used pyrite extensively in practical and religious objects at least as early as

750 AD (examples are illustrated). Cutting of marcasite to imitate rose-cut diamonds began in the 18th century and peaked in Europe during the reign of French King Louis XIV. The stones were set in silver, as were diamonds, but their affordability and availability extended their application to buttons and buckles as well as jewelry. The quality of marcasite jewelry declined as demand grew in the 19th century, and it was regarded poorly as simply a cheap substitute for those who could not afford diamonds. A brief artistic resurgence in marcasite jewelry occurred in the 1920s and 1930s, notably in the Art Deco pieces from Germany. Today, the material is used primarily in inexpensive reproductions, although some marcasite pieces have silver mountings rather than the base metal used after World War I.   *CMS*

Gems—Fact and mythology. H. Levy, *Gem & Jewellery News*, Vol. 6, No. 4, September 1997, pp. 57–59.
Various aspects of sapphire and fancy-colored sapphire are discussed, including biblical references, color change, Roman jewelry, sources, durability, heat treatment, stars, and synthetics. Several pieces of interesting information are presented. For example, the Bible contains several references to sapphire in which the stone is related to wisdom. Sapphire has long symbolized truth, sincerity, and faithfulness, which has made it an excellent choice for engagement rings (Prince Charles and the late Lady Diana Spencer contributed to the revival of this tradition). The Persians believed that the earth rested on a giant sapphire, and that the sky was pale blue in its reflection. In the 18th century, color-change sapphire was used to determine female virtue (a change of color in a color-change sapphire when worn by the subject indicated unfaithfulness, even though the subject might have been required to wear the sapphire both in daylight and when candles or lamps were lit!).   *MD*

PRECIOUS METALS

Platinum blind. *Cigar Aficionado*, December 1997, pp. 456–467 passim.
This article reviews the history of the use of platinum in jewelry, starting with the ancient Egyptians who, about 2,700 years ago, found a way to work naturally occurring gold-platinum alloys into jewelry. Because of its high melting point, however, platinum was not widely used for jewelry until modern times. For example, the Spanish conquistadors, when plundering for silver and gold, thought of platinum as an inferior silver because it would not melt (and so used it as gunshot instead of lead); in fact, the name *platinum* is derived from the Spanish *platina* meaning "little silver" or "lesser silver." However, its pure color, high strength, and inertness (including resistance to tarnishing) encouraged artisans of the early 20th century to work with this metal. They were aided by new, high-temperature furnace technology with which platinum could be melted more easily than before.

Jewelry design based on delicate-looking platinum wirework (open lacework) strong enough to support gemstones began to appear in the era of King Edward VII (who reigned 1901–1910). This new fashion found favor with Louis Cartier, who used it with diamonds in particular. Later, the early 20th century style evolved into the beautiful platinum-based jewelry designs of the Art Deco period.

During World War II, platinum was used only for military purposes, and platinum substitutes (e.g., white gold) were adopted for jewelry. After the war, platinum never regained its exalted status, although Harry Winston, like a few other fine jewelers, continued to design pieces with platinum to support the massive numbers of diamonds used in his jewelry.

Today, platinum-based jewelry is enjoying a resurgence in popularity, although platinum is a relatively rare metal. Only about 150 tons of platinum are mined annually, compared to more than 2,000 tons of gold. About 40% of newly mined platinum is used in jewelry (the remainder is used in numerous industrial applications, e.g., as a catalyst and in computer technology). Japan consumes 85% of the platinum used for jewelry, whereas the U.S. consumes only 3%. However, the U.S. is the fastest-growing market for platinum jewelry.   *MD*

SYNTHETICS AND SIMULANTS

Inclusions in synthetic rubies and synthetic sapphires produced by hydrothermal methods (TAIRUS, Novosibirsk, Russia). A. Peretti, J. Mullis, F. Mouawad, and R. Guggenheim, *Journal of Gemmology*, Vol. 25, No. 8, October 1997, pp. 540–561.
This well-illustrated article examines (by SEM-EDX analysis) the inclusions in Russian hydrothermal ruby and sapphire manufactured by Tairus. Coatings on rough samples were found to be either boehmite or an unknown noncrystalline gel-like material. The following inclusions were observed in both rough and cut samples: solid inclusions of corroded copper (probably remnants of wire), isometric crystals and hexagonal platelets of copper, clouds and linear series of pinpoints of whitish reflective particles, tiny needles, and whitish particles (possibly alkali or calcium carbonates from the mineralizers).

In pinkish red to red samples, the authors found fluid inclusion "fingerprints" or feathers, among which occur large three-phase (liquid-gas-mineral) inclusions associated with large tube-like negative crystals. The daughter minerals in the inclusions were identified (by crossed polarizers and heating/freezing [H/F] experiments) as carbonates. H/F experiments also revealed that the liquid phase is predominantly H_2O. By contrast, three-phase inclusions in natural rubies are often CO_2-rich with daughter minerals of diaspore, graphite, or mica. Of perhaps greatest interest to the practicing gemologist, the authors describe a simple gemological H/F test to distinguish between natural and synthetic hydrothermal rubies

on the basis of three-phase inclusions. The copper inclusions also are indicative of synthetic origin.   *CMS*

Tairus hydrothermal synthetic ruby. L. Qi and S. Lin, *China Gems*, Vol. 7, No. 1, 1998, pp. 122–124 [in Chinese with English abstract].

Gemological investigations of Tairus hydrothermal synthetic ruby revealed characteristic microscopic features, including solid alloy inclusions consisting of mainly copper-iron alloys and wavy growth lines. Chemical analysis by microprobe showed that the chromium concentration in the area of the growth lines averaged 3.81 wt.% Cr_2O_3, as compared to 1.53 wt.% Cr_2O_3 in the remainder of the stone. Characteristic infrared absorption peaks are 3308, 3233, and 3186 cm^{-1}.   *Taijin Lu*

Marketing moissanite. *Modern Jeweler*, March 1998, Vol. 97, No. 3, p. 14.

C3 Inc. of Research Triangle Park in North Carolina is planning to market synthetic moissanite (silicon carbide) as a diamond simulant "later in 1998." The prospect of C3's launch of synthetic moissanite in commercial quantities has drawn the trade's attention, mainly because news reports showed jewelers misidentifying synthetic moissanite as diamond with a standard diamond tester (the thermal conductivity of synthetic moissanite is very similar to that of diamond). This article gives the current and anticipated quality characteristics and prices of synthetic moissanite. (See *Gems & Gemology*, Vol. 33, No. 4, 1997, pp. 260–275, for more details of the physical and optical properties of this material, and methods by which it can be distinguished from diamond and other simulants.)

The synthetic moissanite produced thus far is "M or better" on the GIA color-grading scale. An undisclosed quantity of cut round brilliants under 0.5 ct have been sold: a 3 mm sample for $18 and a 5 mm sample for $80. Future commercial production is expected to be eye-clean, between I and M in color. The company says that per-carat prices will be about 5%–10% of those for diamonds of similar quality. The company plans to target working women, and will offer retailers full marketing support.   *MD*

TREATMENTS

New emerald treatment features I.D. tracer. *National Jeweler*, Vol. 42, No. 7, April 1, 1998, p. 22.

Gematrat, a new enhancement process for emeralds, now features a "secret signature tracer" designed to aid in treatment identification. A small amount of the tracer, added to a colorless epoxy resin, is visible when exposed to ultraviolet radiation. After a thorough cleaning to eliminate any previous treatments, the tracer-containing epoxy resin is injected into the emerald. Although the tracer identifies that the enhancement was performed by the Gematrat process, at present the fluorescence is visible only with 120× magnification. The developer of Gematrat is currently working to make the tracer detectable at lower magnification, so that jewelers can see it with more typical gem-testing equipment. The developer states that the treatment, which has a lifetime warranty, is superior to others on the market, because it does not change color with age and is able to withstand the rigors of repolishing and ultrasonic cleaning without leaking out or damaging the stone.   *MD*

MISCELLANEOUS

Sri Lanka deregulates to raise exports. M. A. Prost, *Colored Stone*, Vol. 10, No. 6, November-December 1997, pp. 10, 12.

Responding to competitive market pressures, Sri Lanka lowered taxes and tariffs in June 1997 to help small and medium-size cutting and manufacturing companies increase productivity. The new policies allow manufacturers to import rough stones duty-free, paying only a 4.5% security levy that is refunded if the stones are re-exported within six months. More important to manufacturers is that any company can trade gems locally and pay only the nonrefunded levy. The government is also offering a 100% tax exemption on imports of goods, such as machinery, to companies that export 50% of their production. In addition, the National Gem and Jewellery Authority, which regulates the jewelry industry in Sri Lanka, has allocated $4.2 million to develop heat-treatment facilities for milky "geuda" corundum mined in Sri Lanka. All these measures are designed to help Sri Lankan industries compete internationally. The export value of cut and polished gems reportedly increased from $13.64 million in 1996 to $18.79 million by July 1997.

Although manufacturers are optimistic, they remain concerned about other restrictions, including time-consuming paperwork required by the Gem Authority in Colombo. That process normally takes two days and is seen as the major remaining obstacle. The cutting industry has also complained about the lack of guidance for industry growth as well as the lack of funds, training skills, and marketing efforts. Because there is not enough raw material to sustain and develop the local lapidary sector, the cutting industry is lobbying to mechanize the mining industry, which is currently described as "pick and shovel." Meanwhile, the Sri Lanka Export Development Board is working to increase the market for Sri Lanka-cut gems with trade fairs and international promotional programs.   *MD*